AD 630843

FINAL REPORT

Contract No. OCD-PS-64-21

OCTOBER 1965

EFFECTS OF IMPULSIVE LOADS ON FIBER-REINFORCED CONCRETE BEAMS

by

JAMES P. ROMUALDI

and

MELVIN R. RAMEY

for

OFFICE OF CIVIL DEFENSE

OFFICE

SECRETARY OF THE ARMY

DEPARTMENT OF DEFENSE

DEPARTMENT of CIVIL ENGINEERING

CARNEGIE INSTITUTE of TECHNOLOGY PITTSBURGH, PENNSYLVANIA, 15213

DEPARTMENT OF CIVIL ENGINEERING

CARNEGIE INSTITUTE OF TECHNOLOGY

PITTSBURGH, PENNSYLVANIA 15213

EFFECTS OF IMPULSIVE LOADS ON FIBER-REINFORCED CONCRETE BEAMS

BY

JAMES P. ROMUALDI AND MELVIN R. RAMEY

FOR

OFFICE OF CIVIL DEFENSE

OFFICE, SECRETARY OF THE ARMY

DEPARTMENT OF DEFENSE

<u>FINAL REPORT</u>

CONTRACT OCD-PS-64-21

OCD Work Unit 1122 C

<u>OCD REVIEW NOTICE</u>

This report has been reviewed in the Office of Civil Defense and approved for publication. Approval does not signify that the contents necessarily reflect the views and policies of the Office of Civil Defense.

OCTOBER 1965

Table of Contents

List of Figures

List of Figures (contd)

List of Figures (contd)

List of Tables

INTRODUCTION

Concrete develops tension cracks as a result of minute flaws that are inherent in its nature. This is one of the things we take for granted when we design structures of concrete. We have developed methods to overcome the loss of tensile resistance, such as adding steel bars to the tensile portion of a beam, or prestressing the entire member. Little, however, has been done to the concrete mix to minimize the effect of the microcracks.

In 1962, at Carnegie Institute of Technology, a method of arresting these cracks was developed by placing short lengths of randomly spaced fine wire* within the concrete mix itself[1,2,3]. Successful studies of the function of the fibers as crack arrestors have been carried out using a fracture mechanics approach. The results of these studies indicate that (1) the fibers increase the tensile strength of the concrete by as much as 100 per cent for static loading, and (2) the material exhibits considerable post-cracking strength. These two effects increase the ability of the material to absorb energy and suggest a study of the material's resistance to impulsive or blast loading.

This report describes such an investigation of the effect of a destructive impulse load upon fiber reinforced concrete beams. The data presented is compared to identical plain beams similarly tested**.

---

* Randomly spaced fine wire shall be referred to as "fiber reinforcement" or "fibers" in this report.

** Concrete beams without fiber reinforcement will be referred to as "plain beams" in this report. In each case, however, conventional steel reinforcement is placed in the tensile zone of the beam.

A suitable apparatus was developed to apply a known impulsive load to the specimens at a high rate of speed. The data were recorded by utilizing oscilloscopes, high speed motion pictures and a specially designed deflection recording device.

EQUIPMENT AND INSTRUMENTATION

Testing Apparatus

The dynamic testing machine is patterned after one previously used at Carnegie Institute of Technology(4,5). The machine is a spring loading device capable of applying a maximum force of 24,000 pounds to the specimen. Fig. 1 indicates essential details of the apparatus. An 18 WF 77 is located on the laboratory floor with its web in a horizontal plane. Holes, 2 inches in diameter, are cut into the web on 40 inch centers symmetrically about the mid-span of the beam. Square holes, 8 inches on a side, are located in the concrete floor directly below the 2 inch diameter holes and two close-coil helical springs are inserted through the holes to bear against the web of the base beam. These springs are 5-1/2 inches outside diameter, 45 inches long, and each has a spring constant of approximately 1,250 pounds per inch. The springs are encased in 6 inch diameter tubes that are bolted to the underside of the web of the base beam. The tubes act as guides for the springs. Rods extend through the middle of the springs and the holes in the base beam. Plates are attached to the bottom of the rods to act as supports for the springs. A needle beam is attached to the upper end of the rods as indicated in Fig. 1. The needle beam serves to transfer the load from the springs to the test specimen at the desired loading points. Plates with holes at their centers are welded to the top of the needle beam symmetrically about the mid-span to provide a connection for the spring rods. The needle beam is guided in a vertical plane between two channels to insure that the needle beam remains in the vertical plane of the test specimen.

The concrete test beam is supported by two reaction cells, 63 inches center-to-center, that are connected to the top of the vertical support columns. The columns are braced by angles fixed to the flange of the column and the web of the base beam.

The reaction cells (Fig. 2) consist of 9 inch lengths of 6 inch diameter double extra strong steel pipe welded to base plates. The base plates are clamped to flat plates welded to the top of the support columns. Only one reaction cell is instrumented to record vertical load.

The load is applied to the specimen at the third points by rods acting through two load cells. One load cell is instrumented to record the variation of load with time; the other is used as a trigger for the oscilloscope. The recording load cell is the same one used successfully by Stewart[4] and Wadlin[5]. A complete description of the cell is found in their reports. The cell consists of a 9 inch length of double extra strong 6 inch diameter pipe. The pipe is cut longitudinally and a 11-1/2 inch by 1/2 inch steel plate is welded into the cut. Two 6 inch long, 2 inch diameter pipes are welded to the ends of the plates through which the loading rods from the needle beam pass. The loading rods are bolted in place against the 2 inch diameter pipes. Fig. 3 shows a photograph of the recording load cell.

The other loading cell contains the mechanism for the oscilloscope trigger. The cell consists of a piezoelectric crystal mounted in a bearing that protects the crystal during testing (Fig. 4).

Each load cell is connected to the needle beam by two rods. The upper ends of the rods are attached to the cell in the manner shown in Figs. 3 and 4. The lower end of the rods are attached to the inside of a 4 inch diameter pipe that formed a part of a yoke around the needle beam.

To activate the machine the springs are compressed against the web of the base beam by raising the needle beam with two hydraulic jacks. When the needle beam is at the proper height, determined by a strain reading taken on the spring rods, a 20 ton railroad quick action track jack is inserted between the needle beam and the base beam. The load is then transferred from the hydraulic jacks to the track jack. The loading cells are properly positioned on the specimen and the connecting rods tightened. The hyraulic jacks are removed and wood blocking inserted in their place to stop the travel of the needle beam after the specimen is destroyed. When the trigger on the track jack is released the load from the springs is transferred to the specimen at a rapid rate.

The machine is versatile in that the loading magnitude can be varied by changing the height of the needle beam and/or changing the position of the loading cells. For tests reported in this report, only third point loading was used. Fig. 5 shows typical views before and after a test.

Instrumentation

Recording of Data: - Data from the dynamic tests are obtained from three sources:

1. Measurements of load and reaction from oscilloscope signals.
2. Review of the high speed camera film.
3. Measurements of deflection by a rotating drum deflection recorder placed at the third point (loading point).

Load and Reaction: - In the earlier stages of the investigation an attempt was made to measure loads and reactions using piezoelectric crystals. This method was abandoned after it was found to be unsatisfactory. A ring type load cell, described earlier, was used in its place. The crystal was retained, however, for the oscilloscope trigger signal.

The recording load cell, as previously mentioned, was used successfully before and is shown in Fig. 3. The cell is sliced into three segments so that the strain in any one section is increased if the load is entirely in that section. In this study, the center section is always used. Strain gages (Budd C-144 foil gages) are mounted on the outside of the cell to form a four arm Wheatstone bridge circuit. One gage is placed on each of the opposite ends of a horizontal diameter of the cell, in the tensile zone, and two gages placed in a similar manner on opposite sides of a vertical diameter, in the compression zone. The gages are connected to an Ellis BAM-1 Bridge Amplifier which, in turn, is connected to a channel of a Tektronix 502-A Dual Beam Oscilloscope. The Wheatstone bridge circuit is balanced by adjustment of the amplifier. When load is applied the bridge is unbalanced and registers on the oscilloscope.

The magnitude of the bridge unbalance indicates the amount of load applied to the cell.

The reaction cell functions the same as the load cell. The reaction cell has strain gages placed on the inside and outside of the cell in the tensile and compressive zones (Fig. 2). The gages are wired into a Wheatstone bridge circuit connected to another BAM-1 amplifier and the other channel of the oscilloscope. Fig. 6 shows the schematic wiring diagram for both load and reaction.

The BAM-1 bridge amplifier is a useful part of the instrumentation. Not only does it supply power to the bridge and amplify the resulting signal, but it has a built-in circuit which permits one to calibrate the cells without removing them from the dynamic testing machine.

The trigger for the oscilloscope is activated by voltage originating from the piezoelectric crystal when the load is applied. This voltage is sent to the external trigger channel of the oscilloscope trigger system and causes the dual beams to sweep. The beams are set to sweep one time at the rate of 25 millisec/cm. These traces are photographed by a Polaroid camera mounted on the face of the oscilloscope with an open shutter.

High Speed Camera: - A Kodak 16 mm high speed camera with an f 2.0 high speed lens was placed 35 feet from the plane of the specimen to photograph the action of the beam during dynamic testing. Originally the camera was only intended to provide a pictorial record of the action of the beams; however, it was later used to obtain an estimate of the angular rotation of the beams. A horizontal black line is marked on the side of the specimens and changes in rotation are measured with reference to this line. Figs. 7, 8, 9, 10, 11 and 12 show typical views of beams during a test. The film, DuPont 931-A Rapid Reversal, is set to run in the camera at approximately 1,000 frames/sec. At this rate of film speed it is necessary to place ten 500 watt photoflood lights 4 feet from the plane of the specimen for proper illumination.

Deflections: - Deflections are recorded only at the location of the load cell. Having the load and deflection at this point makes it possible to calculate the energy input to the beam. The deflection recorder consists of a 6 inch diameter aluminum drum rotating about a vertical axis with a known constant velocity. The drum is placed above the specimen. The upper end of a rod protruding from the beam is attached to a spring loaded pencil scriber fitted with a ball and socket joint. The pencil scriber is guided to move in a vertical path. The lower end of the scriber rod is attached to a wooden block that had been previously glued to the side of the specimen. By this connection, actual beam defelctions are measured directly on the drum. Fig. 13 shows a picture of the device.

Concrete Beam Specimens: - The bulk of this report deals with the results obtained from the third of three series of beams. The beams of the first and second series were used to perfect the instrumentation and observe the behavior of the specimens in order to improve design of the final test beams. The beams of the first series were reinforced solely with No. 6 bars and minimal diagonal tension reinforcement. The tests on these beams indicated that the effect of changing the size of the reinforcement should be investigated. This was done in the third series and is reported in what follows.

The concrete specimens used in all tests were 72 inches long, 4 inches wide, 6 inches deep and supported on a clear span of 63 inches.

There was a total of 20 beams cast; 10 fiber reinforced and 10 plain. All beams had tensile reinforcement. Six were reinforced with one No. 5 bar, eight reinforced with one No. 6 bar, and six reinforced with a No. 7 bar. All reinforcement was intermediate grade except one No. 7 bar which was A 432-59T hard grade reinforcement. All plain beams had diagonal tension reinforcement consisting of No. 3 bars at 2 inch centers. The diagonal tension reinforcement for the plain beams is shown in Fig. 14. Fig. 15 shows pertinent details of a beam. Seven of the fiber reinforced beams had diagonal tension reinforcement of No. 3 bars spaced at 6 inches. The remaining three fiber reinforced beams had no conventional diagonal tension reinforcement.

The beams were cast in groups of four and six using gang forms. Ingredients for the mix were 2.45 parts sand, 1.0 part cement and 0.55 parts water by weight and 2 per cent fiber by volume for the fiber reinforced beams. River sand was used as the only aggregate. The sand was dried and sifted through a screen that would pass particles smaller than 0.05 inches.

The steel fibers used in these studies were 0.5 inch lengths of 0.006 diameter brass coated cold drawn wire. The wire was supplied by the National Standard Company of Niles, Michigan.

The concrete was mixed in a 3 cubic foot rotary drum mixer. The plain beams were mixed in the conventional fashion, poured into the forms and vibrated with an electric immersion-type vibrator. The fiber reinforced beams had to be poured using the following method. The sand and cement were mixed dry in the mixer after which about 80 per cent of the water was added. This made a rather fluid mortar mix. The wires were then added by sifting them through a sieve with 1 inch openings. The wires were added in intervals, allowing each interval to mix thoroughly before the next batch of wires was added. As the wires were being added the remaining 20 per cent of the water was added to keep the mix sufficiently fluid. After the wires were in and mixed thoroughly, the concrete was poured into the forms and vibrated as before. All beams were stripped of their forms after 24 hours and placed in a moisture room for a 28 day moist cure. Fig. 16 shows typical compression stress-strain curves for plain and fiber concrete after a 28 day moist cure.

TEST PROGRAM AND PROCEDURES

Testing Program

Identical specimens of plain concrete and fiber reinforced concrete were tested at the same dynamic load. Static tests were performed on identical specimens as a comparison.Table I summarizes the beams and the type of test performed on them. All dynamic tests were performed with an initial total spring load of 14,000 pounds.

Test Procedure

The sequence of operations for a dynamic test is as follows:

1. Load and reaction recording cells are checked to insure all bridge circuits are functioning properly.
2. The reaction cells are secured on the support columns.
3. The specimen is placed on the reaction cells.

4. The initial zero load readings are taken from strain gages on the spring rods.

5. The hydraulic jacks are inserted and the needle beam raised to its proper height.

6. The track jack is centered and the load transferred from the hydraulic jacks to the track jack.

7. The load cells are positioned on the specimen and the rods connecting the cells to the needle beam are tightened.

8. The pencil scriber is positioned and the rod of the scriber attached to the wooden block on the specimen.

9. The proper settings are made on the oscilloscope (intensity, sweep rate, etc.)

10. The track jack trigger is set and wood blocking put into place. This blocking is positioned to permit a deflection of 6 inches before the needle beam would be stopped.

11. The bridge circuits were balanced.

12. On the given signal, the lights, high speed camera, and deflection recorder are started.

13. After 25 feet of film passes through the high speed camera, a circuit breaker in the camera sets off a flash bulb that is visible to the operator of the track jack. The flash is the signal for the jack operator to pull the trigger lever. The delay between the start of the camera and the flash is about 1 second. This time delay is necessary to permit the camera to reach a constant speed of about 1,000 frames/sec.

14. When the track jack is triggered, the springs expanded and applied the load to the specimen. All of the action recorded is within 0.1 second.

ANALYSIS OF DATA

Load and Reaction as a Function of Time

The variations of load and reaction with time is shown in Figs. 17 to 25. These figures were obtained from the Polaroid photographic record and scaled to the size shown by use of a pantograph. It is seen from these figures that, in general, for beams made of the same type of concrete, the initial behavior is essentially the same regardless of the size of reinforcement. By examining the curves for all the beams, one observes that the initial maximum load was reached in about 0.005 to 0.008 seconds, after which the load decreased as the beam responded. Also to be noted is the smaller peak that occurs at about 0.003 seconds. At this time the load is about 3,000 pounds and then drops off slightly. This smaller peak is due to the beam accelerating away from the load that has just come on to the beam. The load, however, catches up with the beam and is again increased.

By comparing beams reinforced with the same size of bar, but made of different concrete, it is seen that the behavior of the load is about the same for the first 0.020 to 0.025 seconds. After this time, the plain beams fail in compression and all load is lost (see Figs. 26a, b, c). The fiber reinforced beams on the other hand, continue to support the load, executing diminishing oscillations, until the beam stops at some final residual load. The significance of this result is that the internal resisting capacity of the fiber beams is higher than that of the plain beams, evidenced by the fact that the fiber beams were able to stop the motion of the load. The fiber beams, even though damaged considerably, were able to maintain their structural integrity (Figs. 27a, b, c). For a summary of residual loads, see Table II.

The reactions varied essentially in the same manner as the loads. It was reported by Stewart[4] and Wadlin[5] that during the initial phase of the loading there was a significant difference between the magnitude of the load and reaction due to the beam's acceleration. This difference is due to the inertia of the beam. In this testing program a great difference between load and reaction was not observed. This can be attributed to the fact that the mass of the specimens in this program is considerably smaller than the mass of specimens used in the Stewart and Wadlin programs.

Deflection versus Time

The variations of deflection at a load point as a function of time is shown in Figs. 28 to 32. It can be seen from these graphs that, in general, the deflections were the same for the first 0.005 seconds for beams reinforced with the same size bar. At this time the peak load was applied to the member. After the load reached its peak value, however, deflections begin to differ. In every case the deflections of the plain beams continue to increase, while the fiber beam deflections cease at a final static deflection. This behavior demonstrates that the fiber beams are able to absorb all the kinetic energy of the beam and bring its motion to rest.

Load versus Deflection

The load-deflection curves, Figs. 33 to 47, have been plotted for beams tested both dynamically and statically. All beams not destroyed in the dynamic tests were statically tested to destruction. The static tests were all conducted with third point loading. The area under these curves is a measure of the work done on the beam during the test. Table III summarizes the work done up to a deflection of 5 inches at the third point. This deflection was chosen because it was the maximum deflection of beam 25F which was used as a reference. From the tabulation, it is seen that the work done on the fiber reinforced beams significantly exceeds the work done on the plain beams.

Static Tests

One of the most significant results of the testing was obtained from the static bend tests. After the dynamic tests were concluded, two fiber reinforced beams reinforced with a No. 5 intermediate grade steel bar, 25F and 15FS, were placed in a universal testing machine and statically tested. As the load was applied, and the reinforcing bar strained past its yield point, large cracks were opened in the tensile side of the beam but there was no sign of an ensuing compressive failure in the top of the beam (Fig. 48). The load was continuously applied until the reinforcing bar broke, leaving the concrete in the compression zone intact. This same behavior was also duplicated with one of the fiber reinforced beams reinforced with a No. 6 intermediate grade bar and a fiber beam, tested only statically, reinforced with a No. 5 intermediate grade bar. This behavior is in contrast to that of plain concrete beams. When the steel yields in a plain concrete beam, the stresses in the compression zone increase to the ultimate value for the concrete and the compression zone crushes out of the beam. However, with the fiber beams, even though the stresses are again increased to the maximum value as in the plain concrete (assuming the same compressive strength for both concretes), the fiber concrete will continue to support this stress and not crush out of the beam. The concrete, by remaining in place, provides a fulcrum around which the reinforcing steel can be continuously strained to a higher level. Fig. 49 shows photograph of the broken bar in beam 25F.

It was not possible to break any additional reinforcing bars, but it was observed that even when the compression zone failed, it was a gradual yielding and not a sudden movement. This trend can be seen on the load deflection curves where the loads on the fiber reinforced beam are seen generally to gradually decrease as the deflection is increased.

As further eveidence that the fiber reinforced concrete beams would permit higher steel strains, a fiber reinforced beam was cast with one No. 7, A 432-59T reinforcing bar. The yield point for this bar was 69.5 ksi as determined from a tensile coupon test. Fig. 50 is the A 432-59T stress-strain diagram and a typical intermediate reinforcing bar stress-strain diagram. The beam was tested dynamically in the same manner as all other beams and later statically tested to destruction. The results of these tests are shown in Fig. 53, which is a plot of moment versus rotation. The values of ϕ were obtained from the high speed camera record by projecting the film on to a large screen and measuring the change in angle made between two tangents of a reference line painted on the beam.

We see that the beam supported a maximum moment of 238 inch-kips. It was observed during the static tests that the compression zone in the latter stages of loading was approximately 1.75 inches deep. Using this value, and assuming the compressive stress distributed uniformly over this depth, one can calculate the stress in the reinforcing bar by considering the internal couple, i.e., (Refer to Fig. 51)

$$M = T \cdot X$$

therefore,

$$T = M/X = 238/4.02 = 59.2^{k}. \ . \ . \ . \qquad (1)$$

$$f_s = T/A_s = 59.2/0.6 = 98.5^{ksi} > 69.5^{ksi}. \ . \ . \ . \qquad (2)$$

Therefore, to sustain this moment the reinforcing bar is stressed well beyond its yield point. The maximum ultimate moment of a similarly designed plain beam can be calculated from the ACI[6] equation

$$M_u = \phi[bd^2 \ f'_c \ q(1 - 0.59 \ q)]. \ . \ . \ . \qquad (3)$$

for

$$f'_c = 8{,}000, \ \phi = 0.9, \ f_y = 70^{ksi}, \ d = 4.90, \text{ and } b = 4.0$$

$$q = \frac{A_s \ f_y}{bd \ f'_c} = 0.262$$

substituting, we find

$$M = 155 \text{ inch kips}$$

Therefore, the maximum moment a plain beam could support would be 155 in · kips, much less than the 238 in · kips of the fiber reinforced beam.

To evaluate the effectiveness of the fiber reinforced concrete one can calculate the amount of steel necessary to sustain a 238^{in-k} moment in a plain beam. Solving Equation (3) for A_s it is found that the required steel area is 1.90 in^2. This is more than three times the steel area (0.6 in^2) used in the fiber reinforced beam.

Moment-Rotation Relationship

Curves of moment versus rotation (Figs. 52-57) were plotted to obtain a measure of the amount of energy absorbed by the specimens. The areas under these curves is a measure of the energy absorbed by the beams. The energy was measured up to a total angle change of 0.460 radians, the value at which the bar in Test 25F broke. Table IV summarizes the data. From the values shown in the tabulation it is seen that for beams reinforced with the same size bar, the fiber reinforced beams absorb more energy than the beams using plain concrete.

The Effect of Shear

It was mentioned earlier that the first two casts of specimens were made with a minimum amount of shear or diagonal tension reinforcement. Those of the first cast had no shear reinforcement and those of the second cast had No. 3 bars spaced at 6 inches. When these specimens were tested dynamically, all of the plain beams failed in shear, as expected, but none of the fiber beams. Close examination of the fiber beams showed very few shear cracks present while the specimen carried its residual load. The fiber beams of the third cast were then designed with some beams having shear reinforcement and others without shear reinforcement. The specimens were tested and no shear failures were observed. As an estimate of the average shearing stress resisted by a specimen, consider Beam 17F.

The maximum shearing load was 8,750 pounds. Therefore, the average shear shress is given by

$$\tau = \frac{P}{bd} = \frac{8750}{(4)\ (4.9)} = 444 \text{ psi} \quad . \quad . \quad . \quad . \qquad (4)$$

The maximum shearing stress was actually 1.5 times this value, or 666 pounds per square inch. The resistance of such a high shearing force is attributed to the increase in tensile strength of the concrete made possible by the addition of the steel fibers. The addition of shear reinforcement, however, did somewhat reduce the residual deflections of the fiber reinforced beams. Table V summarizes the final deflections for the dynamic tests.

DISCUSSION

The dynamic and static behavior of singly reinforced beams made with steel fiber reinforced concrete is markedly different than the behavior conventionally reinforced beams. The primary difference is in the ability of the fiber reinforced beam to resist high shear stresses without cracking (without the aid of conventional shear reinforcement) and the extent to which the compression zone remains intact through large angular distortions.

The latter attribute is of essential significance. To the author's knowledge, there have been no recorded instances where a steel bar, in a singly reinforced concrete beam of normal dimensions, has broken. The usual behavior--for under and over reinforced beams--is a breaking up, into fairly large pieces, of the compression concrete zone long before the steel bar could be strained to its breaking point.

This behavior is particularly significant when one considers the history of the engineering opinions regarding blast-resistant design. In the earlier days it was assumed that high strength (hard grade) steel reinforcing bars would be inadequate because of their relatively small ductility. One supposed that the greater unit volume energy absorbing capacity of structural grade steel would be reflected in a higher toughness of the reinforced concrete beam. Mavis and Greaves[7], however, demonstrated that whether one used structural grade or hard grade steel, the maximum steel strain at fracture was always less than ten per cent as a result of failure of the concrete in the compression zone. In other words, the weak link is the concrete---and the higher energy absorbing capacity of the structural grade steel is never realized.

The lesson learned from the data obtained to date in this study, however, is that the compression zone in beams made with steel fiber reinforced concrete develops its full compression load-carrying capacity and continues to remain intact through large angular deflections. Indeed, the behavior is very much like that of a plastic material. This ability to carry full compression through large angular beam distortion means that the ductility of the reinforcing rod is once more an item of extreme importance. In fact, the energy absorbing capacity of the steel reinforcing rod will be reflected in the ability of the entire beam to absorb energy.

Furthermore, one is now in the position to investigate the feasibility of using high strength steel rods or prestressing tendons as reinforcement. In conventional concrete design, the use of such steels is redundant because the high strains required to develop the strength of the steel could not be realized because of the brittleness of the compression zone.

CONCLUSIONS

1. Impulsive loading of the magnitude used in these tests does not cause sudden failure in the fiber reinforced beams such as the sudden failure observed in plain beams.
2. The internal resisting moment is significantly greater in the fiber beams and, therefore, permits the beam to absorb more energy. The beams retain their structural integrity and carry considerable residual load through a relatively large angular distortion.
3. In the event that the fiber concrete does fail in compression, the failure is not sudden but is preceded by extensive deformation.
4. The increased tensile strength of the concrete permits the use of fiber concrete without special shear reinforcement.

BIBLIOGRAPHY

1. Romualdi, J. P. and G. B. Batson, "Behavior of Reinforced Concrete Beams with Closely Spaced Reinforcement". Journal ACI, Vol. 60, June 1963.

2. Romualdi, J. P. and G. B. Batson, "Mechanics of Crack Arrest in Concrete", ASCE Engineering Mechanics Division, June 1963.

3. Romualdi, J. P. and J. A. Mandel, "Tensile Strength of Concrete Affected by Uniformly Distributed and Closely Spaced Short Lengths of Wire Reinforcement", Journal ACI, Vol. 61, No. 6, June 1964, pp. 657-671.

4. Stewart, J. J., "Effects of Impulsive Loads Upon Reinforced Concrete Beams", Ph.D. Thesis, Carnegie Institute of Technology, 1957.

5. Wadlin, G. K., "Impact Loadings on Pretensioned, Prestressed Concrete Beams", Ph.D. Thesis, Carnegie Institute of Technology, 1959.

6. ACI Building Code Requirements for Reinforced Concrete, ACI, p. 318-363.

7. Mavis, F.T. and M. J. Greaves, "Destructive Impulse Loading of Reinforced Concrete Beams", Journal ACI, Proc. V. 52, pp. 93-102, September 1955.

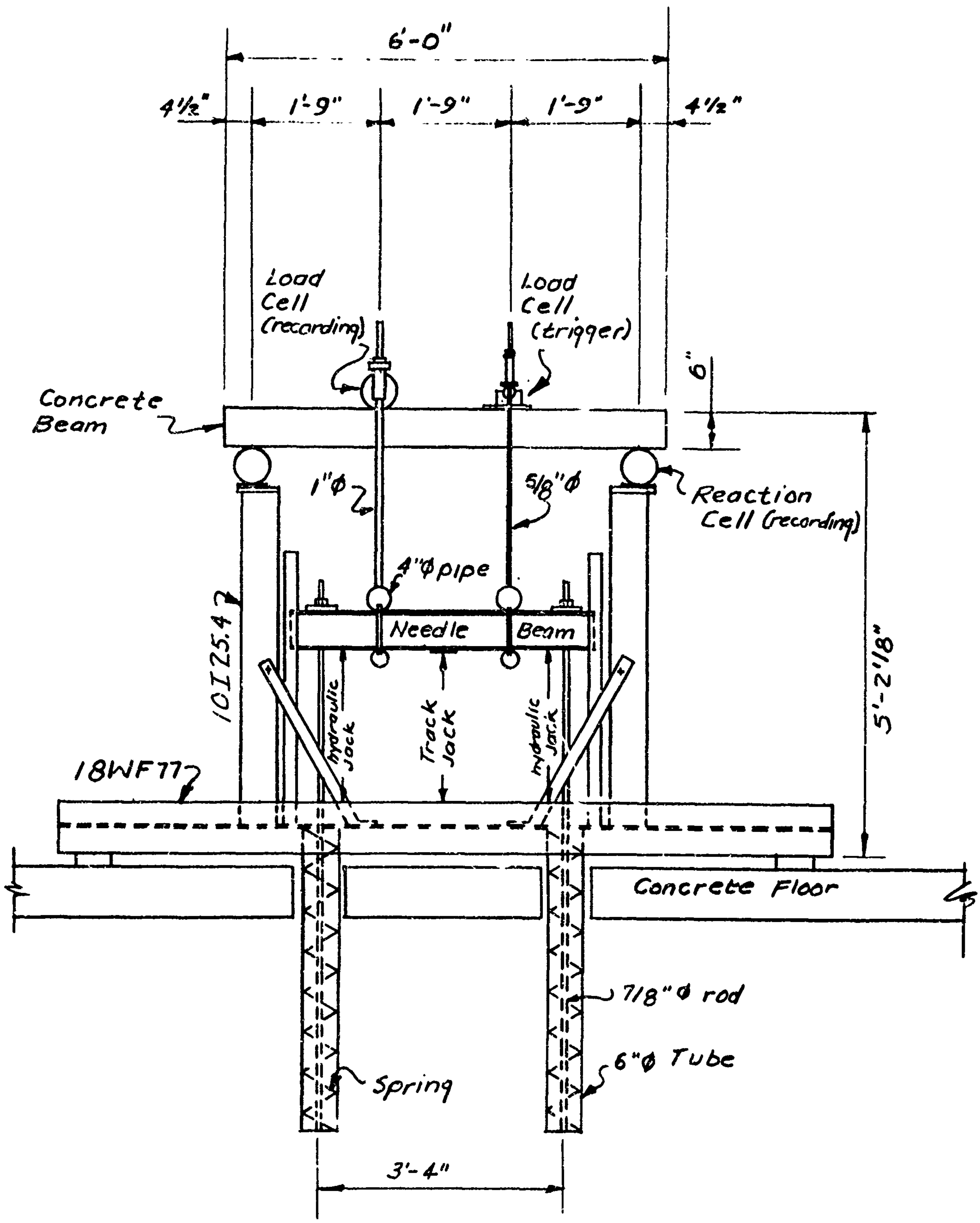

DYNAMIC TESTING MACHINE
Front Elevation (½"=1'-0")

FIGURE 1

REACTION CELL

FIGURE 2

RECORDING LOAD CELL

FIGURE 3

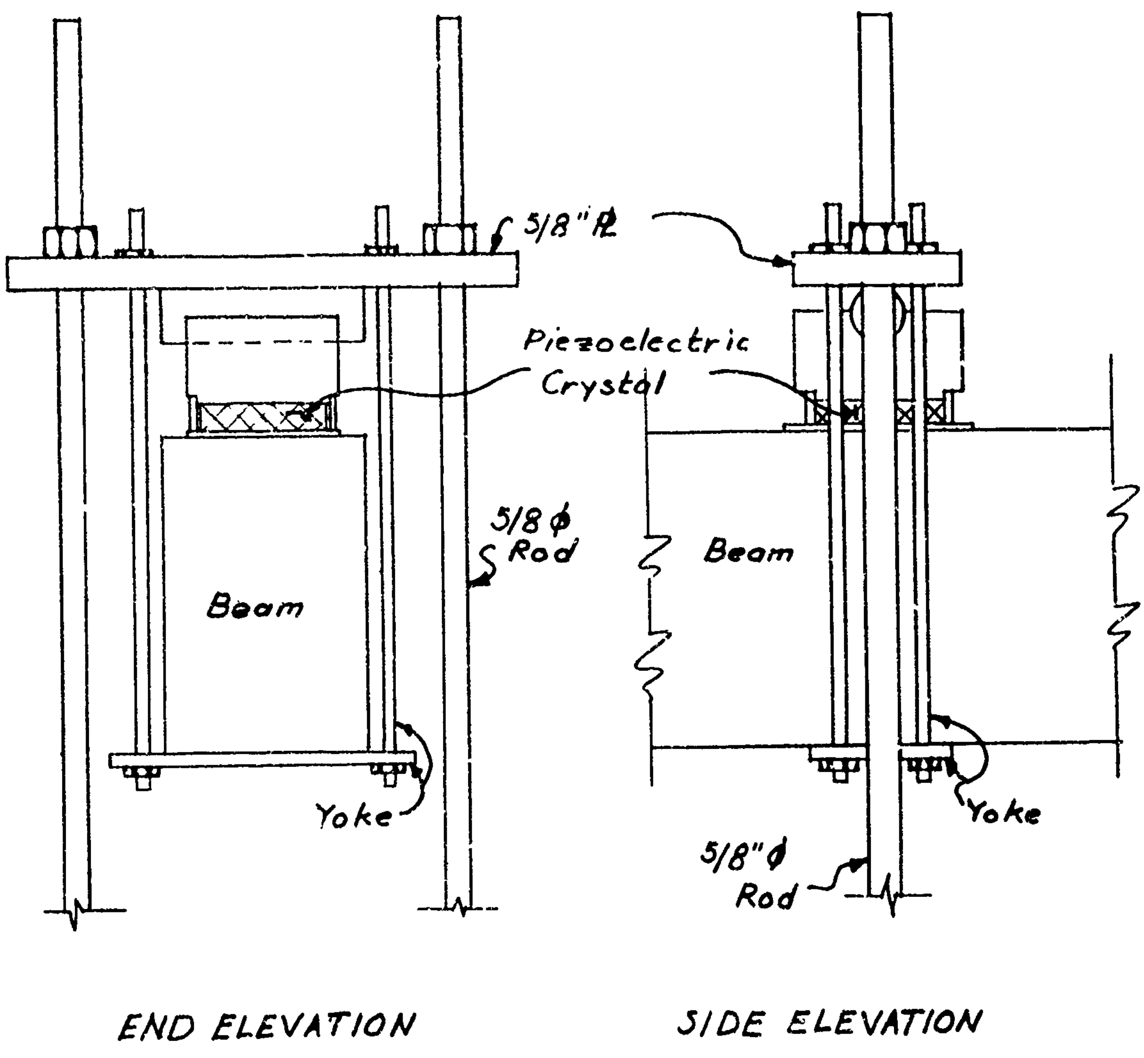

TRIGGER LOAD CELL

FIGURE 4

(a) TESTING MACHINE BEFORE TEST

(b) TESTING MACHINE AFTER TEST

FIGURE 5

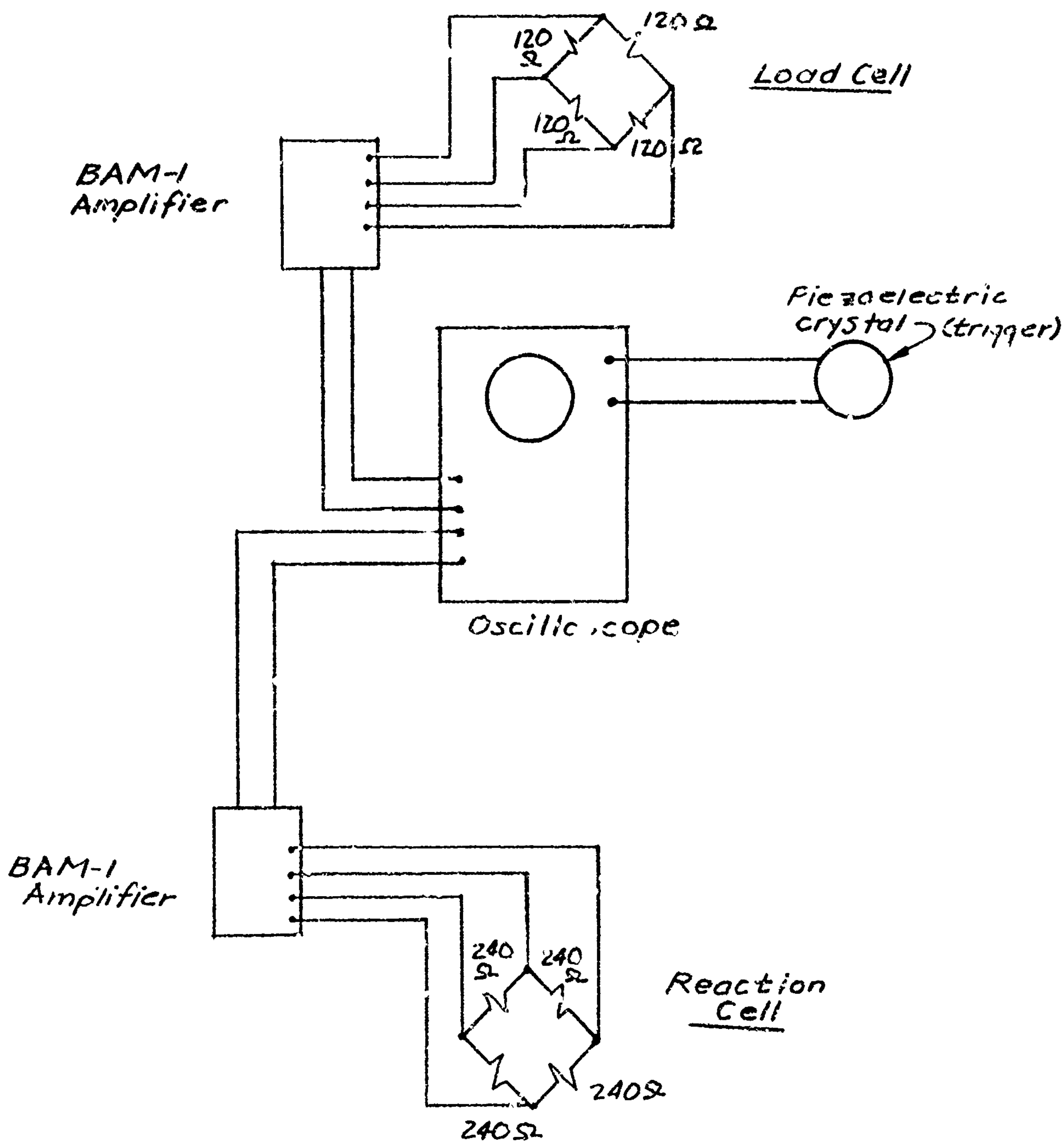

SCHEMATIC CIRCUIT DIAGRAM

FIGURE 6

(a) t = 0,018 seconds

(b) t = 0.054 seconds

(c) t = 0.207 seconds

FIBER REINFORCED BEAM
DURING DYNAMIC TEST
(1 No. 5 Bar)

FIGURE 7

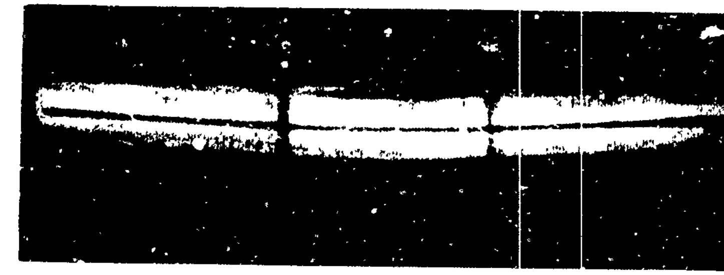

(a) t = 0.018 seconds

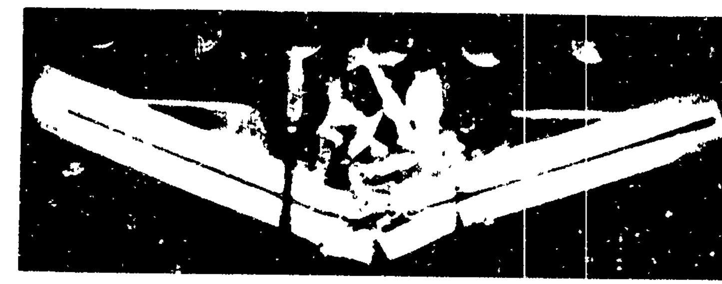

(b) t = 0.054 seconds

PLAIN CONCRETE BEAM
DURING DYNAMIC TEST
(1 No. 5 Bar)

FIGURE 8

(a) t = 0.018 seconds

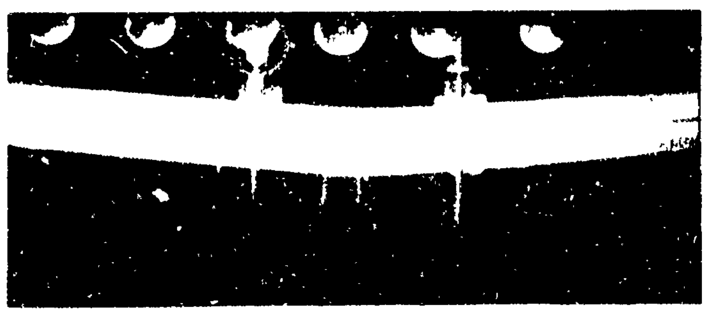

(b) t = 0.315 seconds

FIBER REINFORCED BEAM DURING DYNAMIC TEST

(1 No. 6 Bar)

FIGURE 9

(a) t = 0.018 seconds

(b) t = 0.063 seconds

PLAIN CONCRETE BEAM DURING DYNAMIC TEST

(1 No. 6 Bar)

FIGURE 10

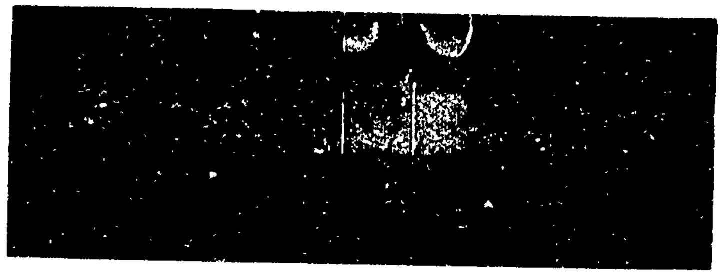

(a) t = 0.027 seconds

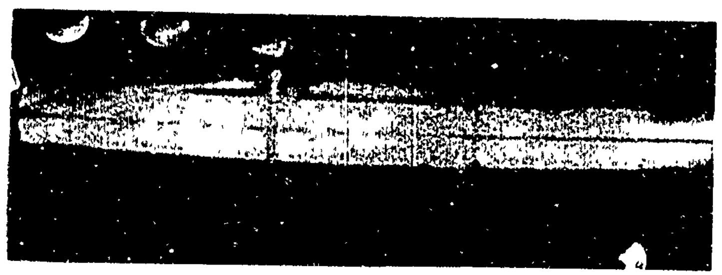

(b) t = 0.063 seconds

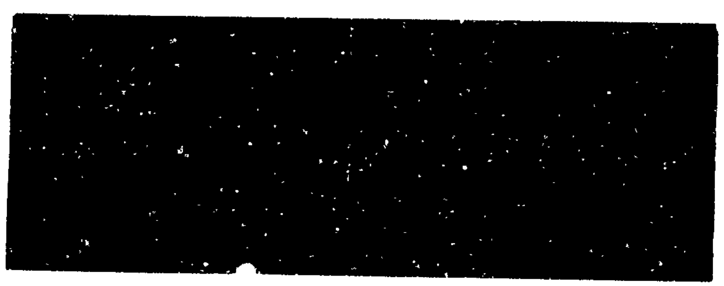

(c) t = 0.313 seconds

FIBER REINFORCED CONCRETE DURING DYNAMIC TEST

(1 No. 7 Bar)

FIGURE 11

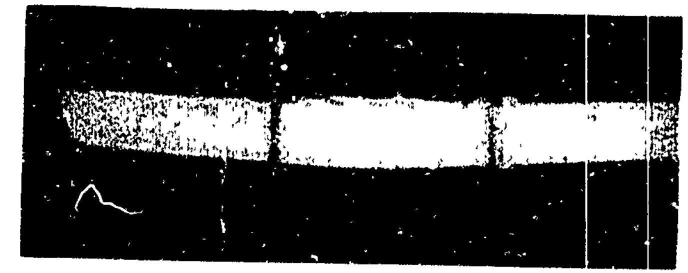

(a) t = 0.027 seconds

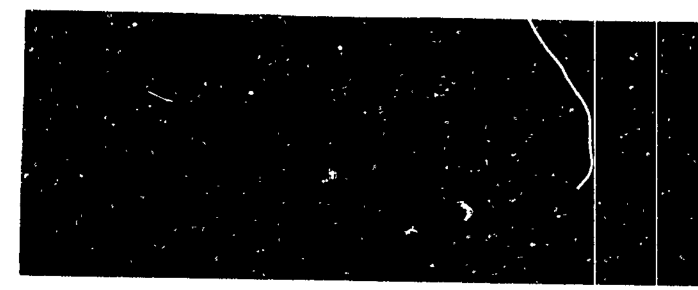

(b) t = 0.063 seconds

PLAIN CONCRETE BEAM DURING DYNAMIC TEST

(1 No. 7 Bar)

FIGURE 12

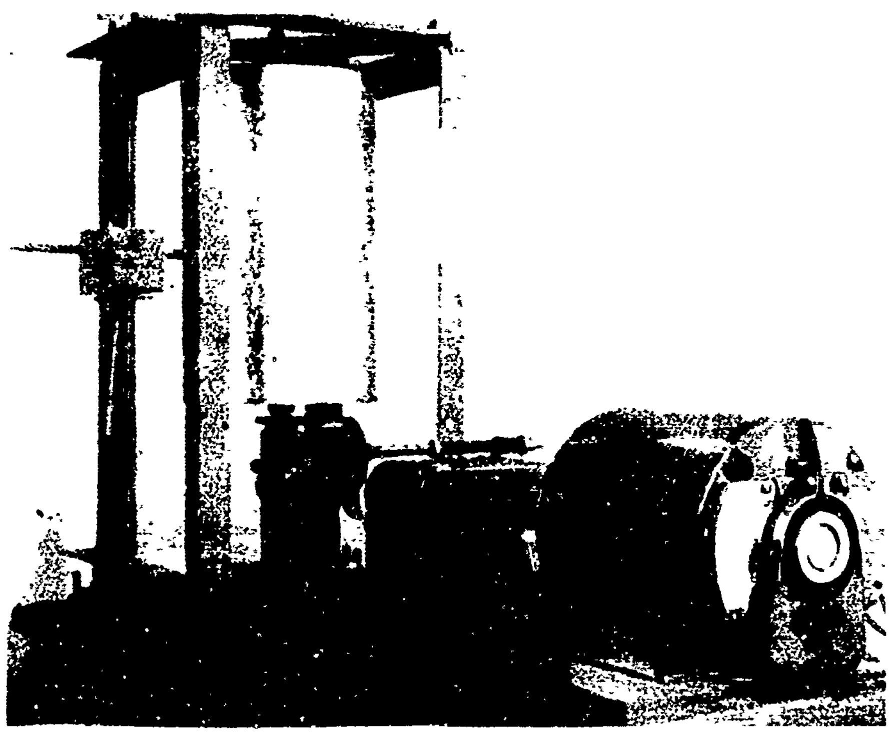

DEFLECTION RECORDER

FIGURE 13

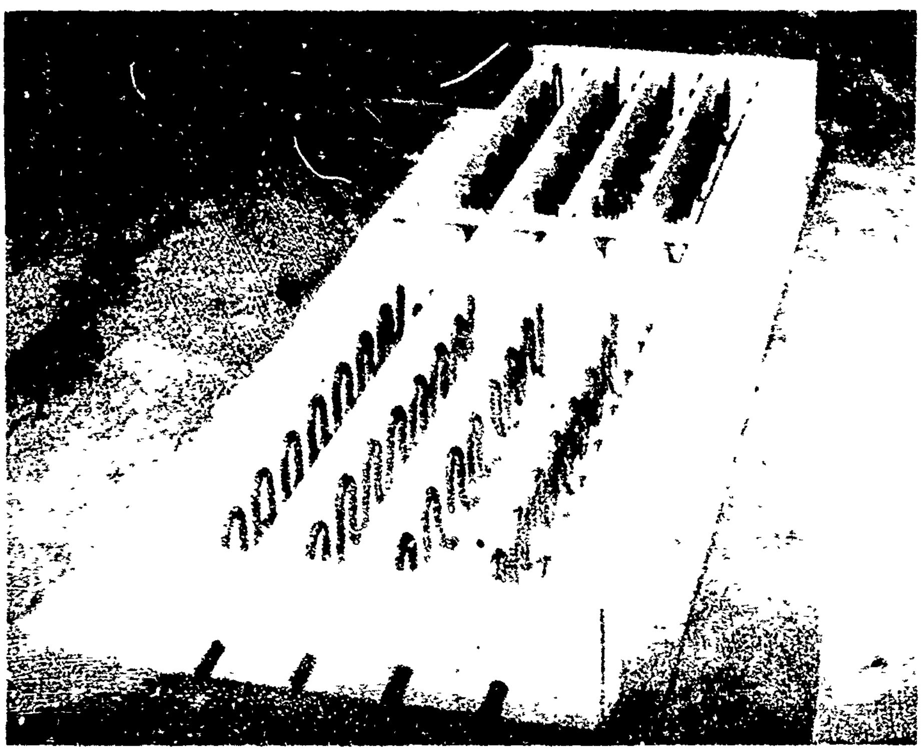

FORMS AND REINFORCEMENT
FOR PLAIN CONCRETE SPECIMENS

FIGURE 14

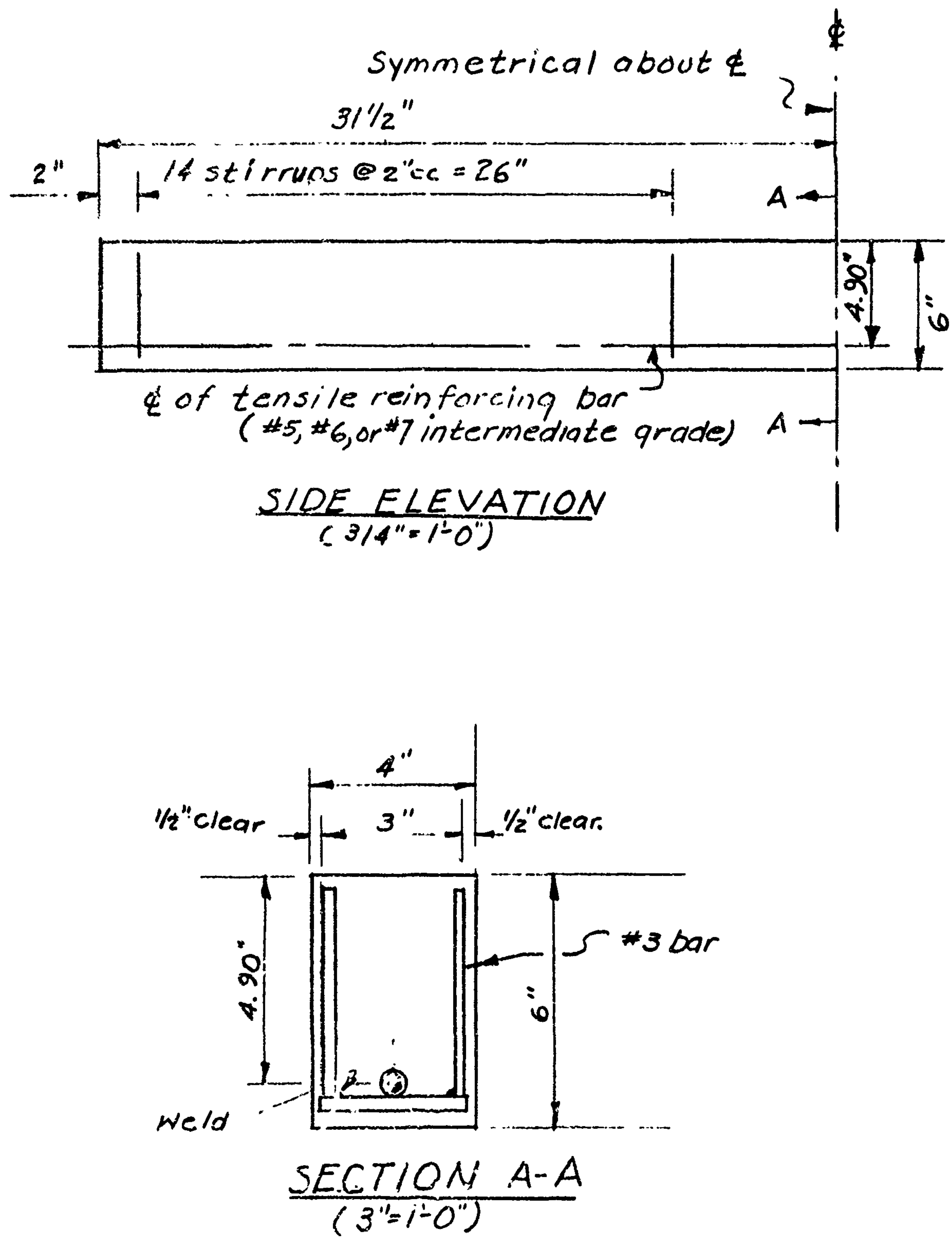

CONCRETE SPECIMEN DETAILS

FIGURE 15

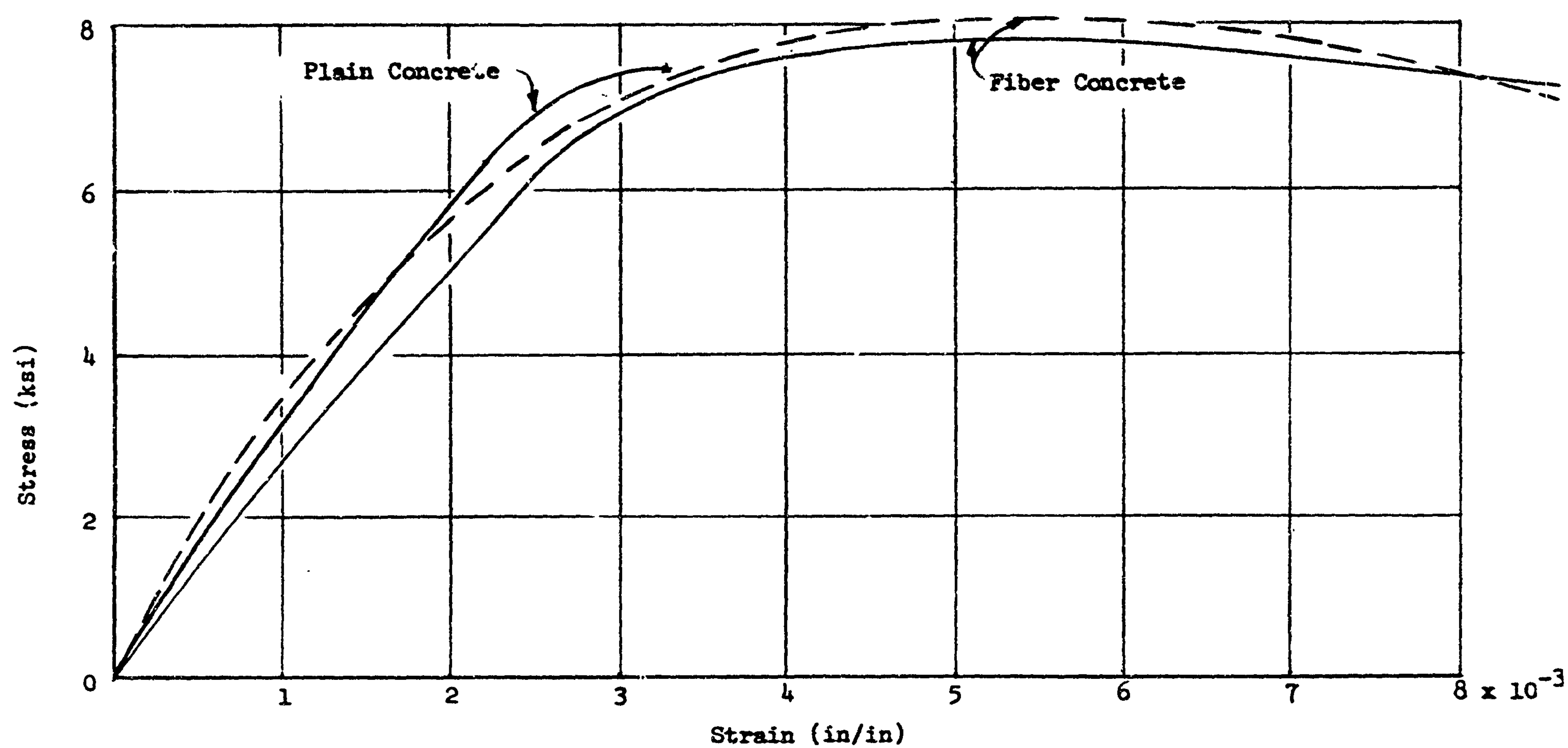

Fig. 16 COMPRESSION STRESS VS. STRAIN FOR PLAIN AND FIBER CONCRETE

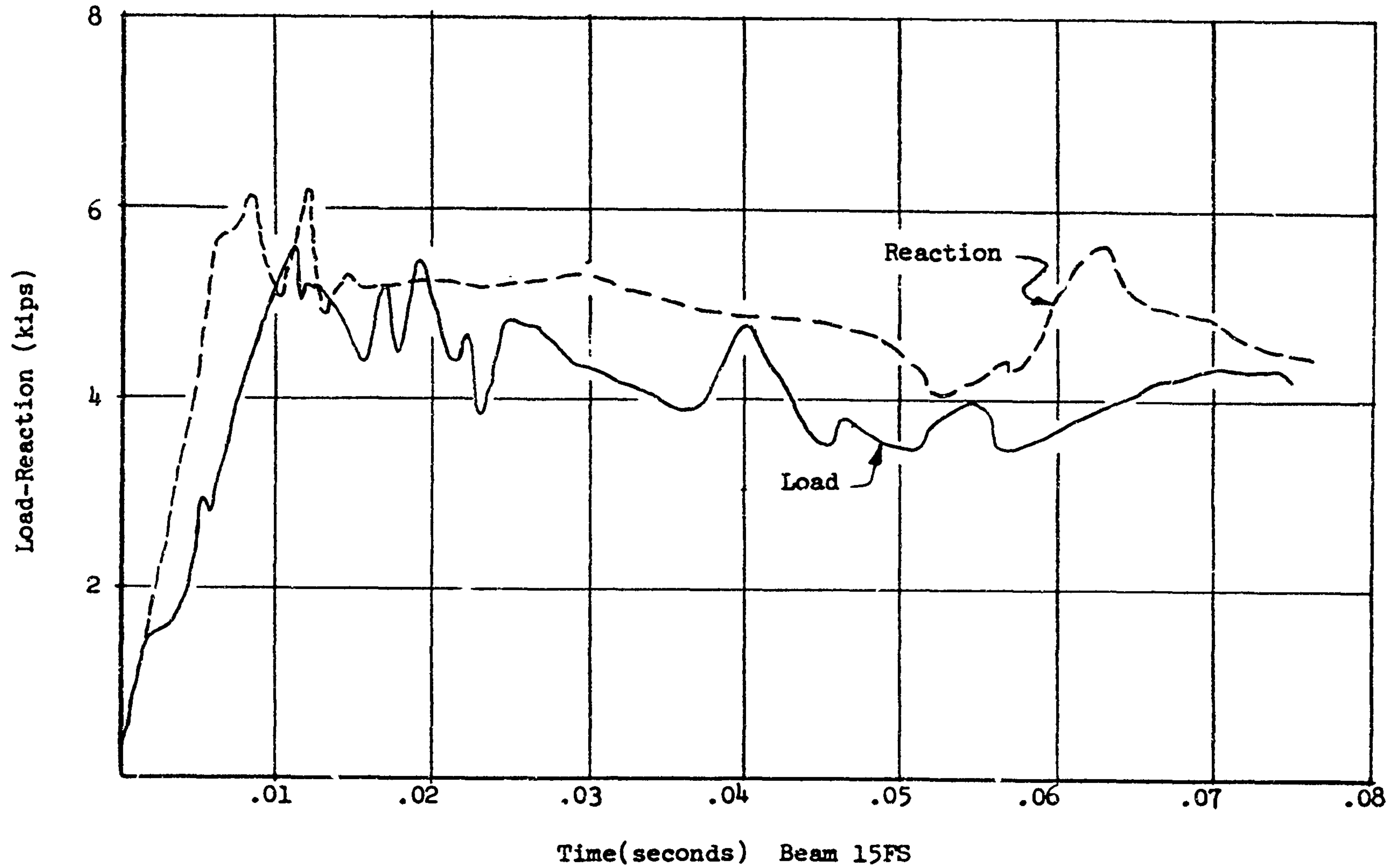

Fig. 17   THIRD POINT LOAD-REACTION VS. TIME

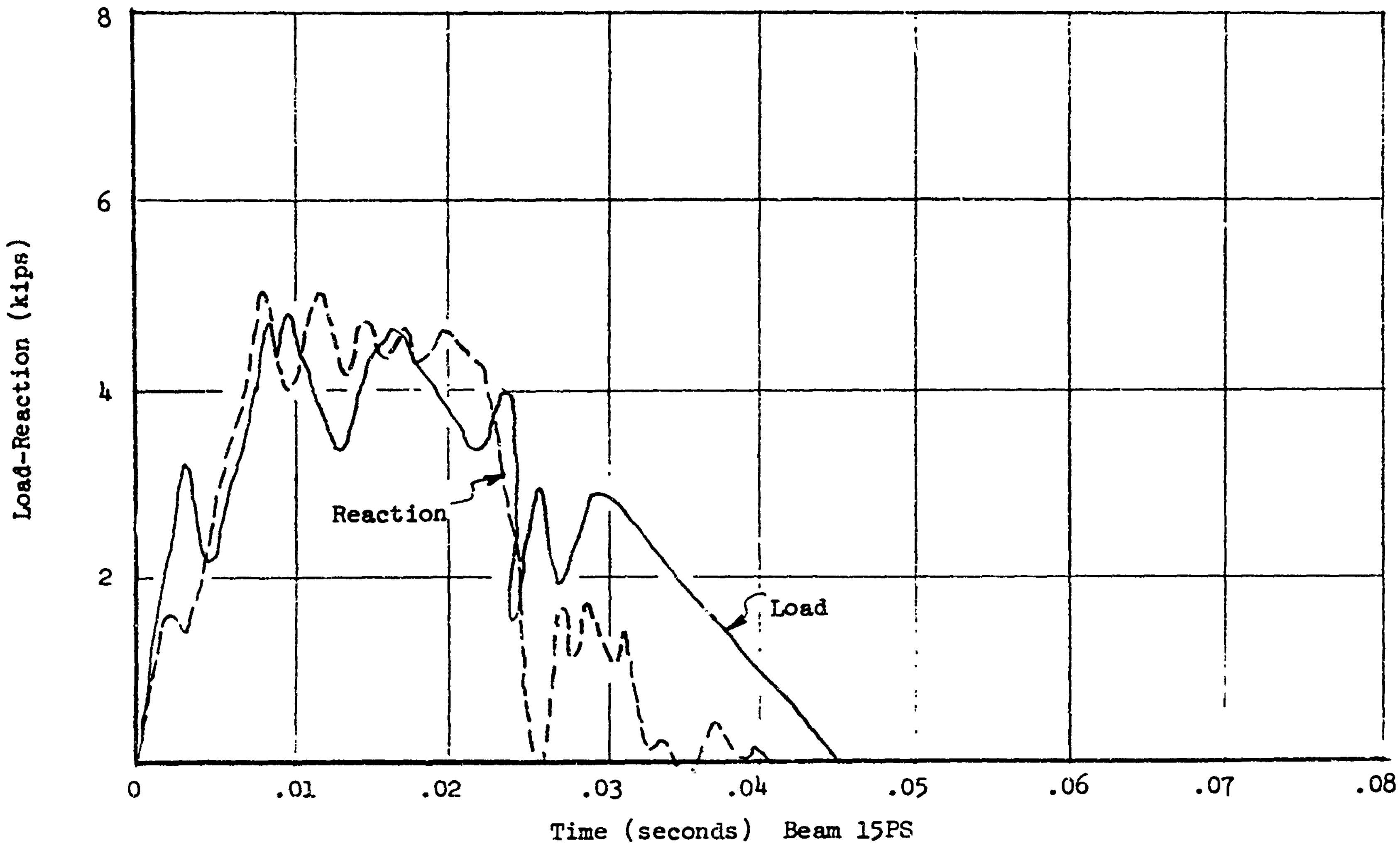

Fig. 18 THIRD POINT LOAD-REACTION VS. TIME

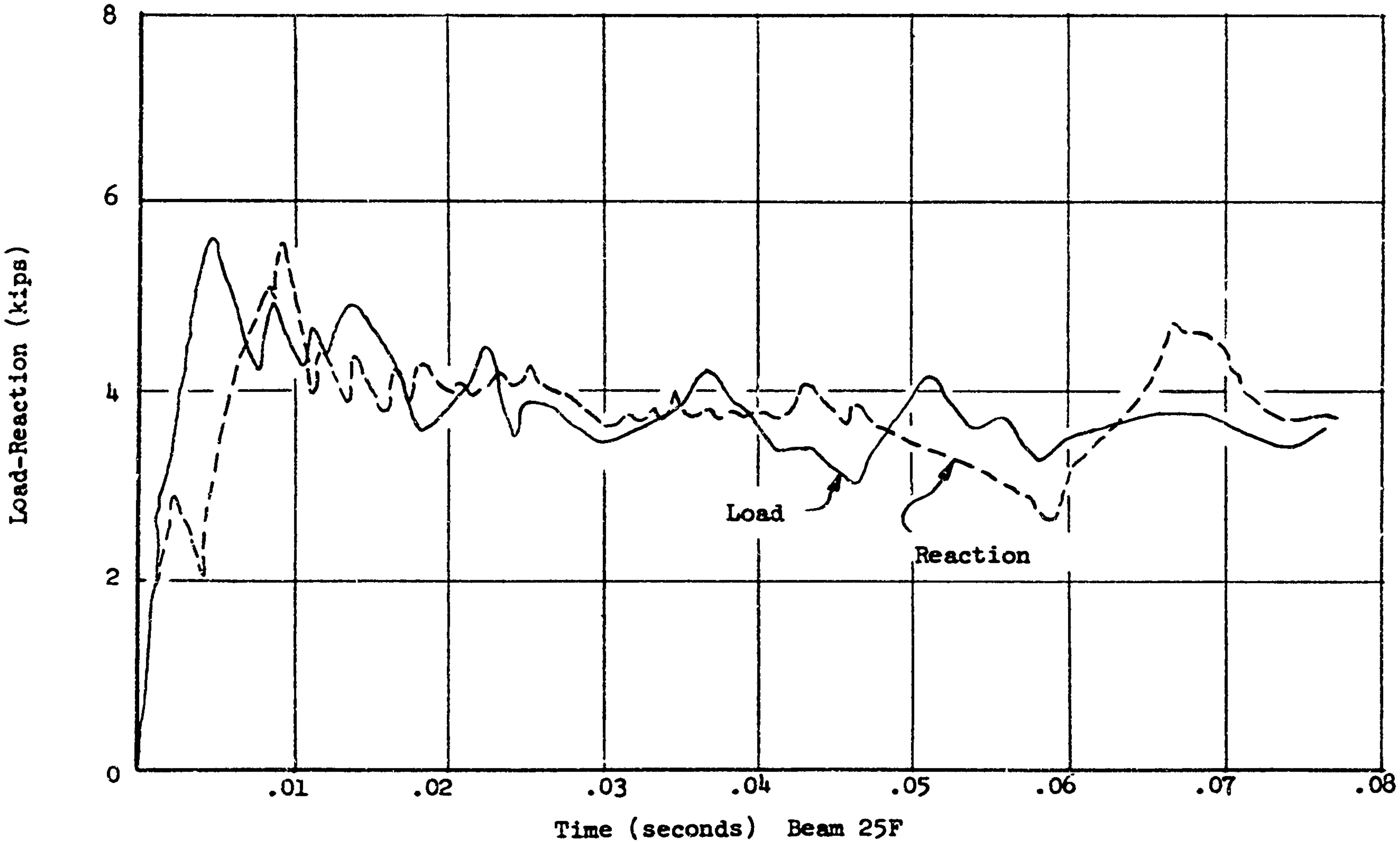

Fig. 19 THIRD POINT LOAD-REACTION VS. TIME

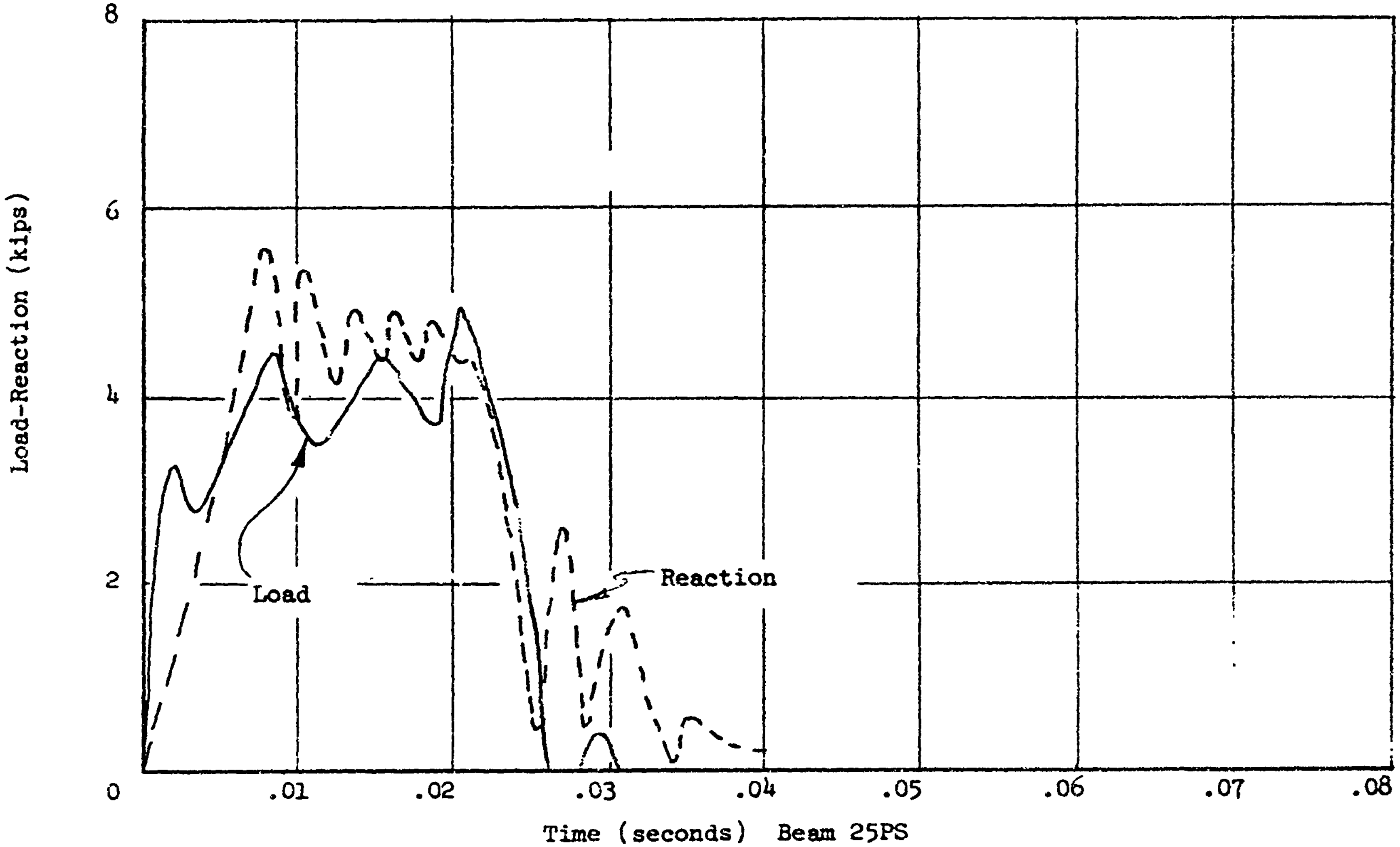

Fig. 20 THIRD POINT LOAD-REACTION VS. TIME

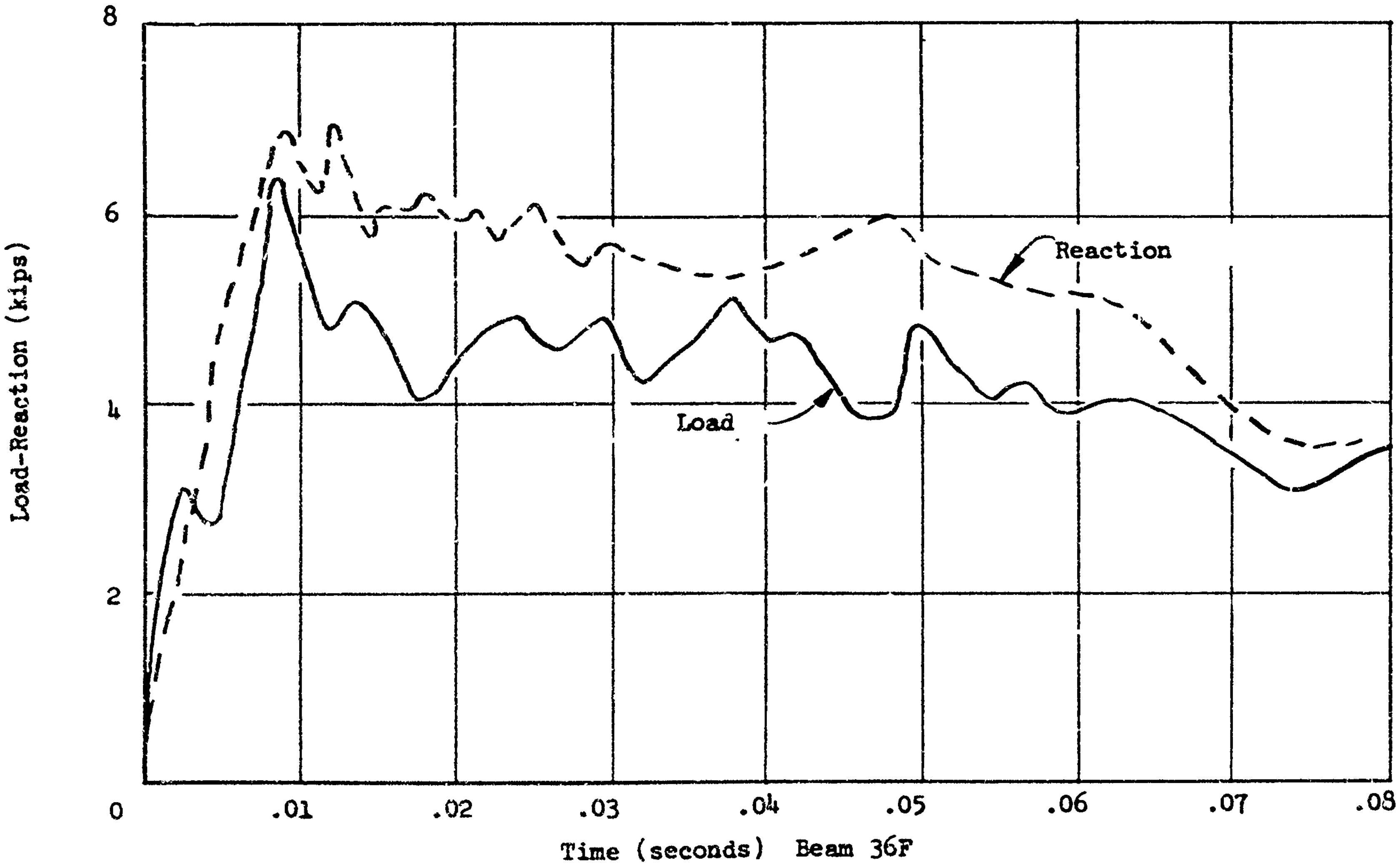

Fig. 21 THIRD POINT LOAD-REACTION VS. TIME

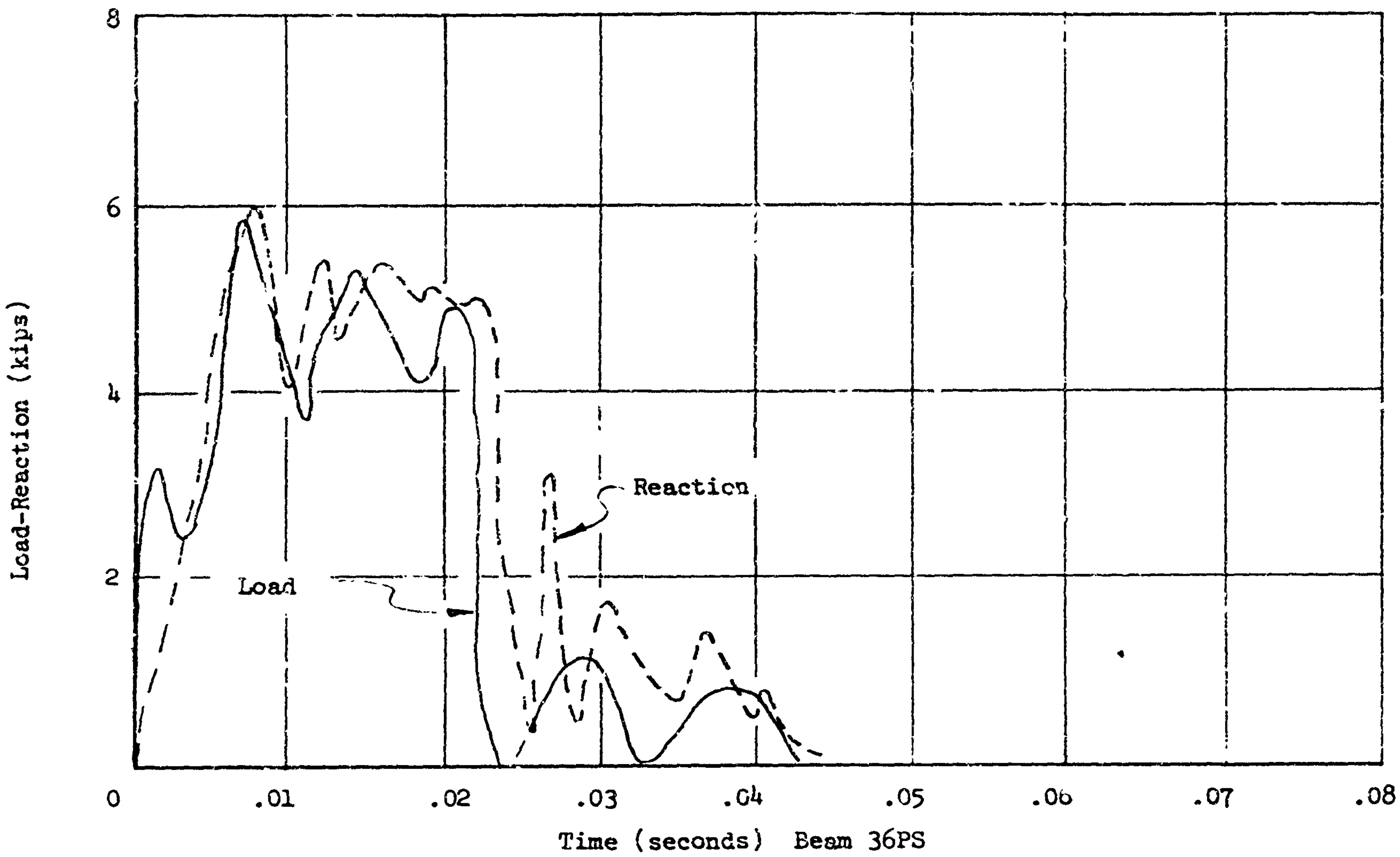

Fig. 22 THIRD POINT LOAD-REACTION VS. TIME

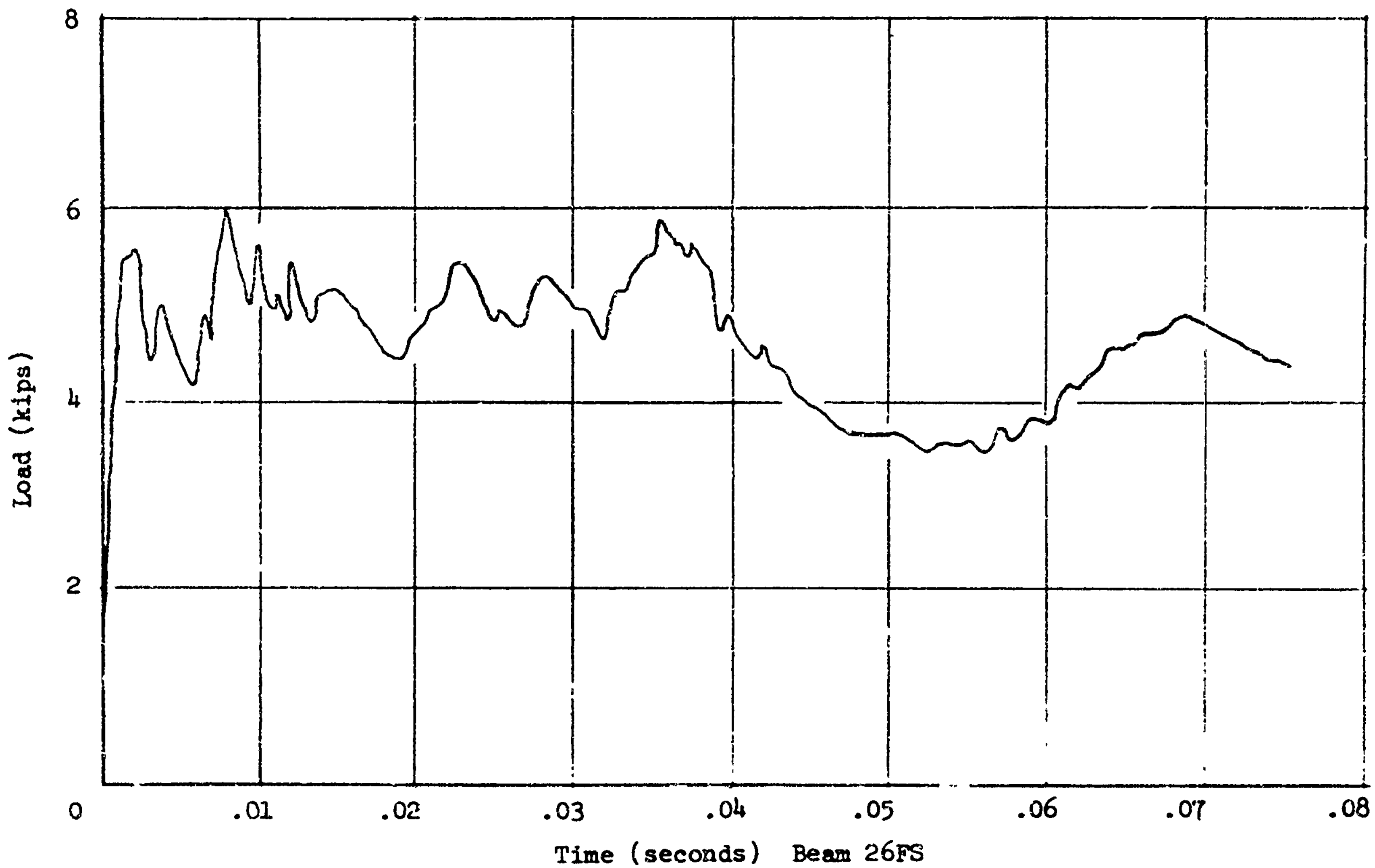

Fig. 23 THIRD POINT LOAD VS. TIME

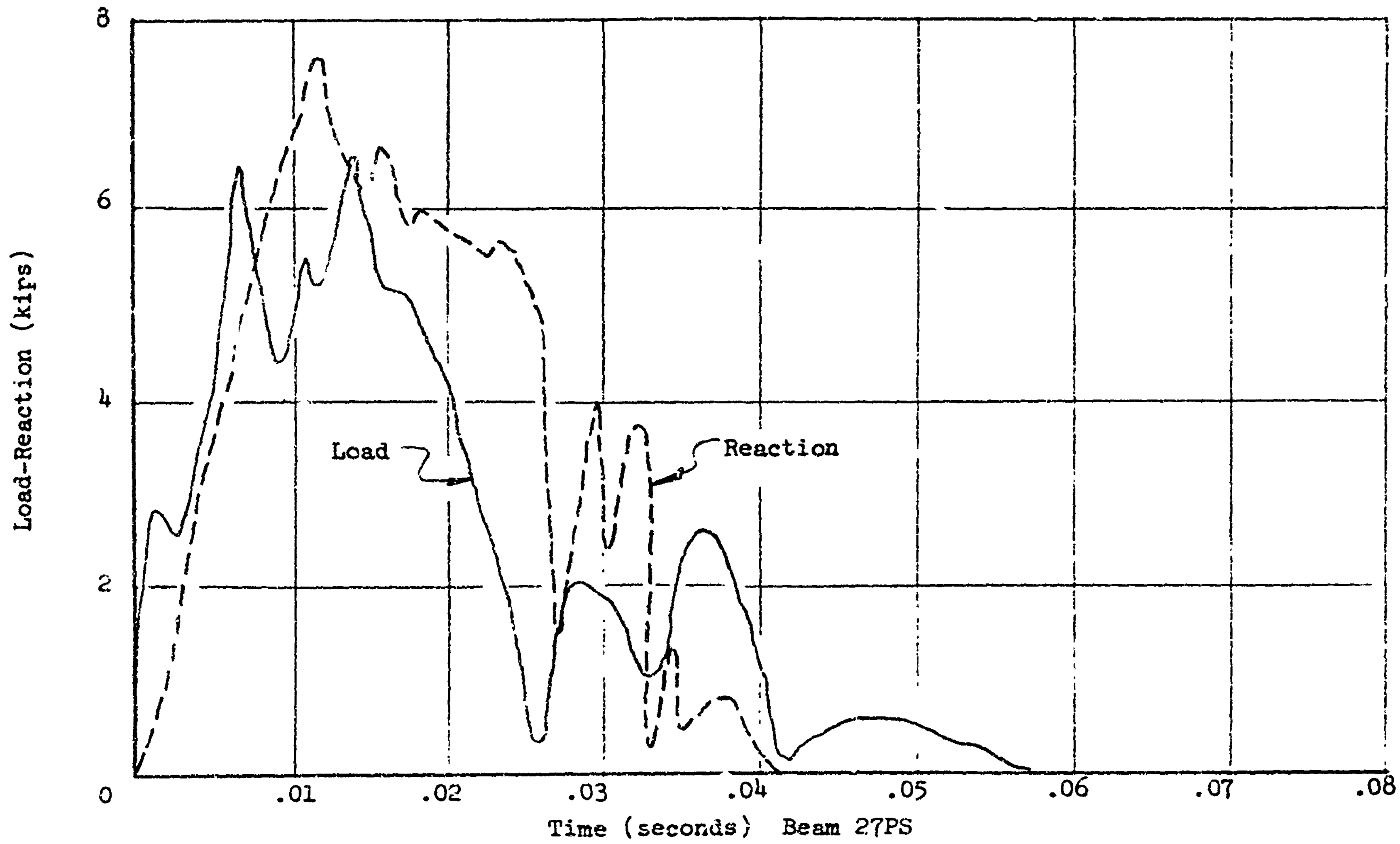

Fig. 24 THIRD POINT LOAD-REACTION VS. TIME

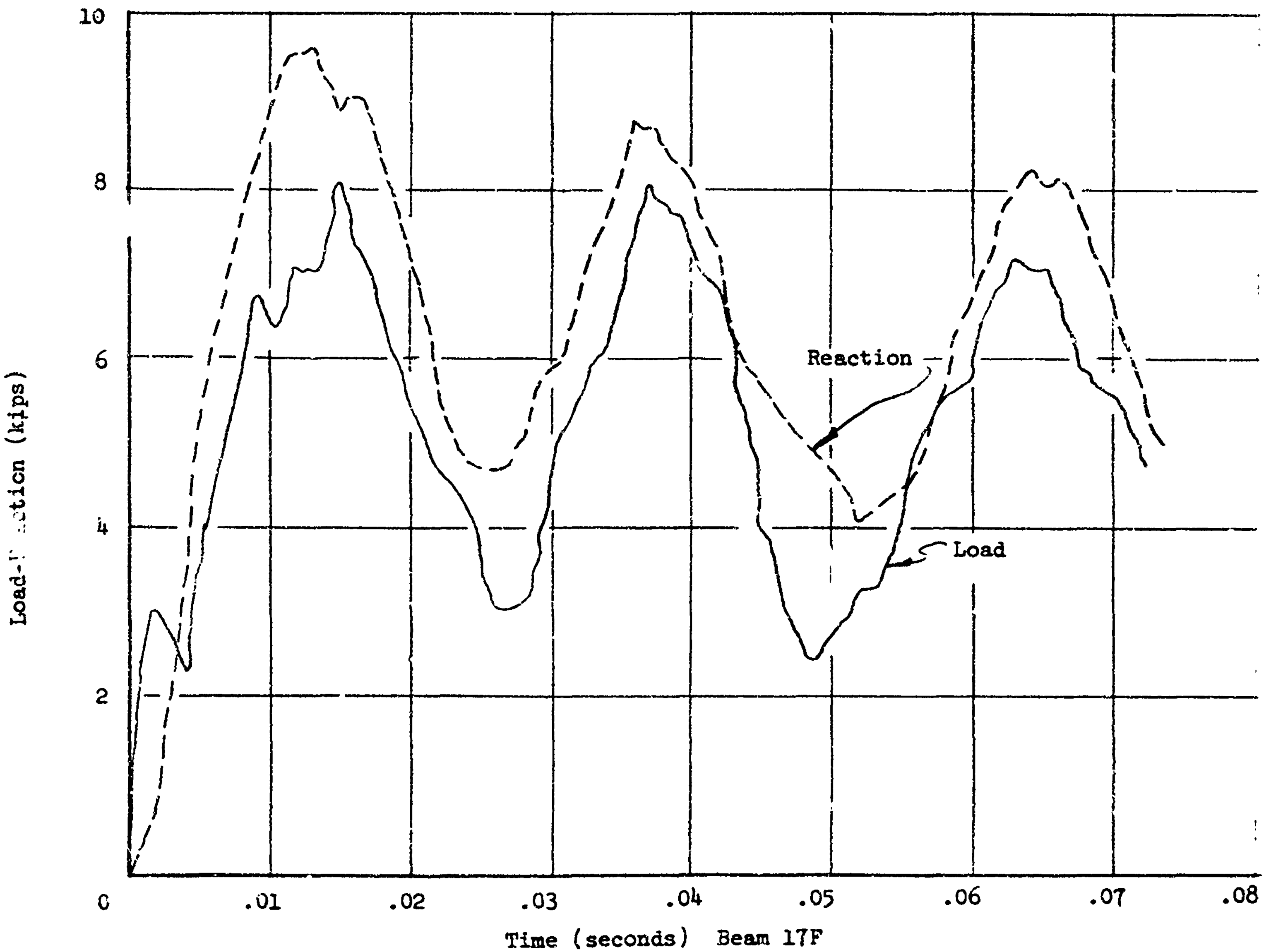

Fig. 25 THIRD POINT LOAD-REACTION VS. TIME

(a)

25PS

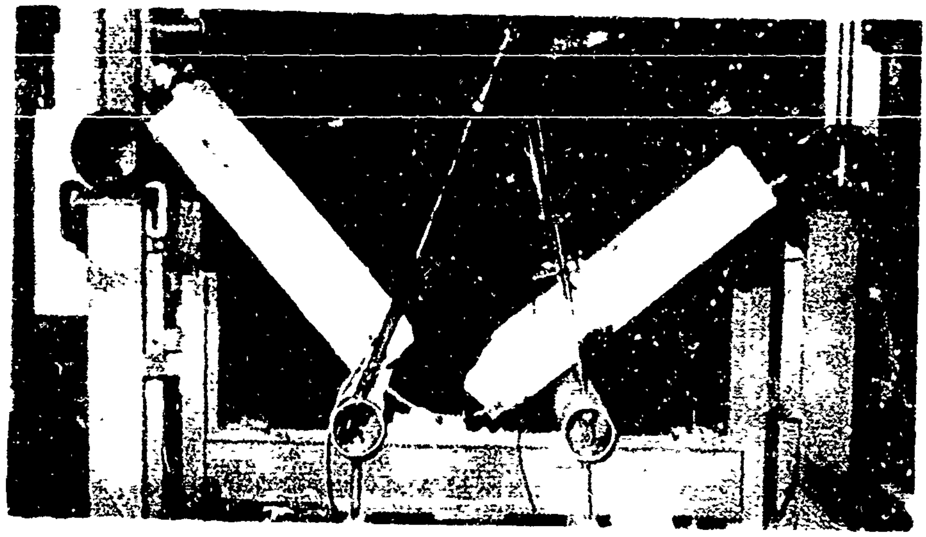

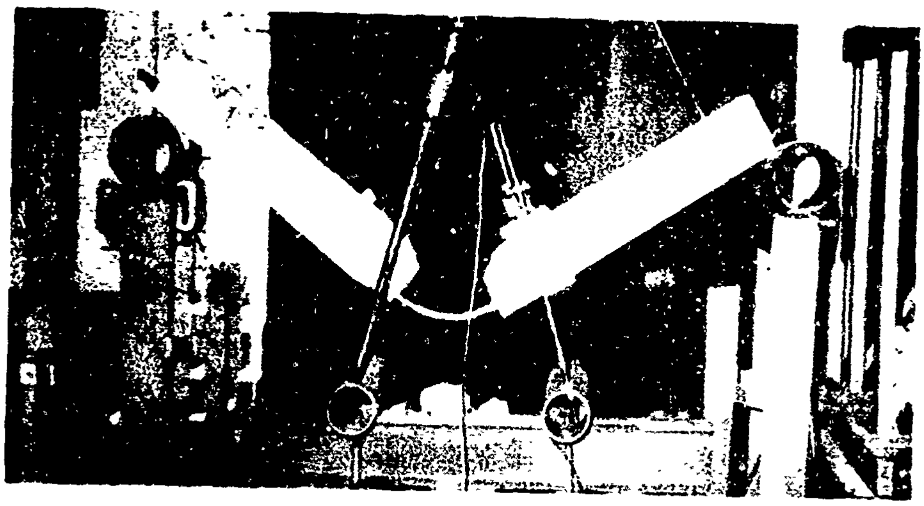

(b)

26PS

(c)

27PS

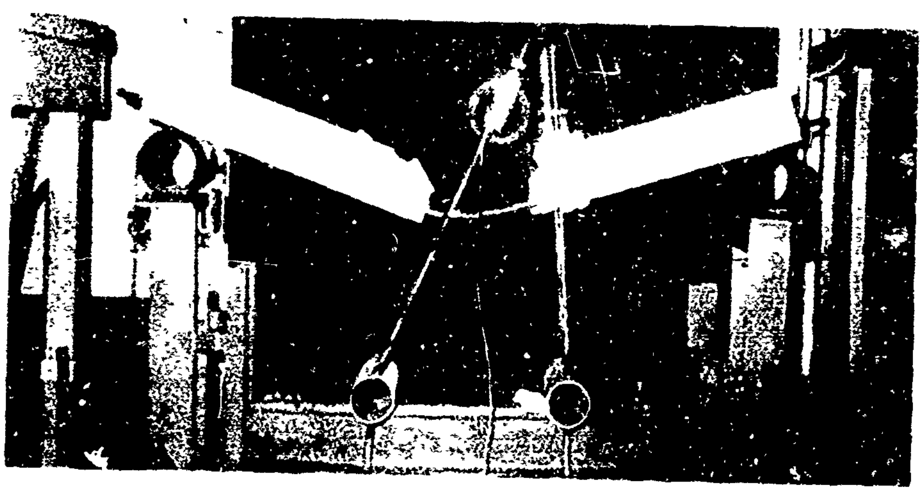

PLAIN BEAMS AFTER DYNAMIC TESTS

FIGURE 26

(a)
15FS

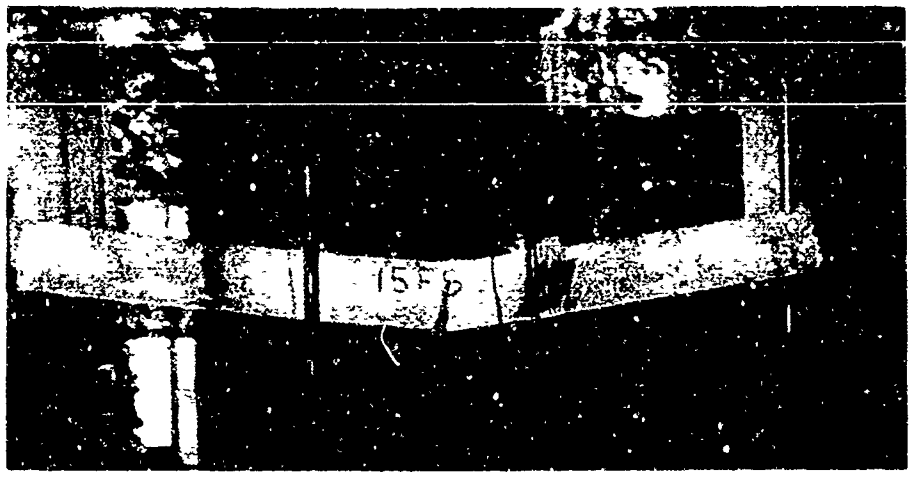

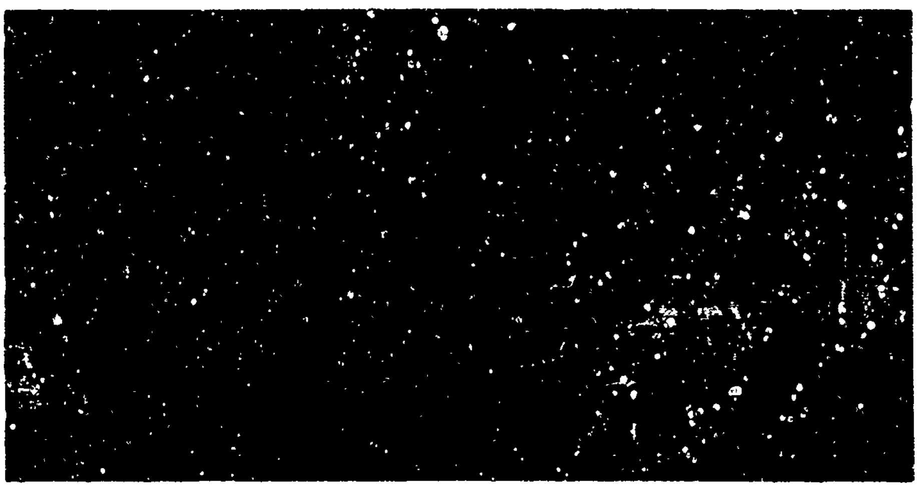

(b)
26FS

(c)
27FS
After five tests

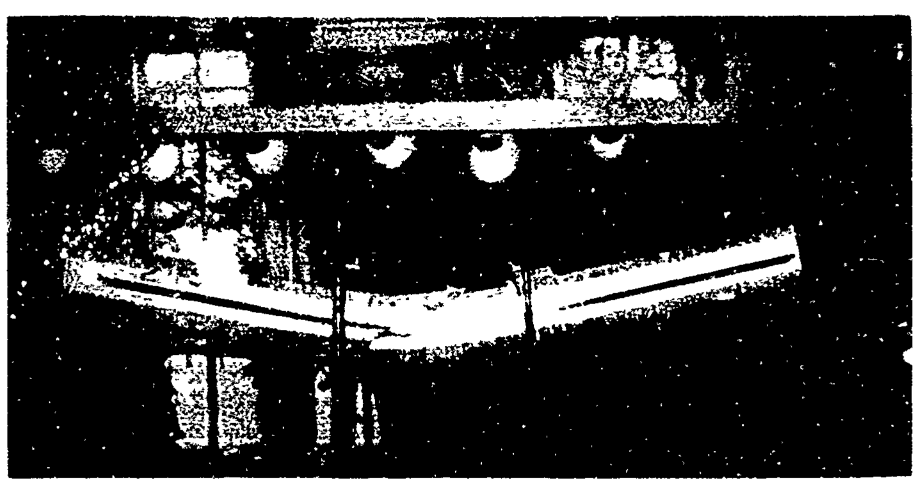

FIBER BEAMS AFTER DYNAMIC TESTS

FIGURE 27

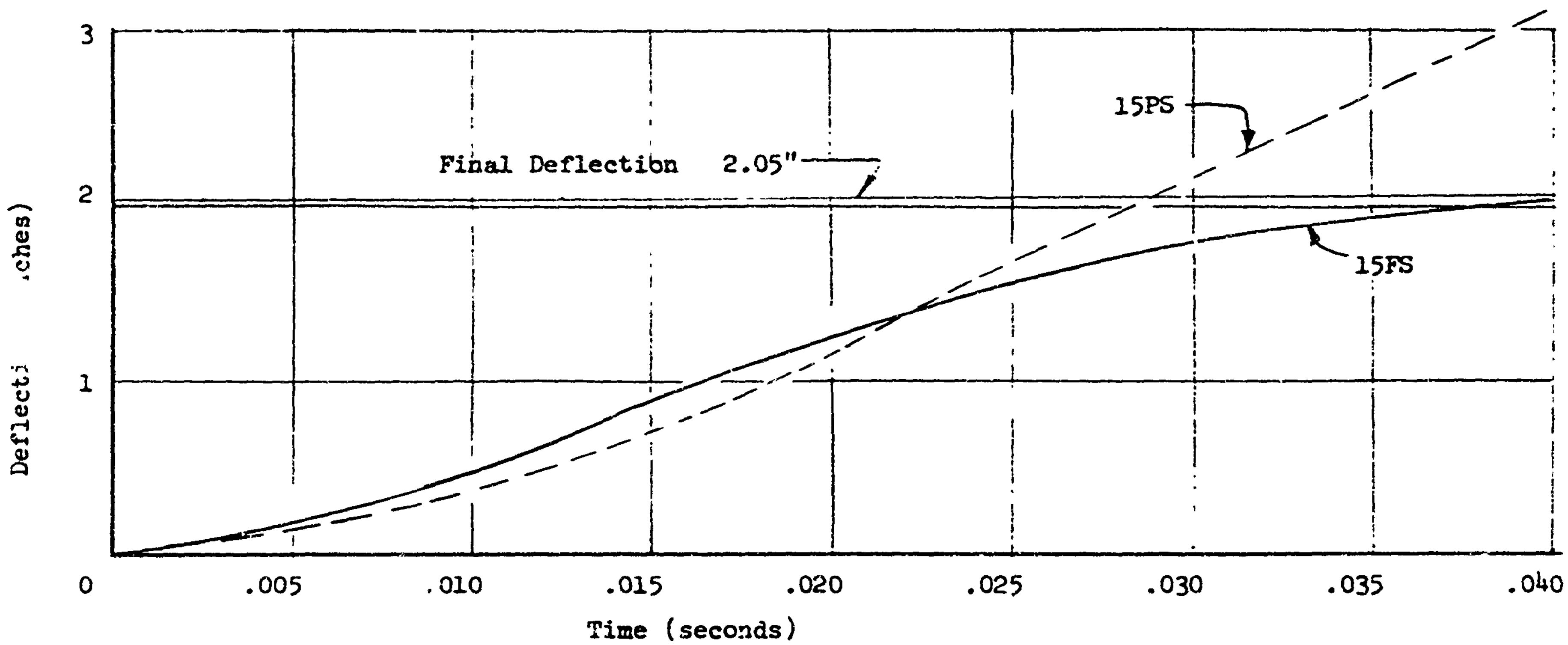

Fig. 28 DEFLECTION VS. TIME

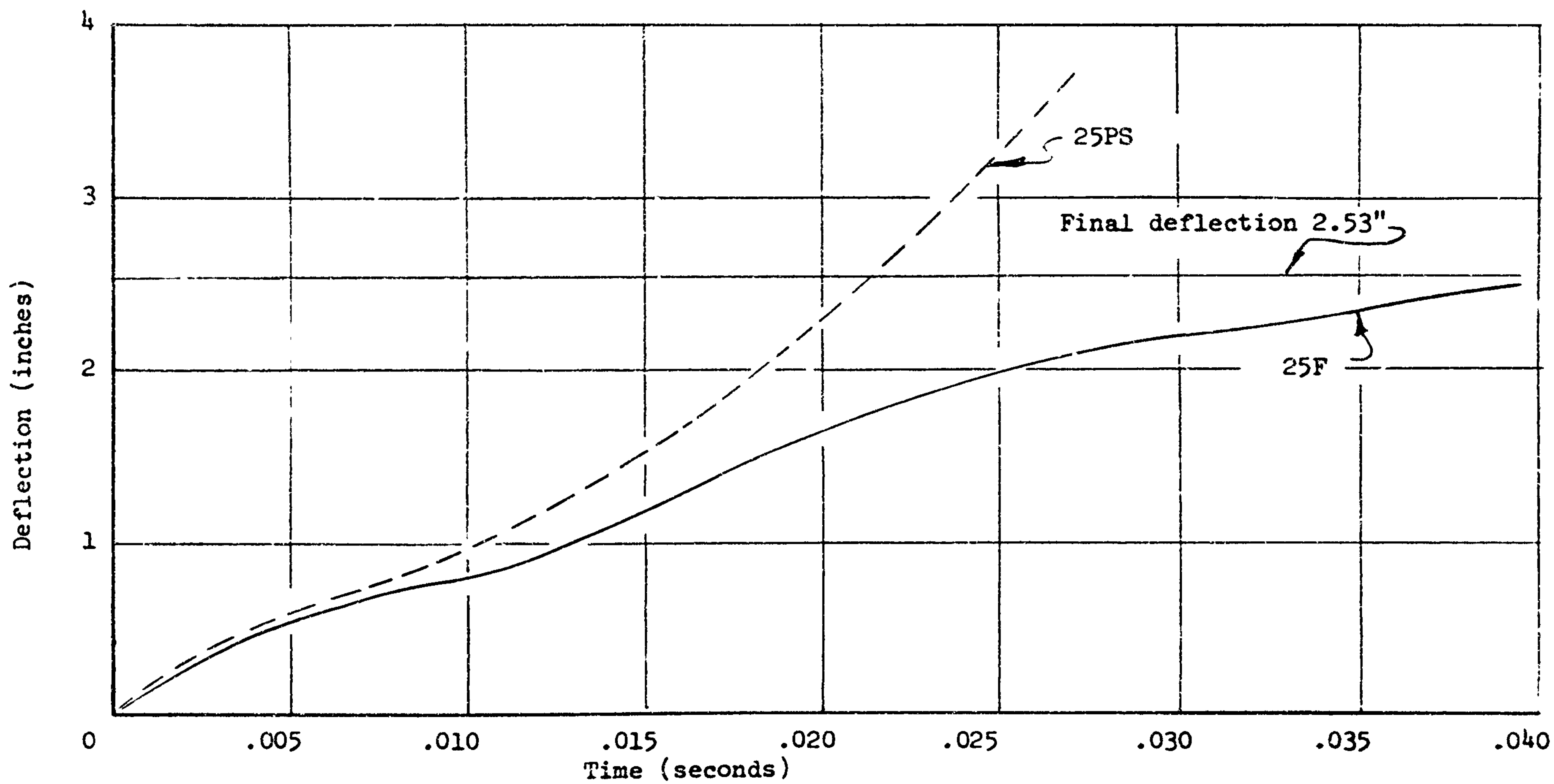

Fig. 29 DEFLECTION VS. TIME

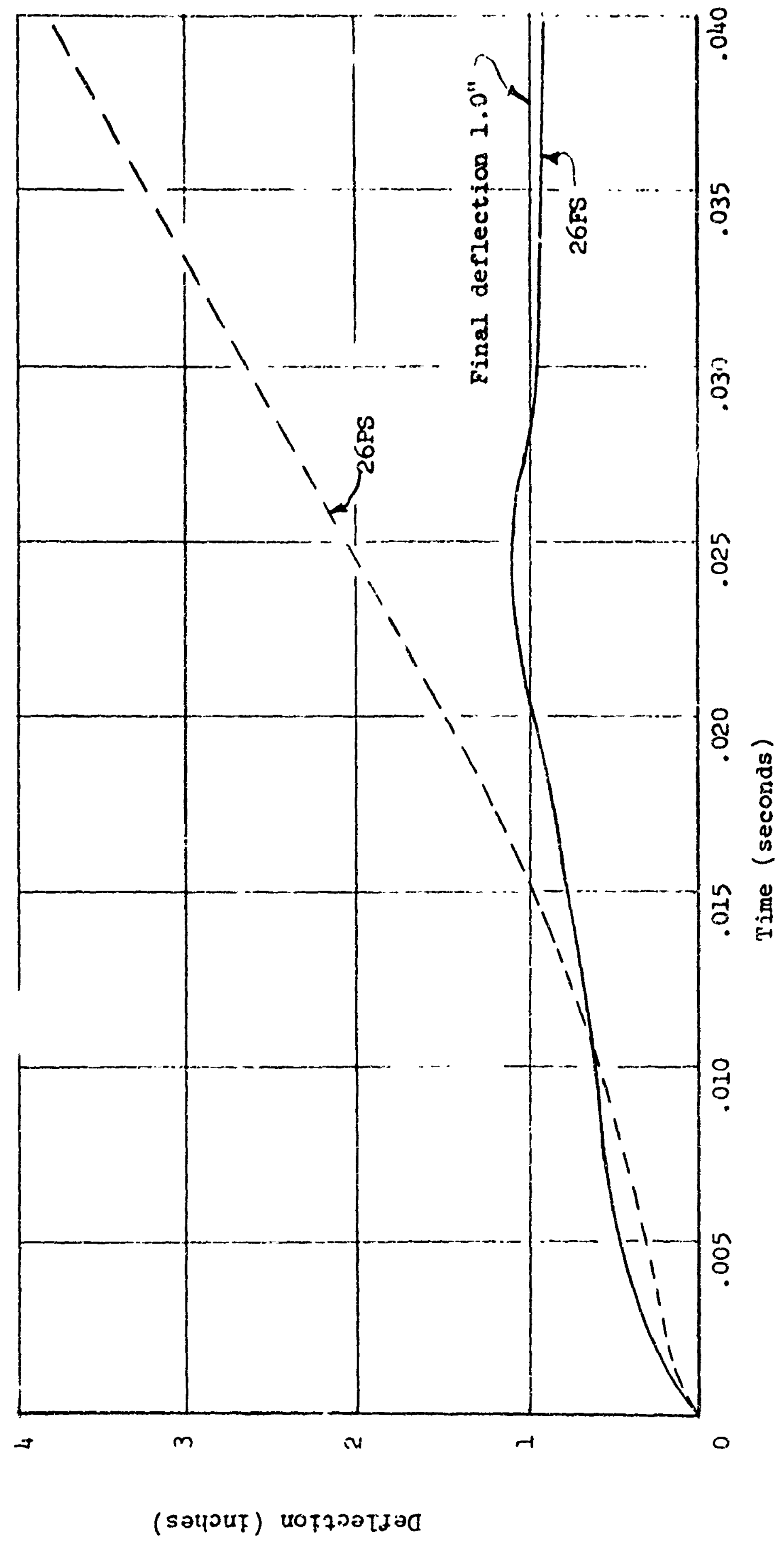

Fig. 30 DEFLECTION VS. TIME

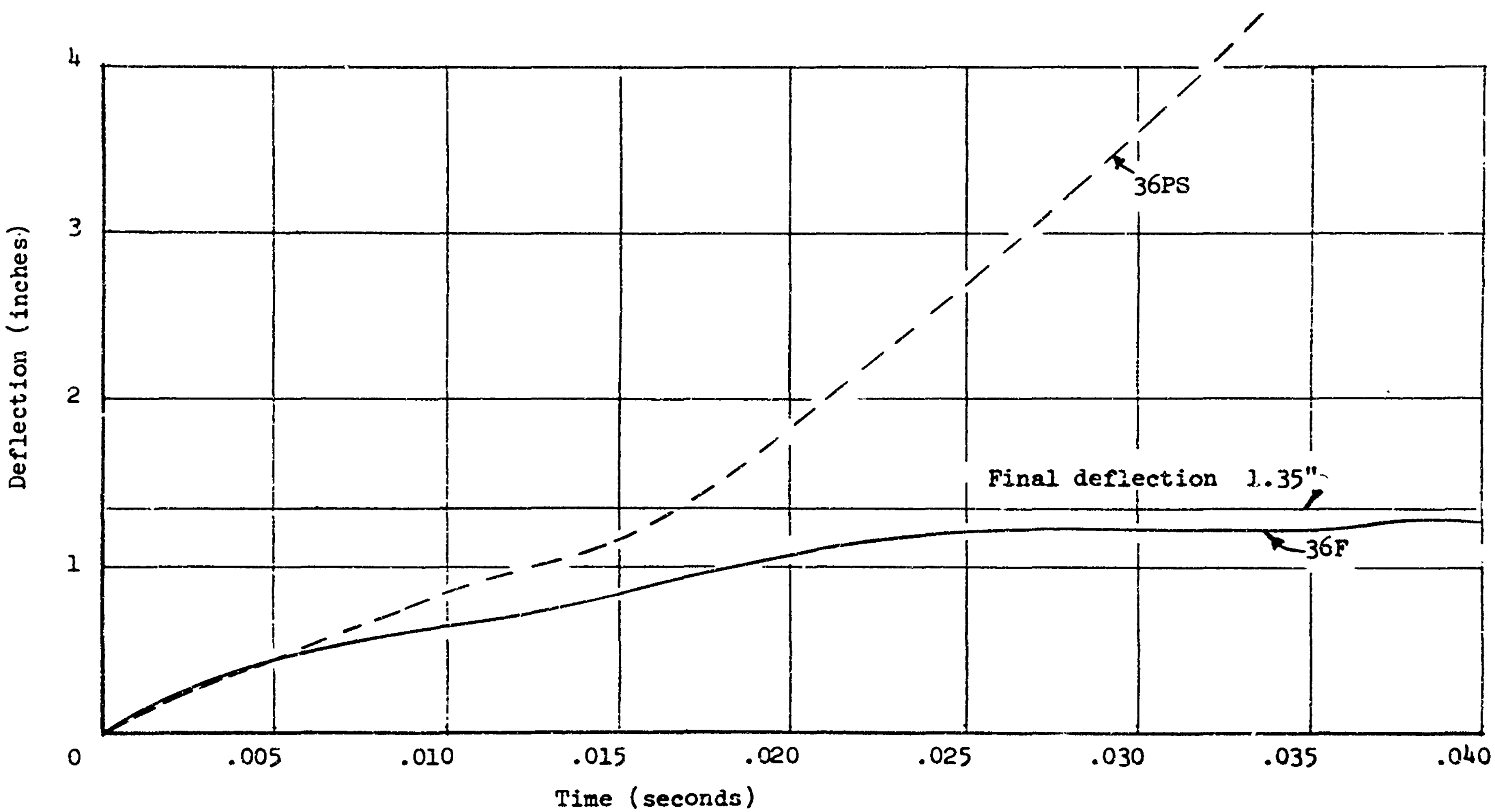

Fig. 31 DEFLECTION VS. TIME

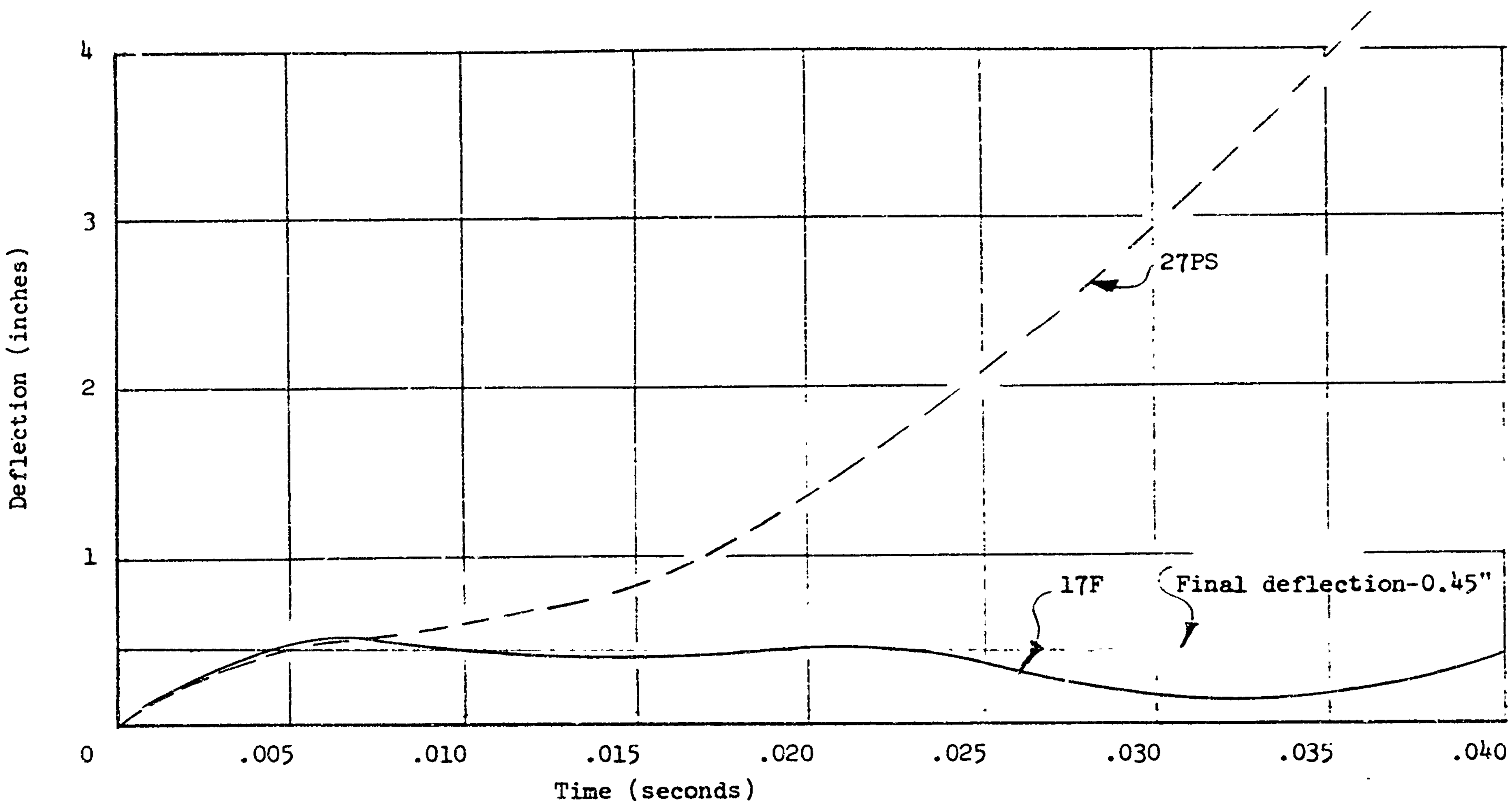

Fig. 32 DEFLECTION VS TIME

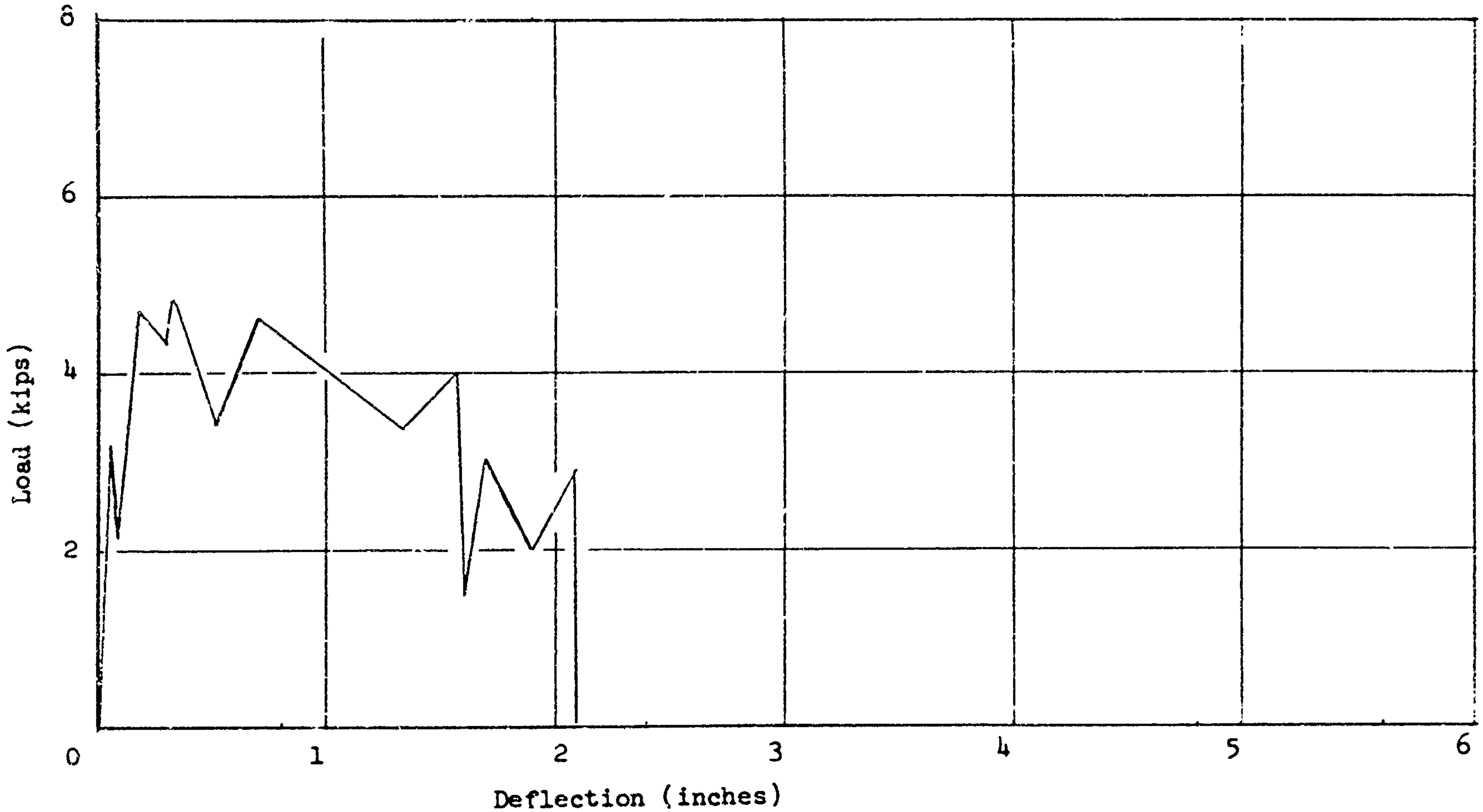

Fig. 33 LOAD VS. DEFLECTION AT THIRD POINT BEAM 15PS

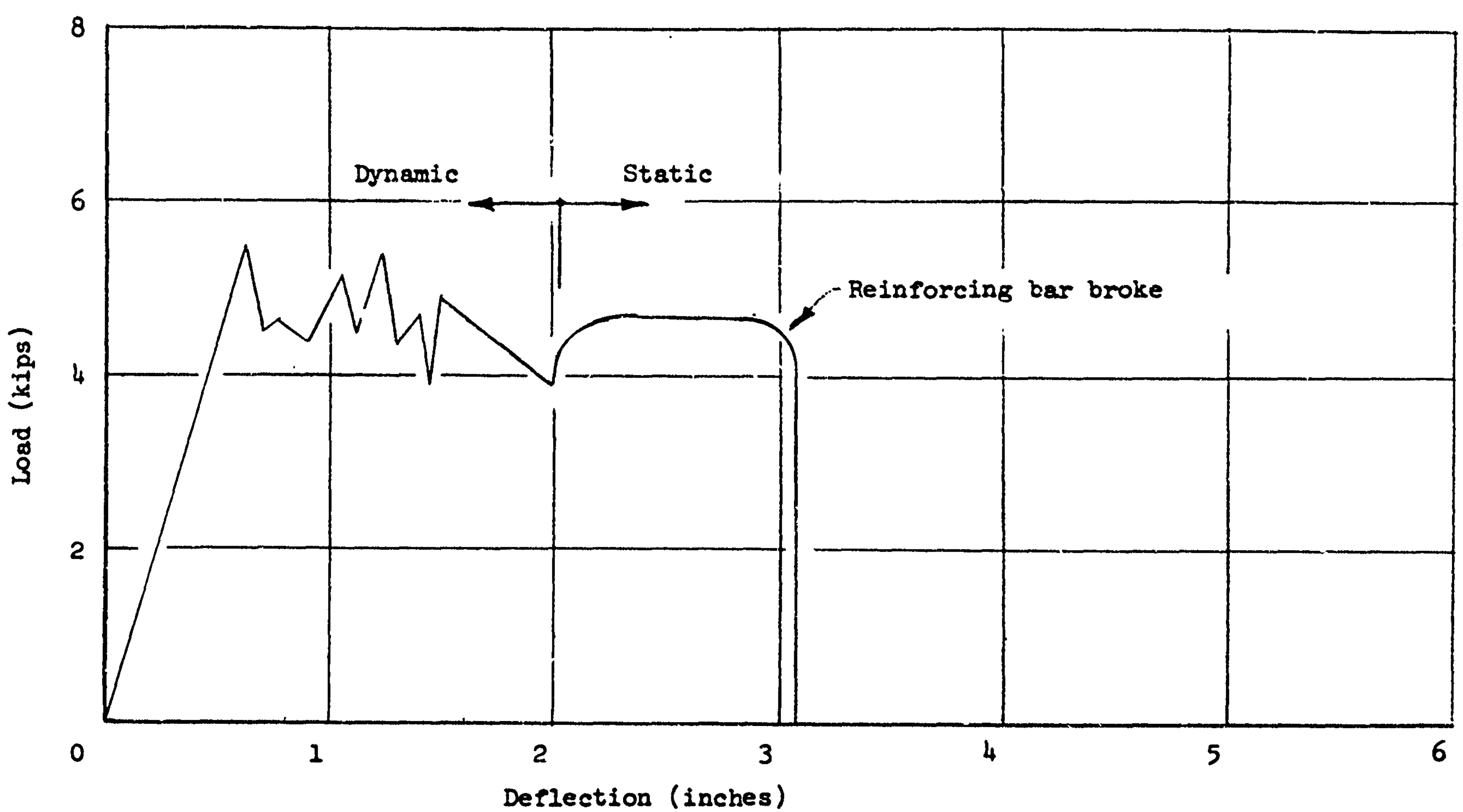

Fig. 34 LOAD VS. DEFLECTION AT THIRD POINT BEAM 15FS

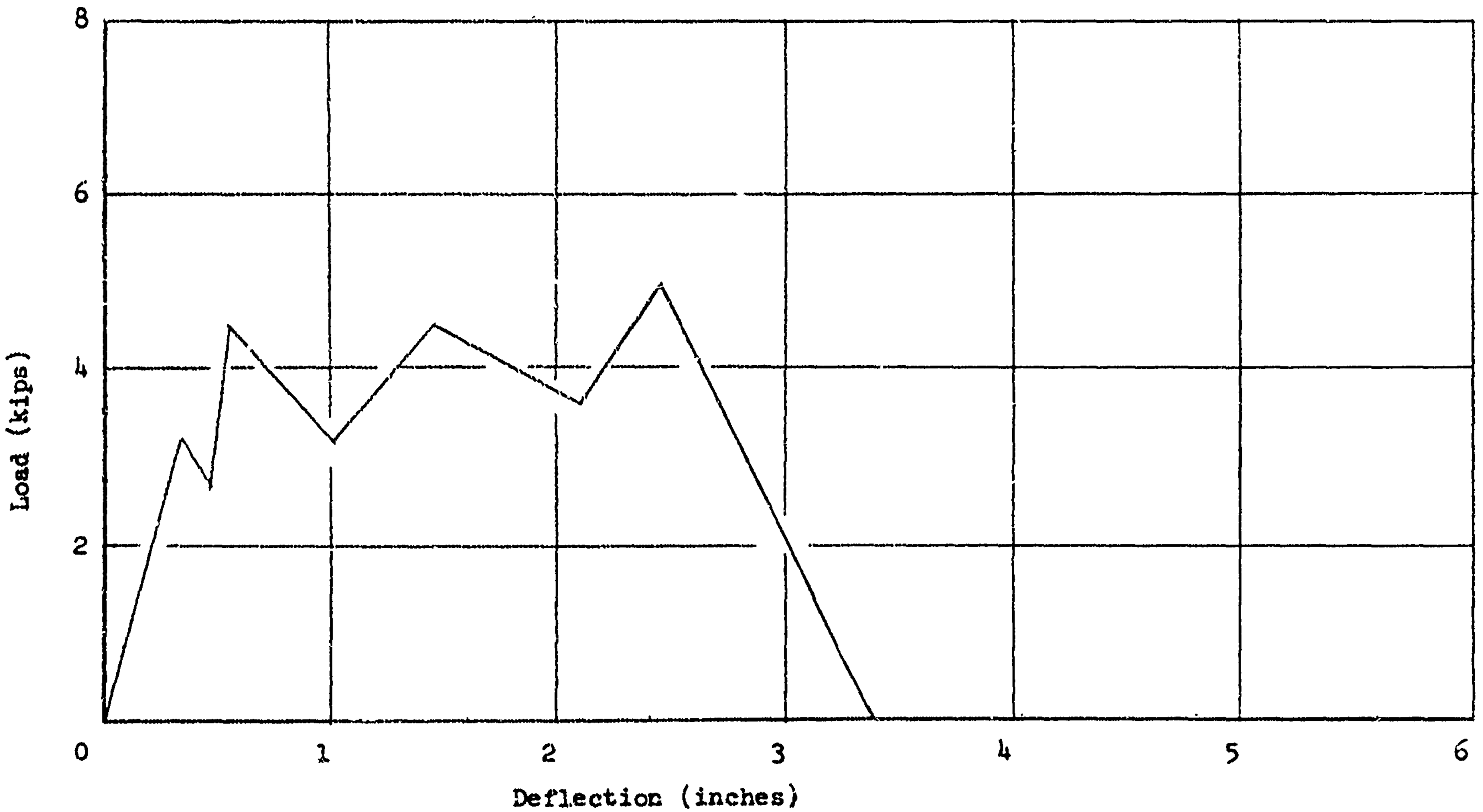

Fig. 35 LOAD VS. DEFLECTION AT THIRD POINT BEAM 25PS

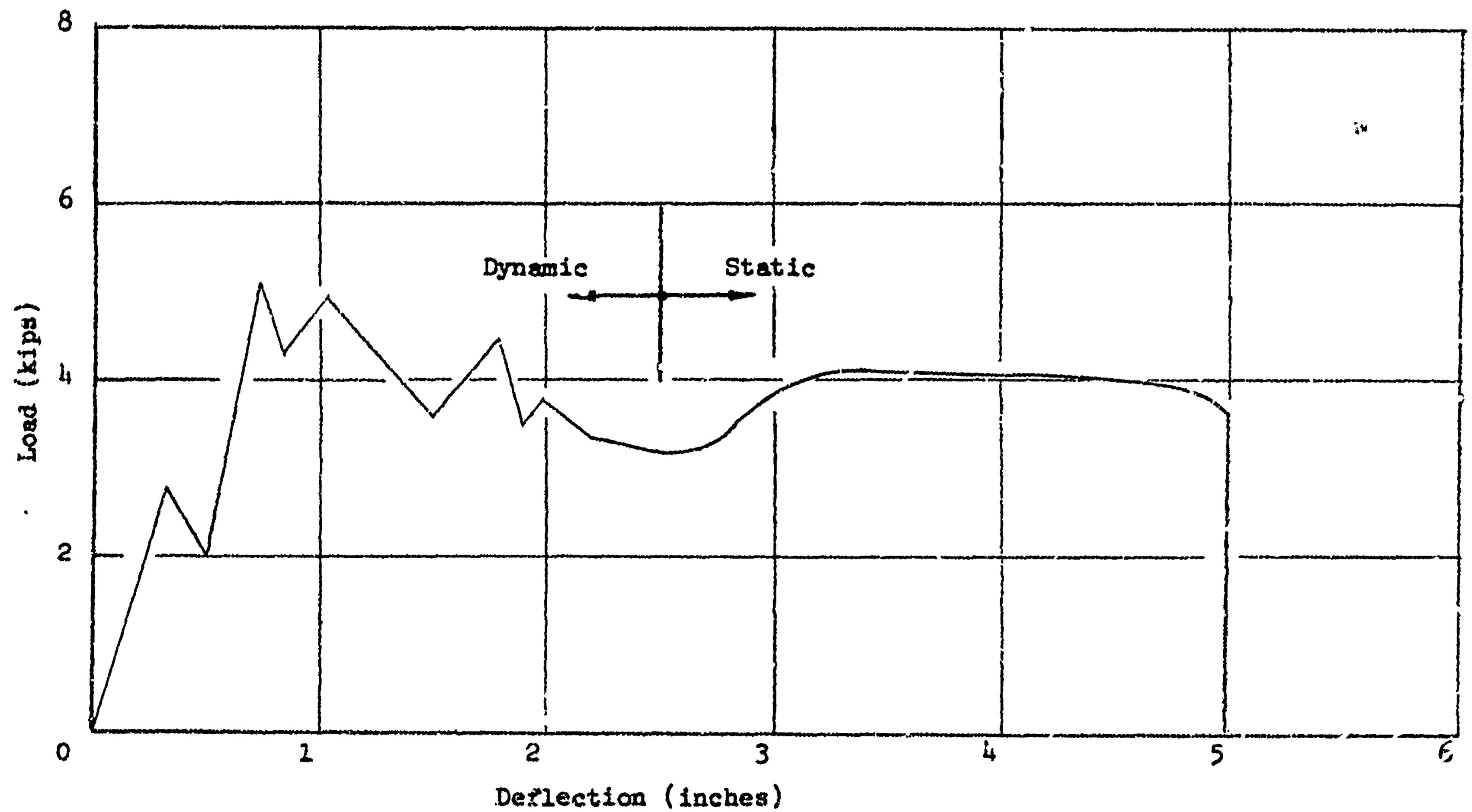

Fig. 36 LOAD VS. DEFLECTION AT THIRD POINT BEAM 25F

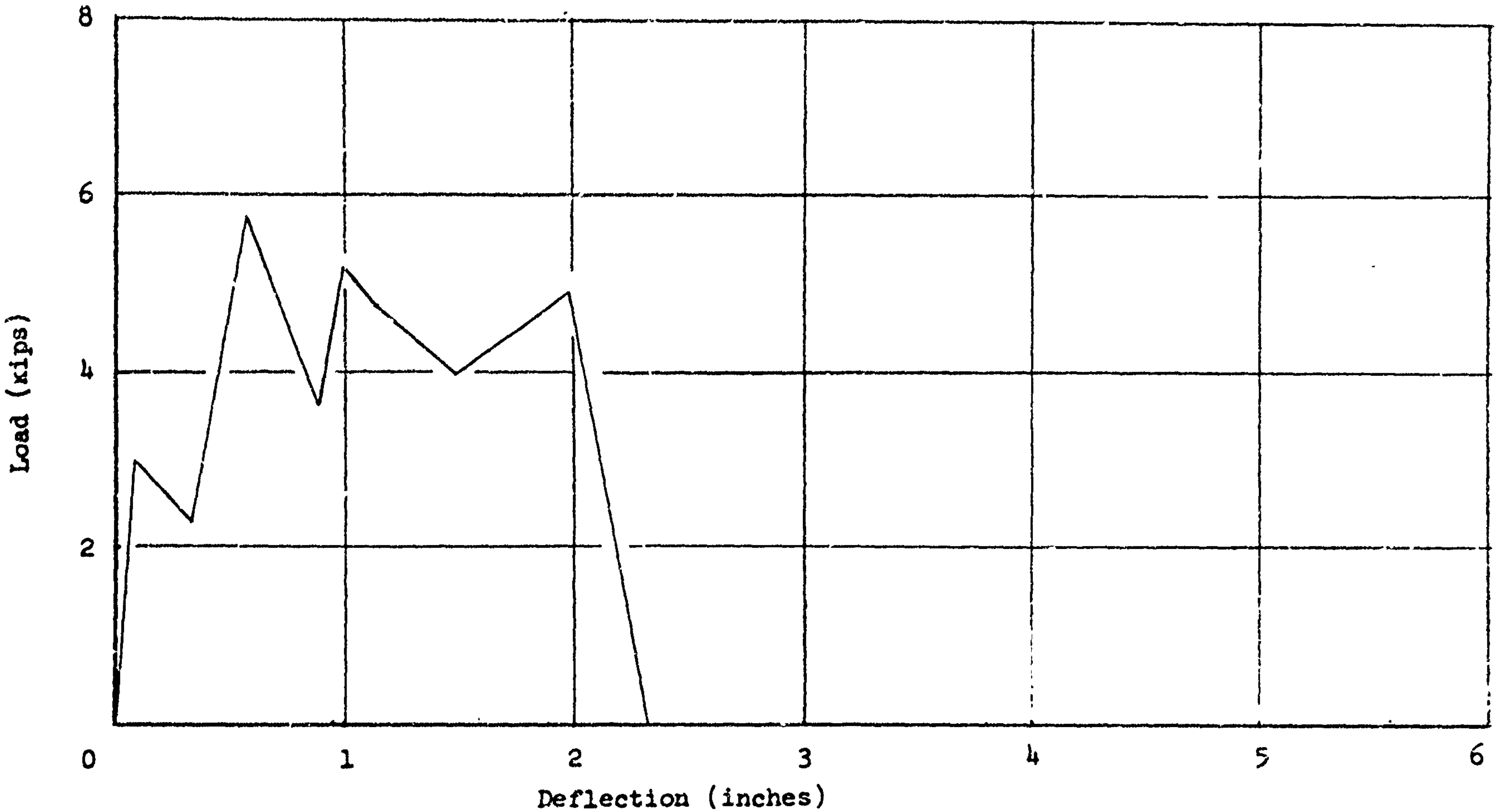

Fig. 37 LOAD VS. DEFLECTION AT THIRD POINT BEAM 36PS

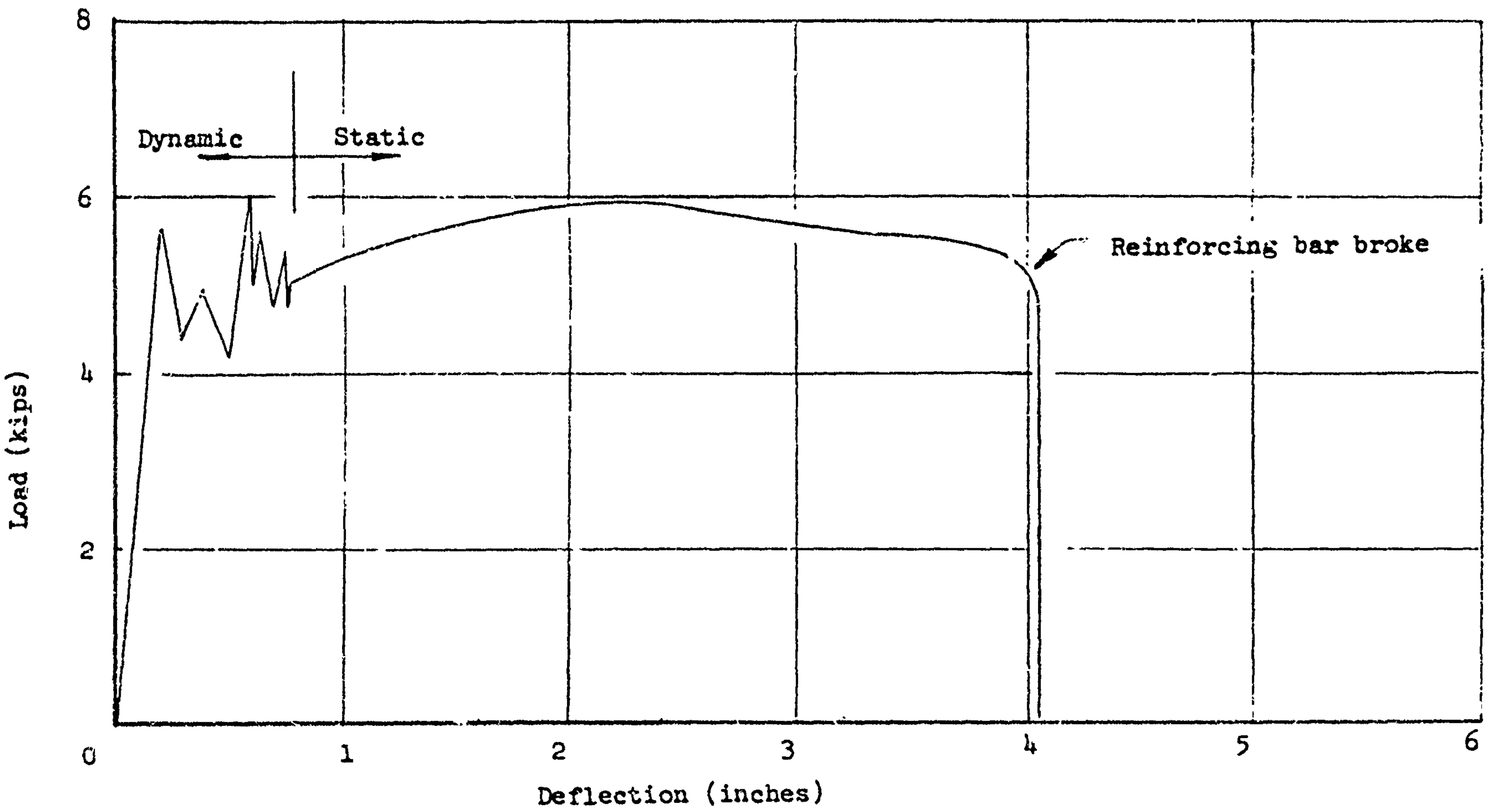

Fig. 38 LOAD VS. DEFLECTION AT THIRD POINT BEAM 26FS

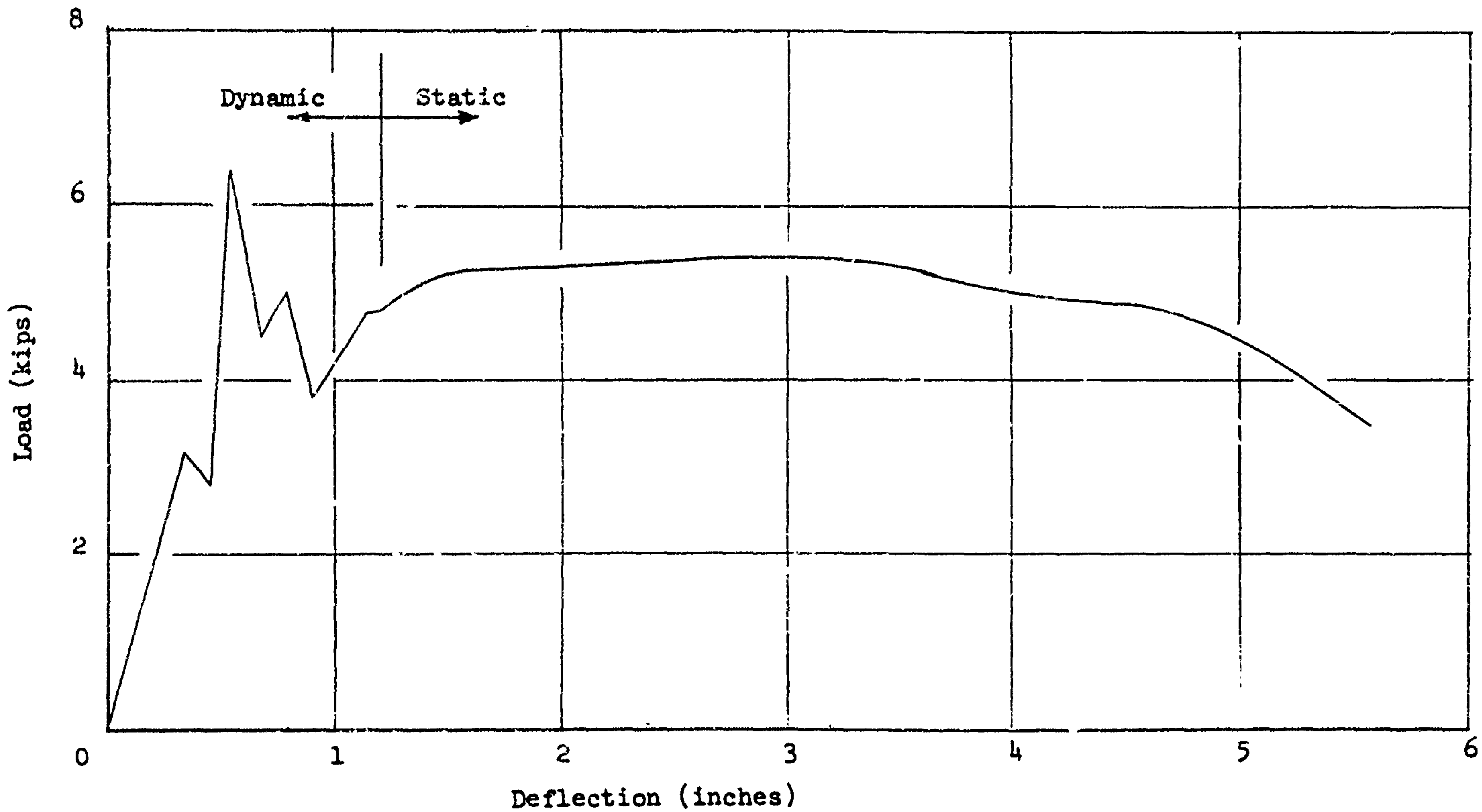

Fig. 39 LOAD VS. DEFLECTION AT THIRD POINT BEAM 36F

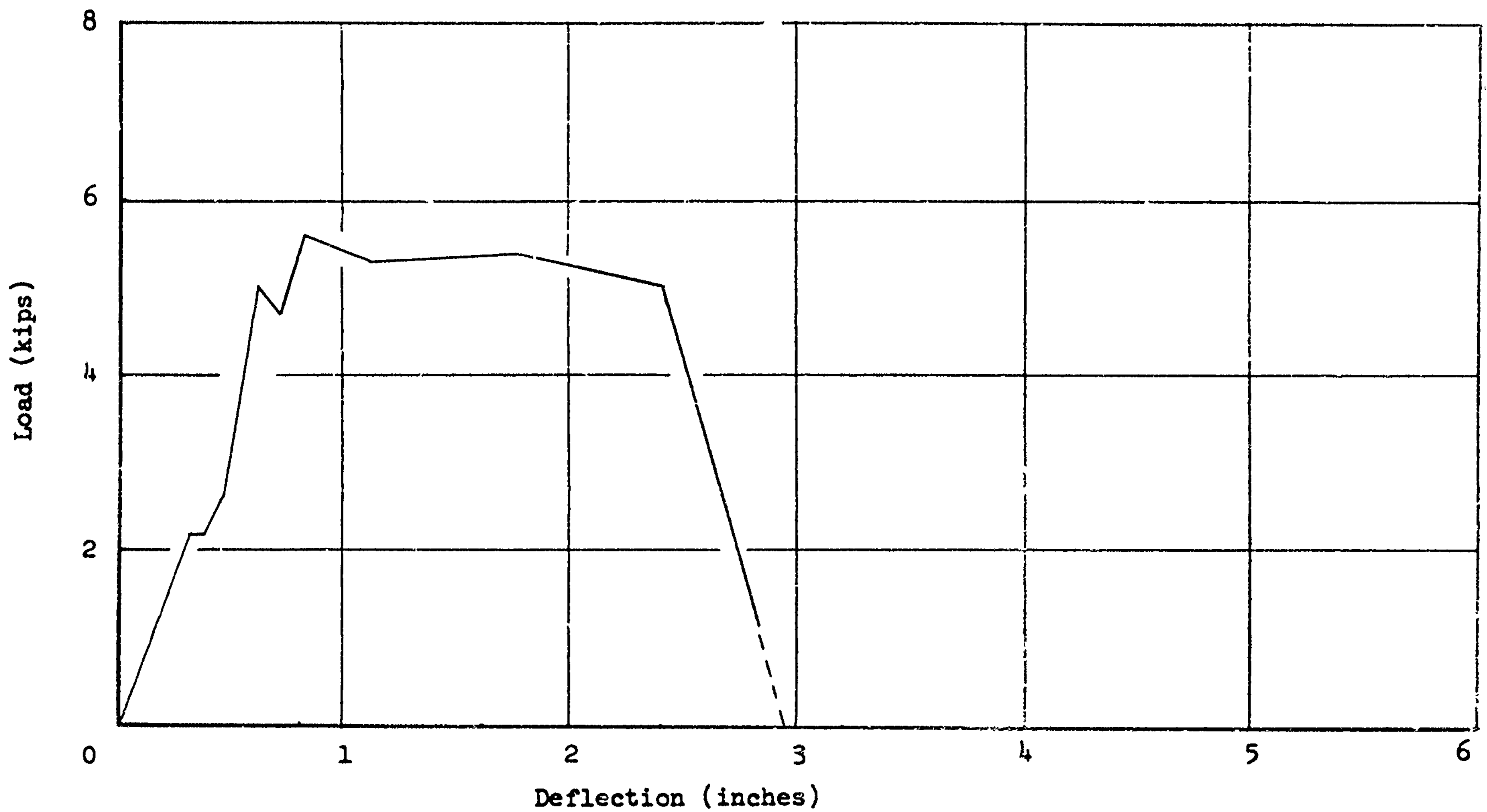

Fig. 40 LOAD VS. DEFLECTION AT THIRD POINT BEAM 27PS

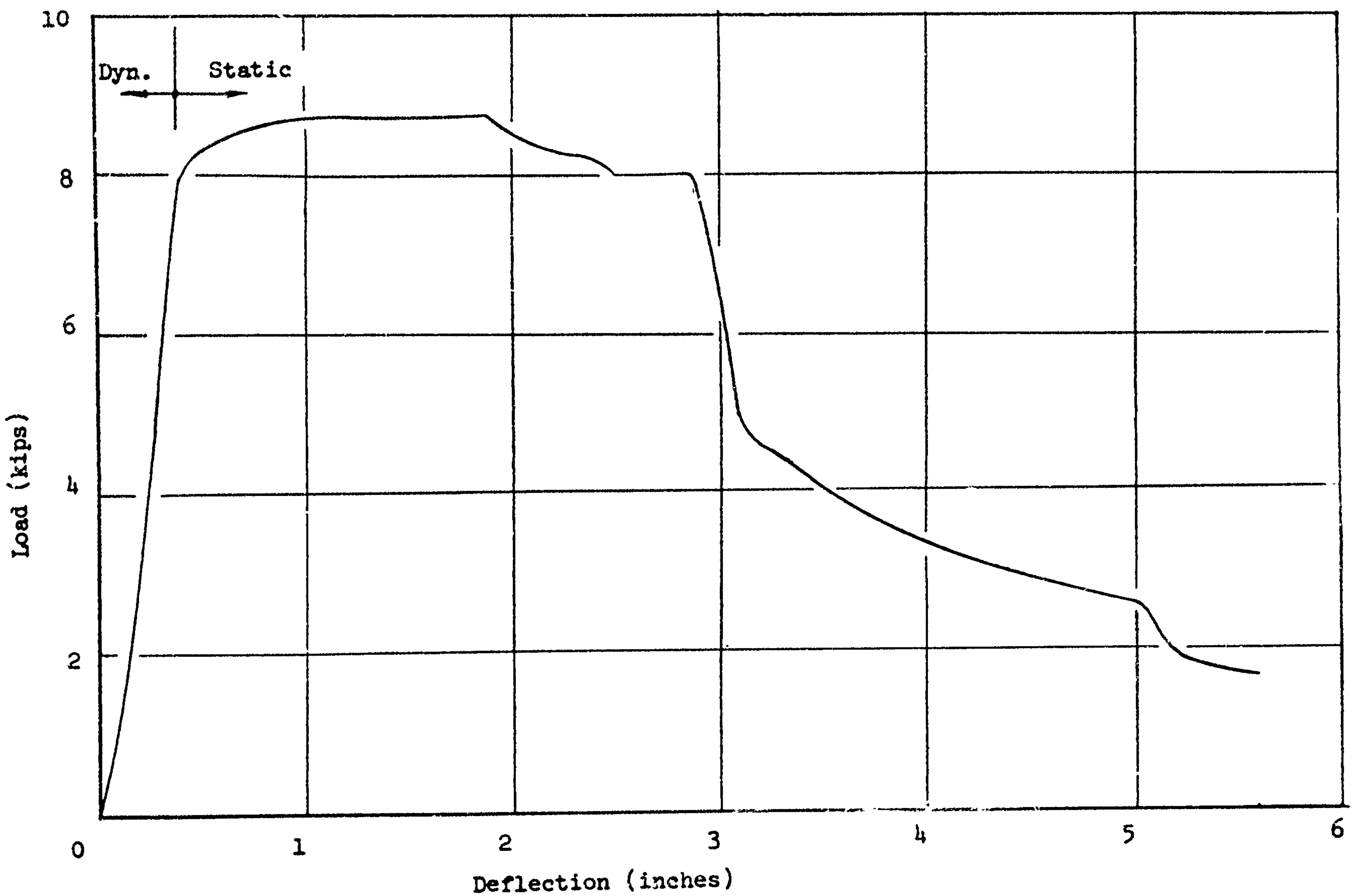

Fig. 41 LOAD VS. DEFLECTION AT THIRD POINT BEAM 17F

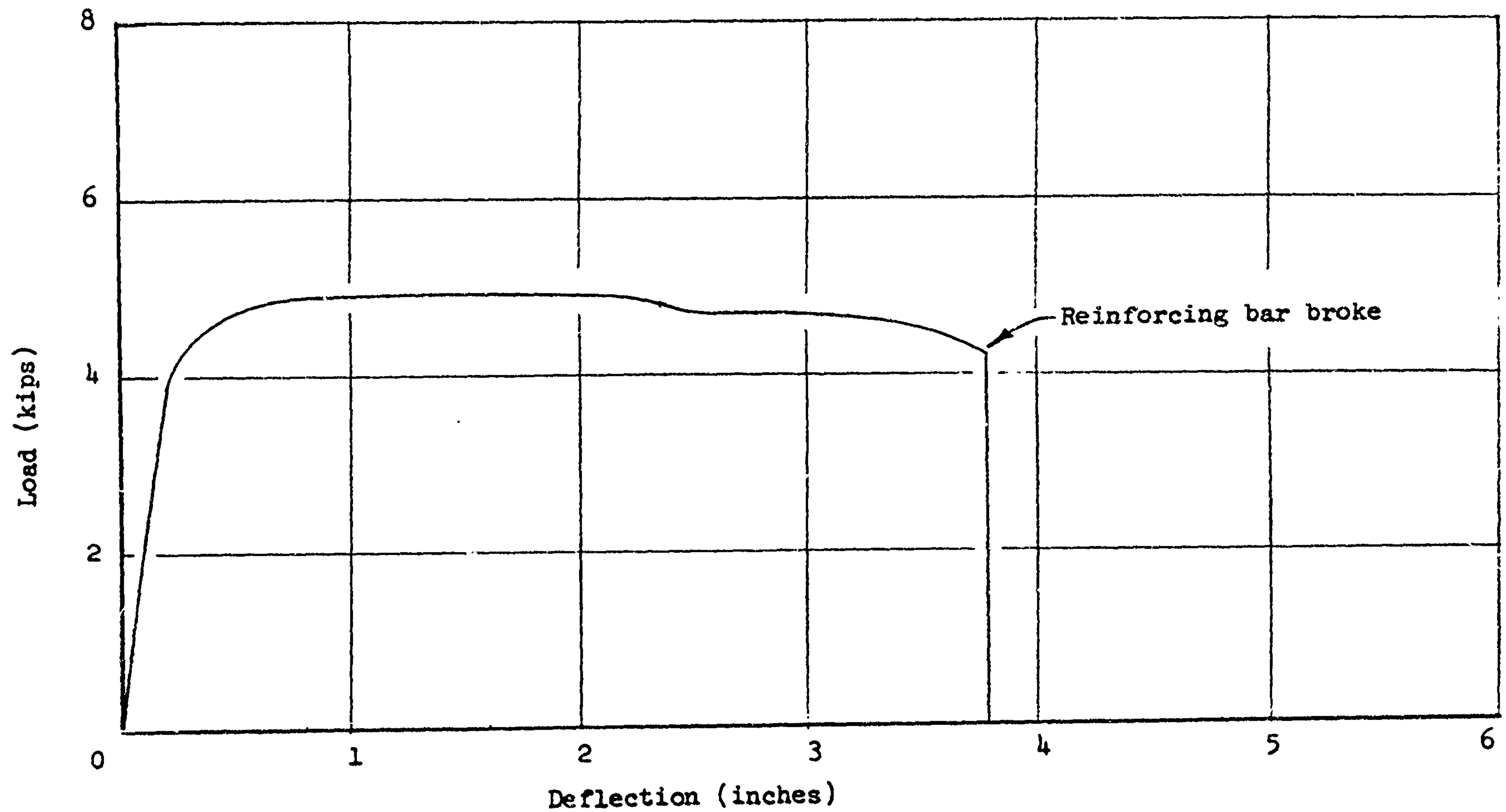

Fig. 42 LOAD VS. DEFLECTION AT THIRD POINT BEAM S5F

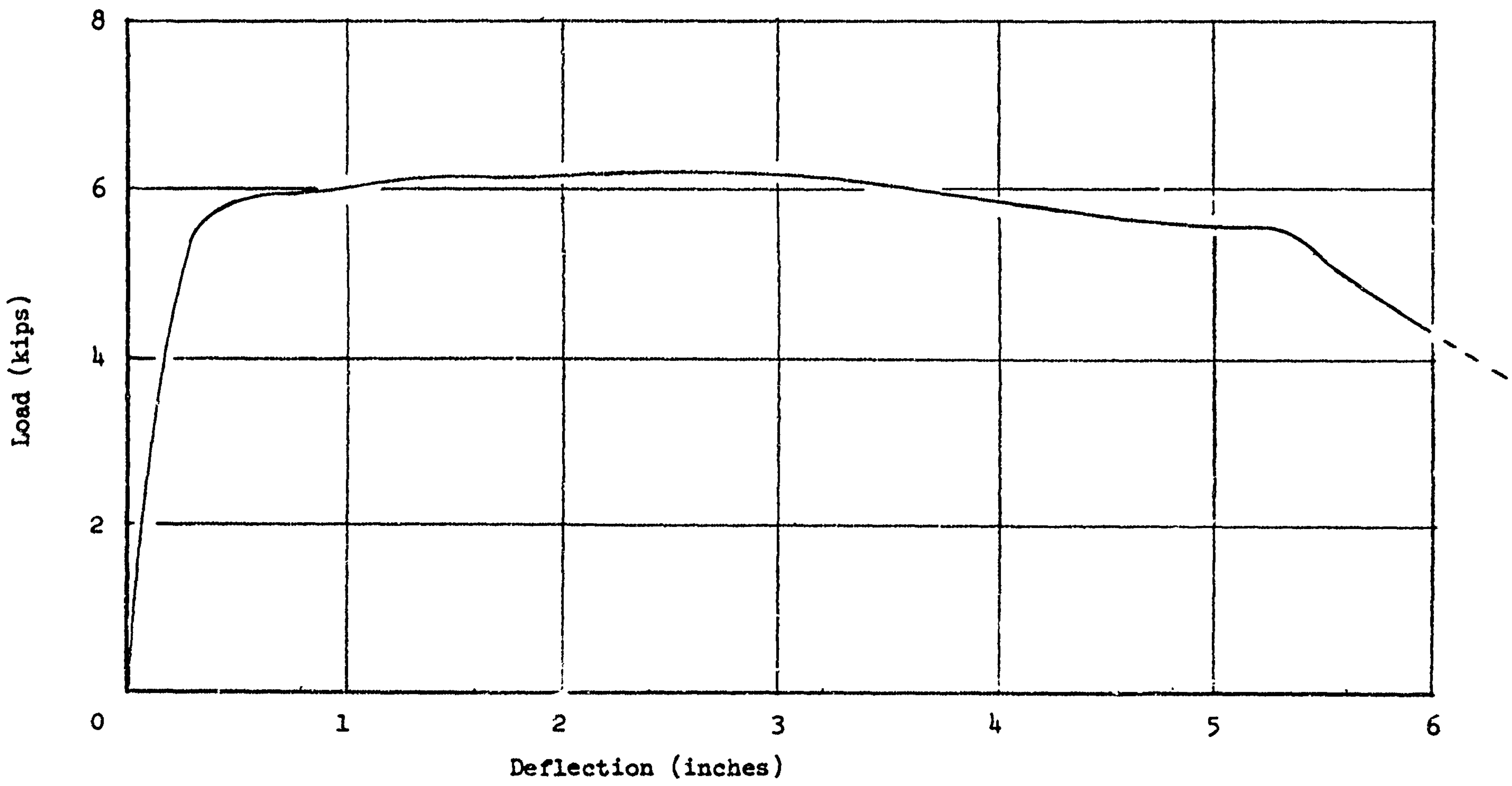

Fig. 43 LOAD VS. DEFLECTION AT THIRD POINT BEAM S6F

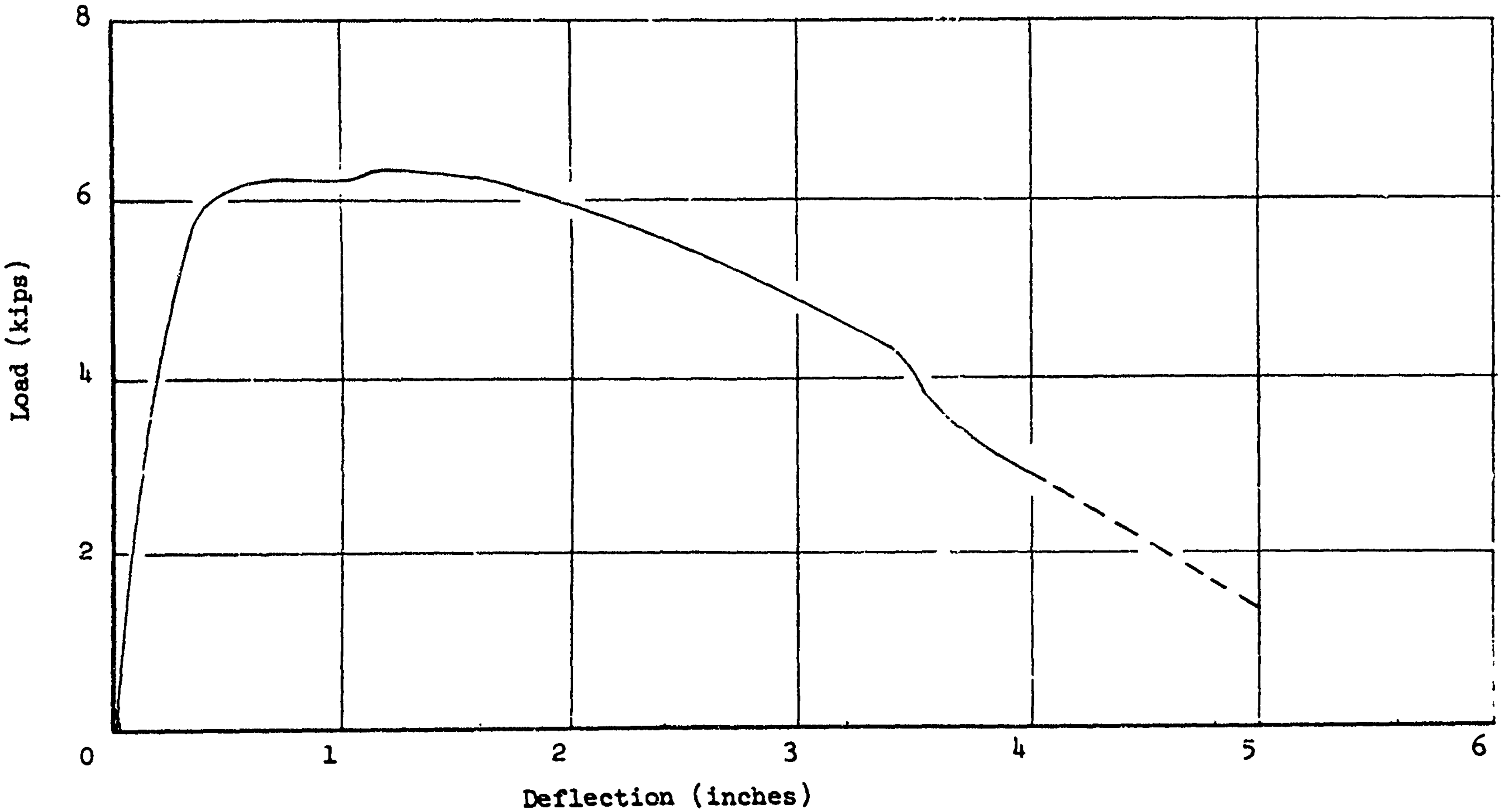

Fig. 44 LOAD VS. DEFLECTION AT THIRD POINT BEAM S7F

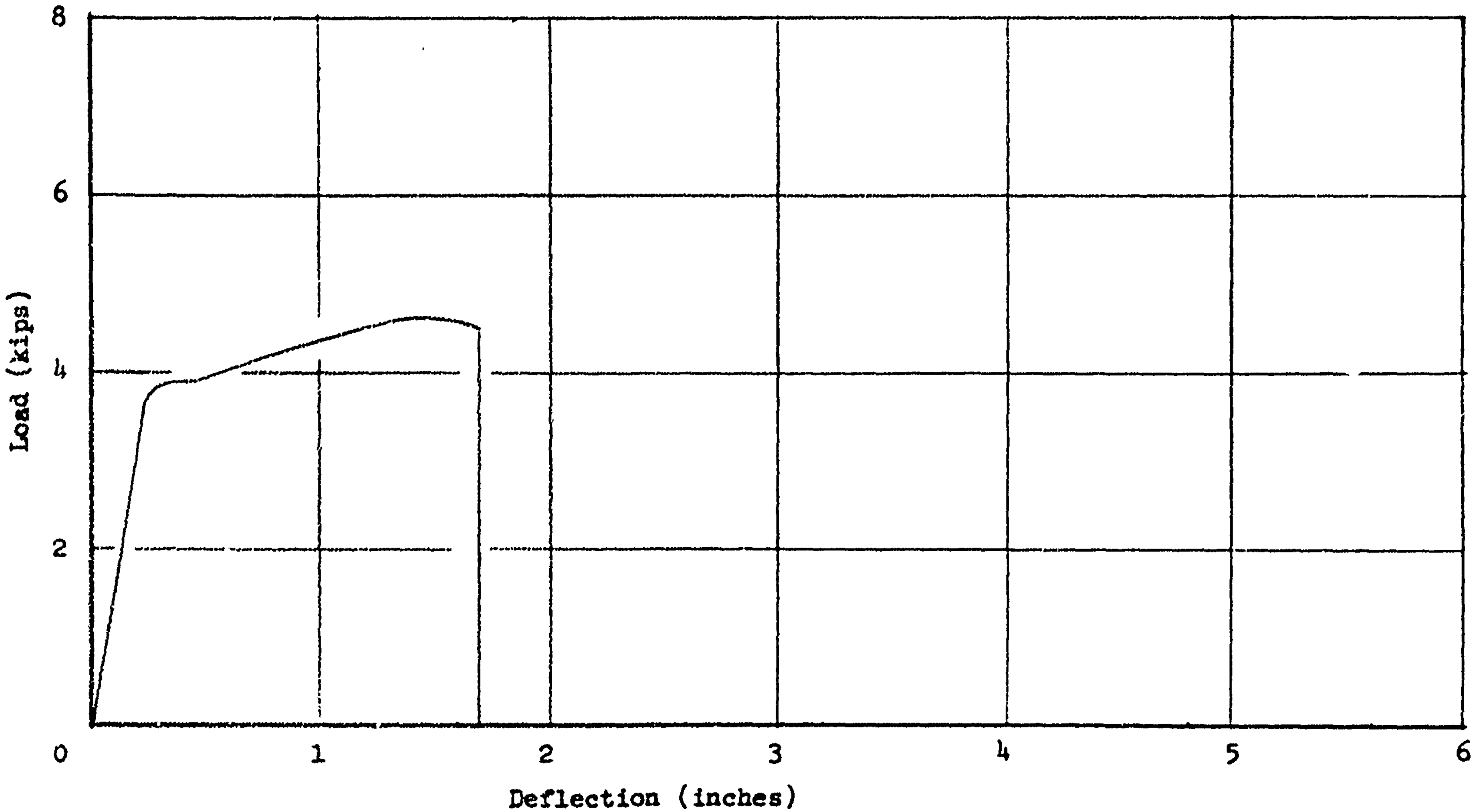

Fig. 45 LOAD VS. DEFLECTION AT THIRD POINT BEAM S5P

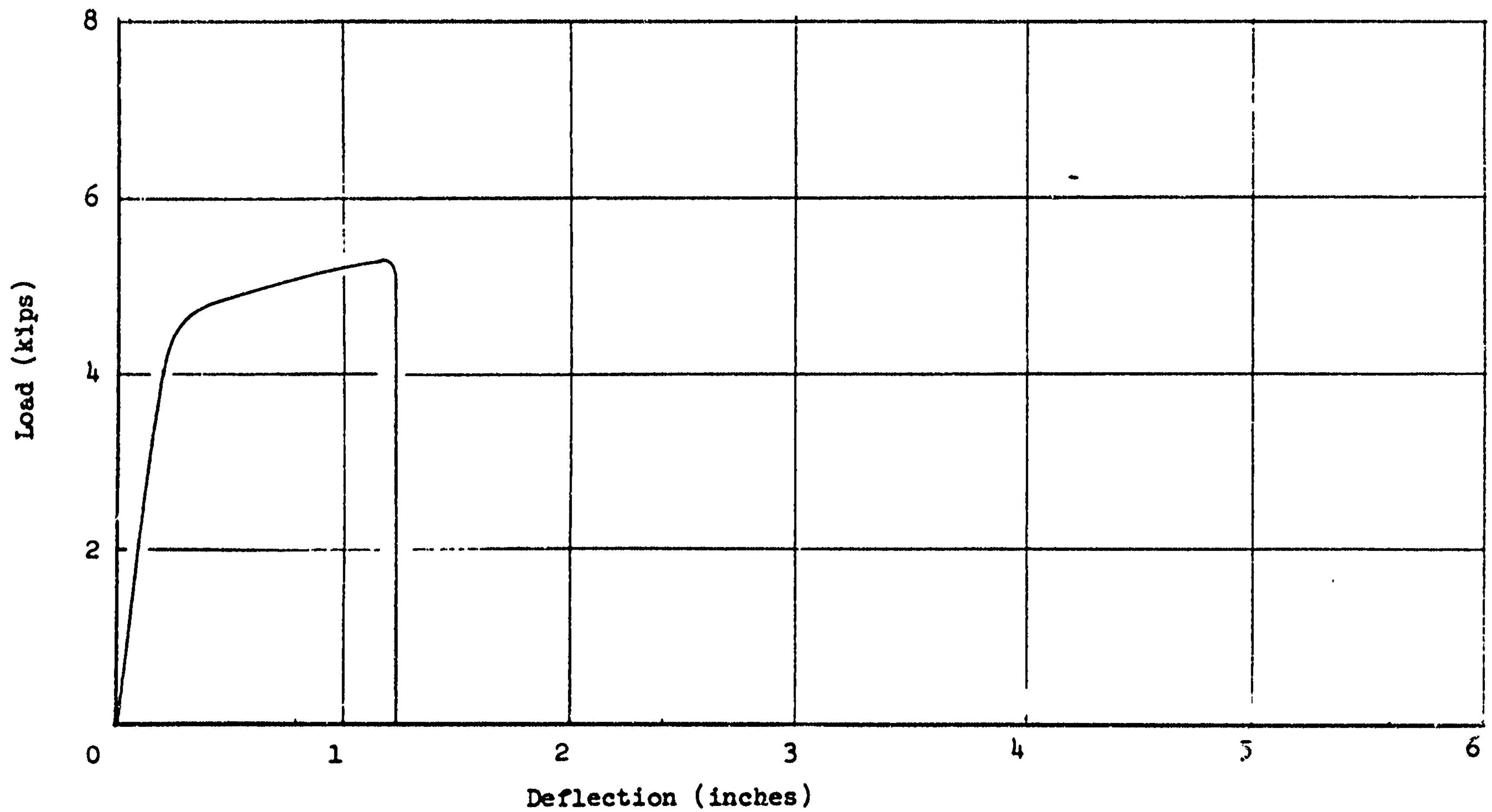

Fig. 46 LOAD VS. DEFLECTION AT THIRD POINT BEAM S6P

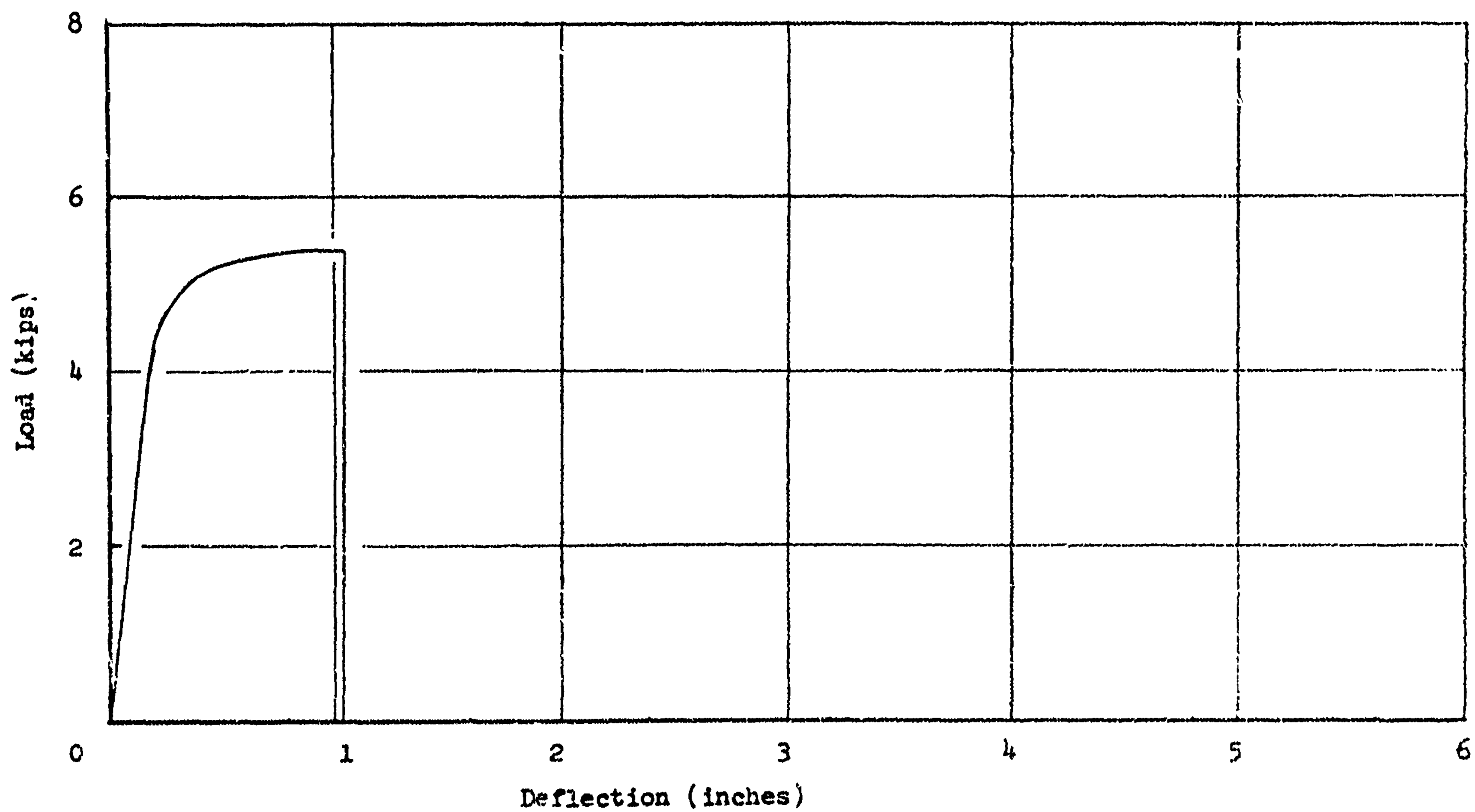

Fig. 47 LOAD VS. DEFLECTION AT THIRD POINT BEAM S7P

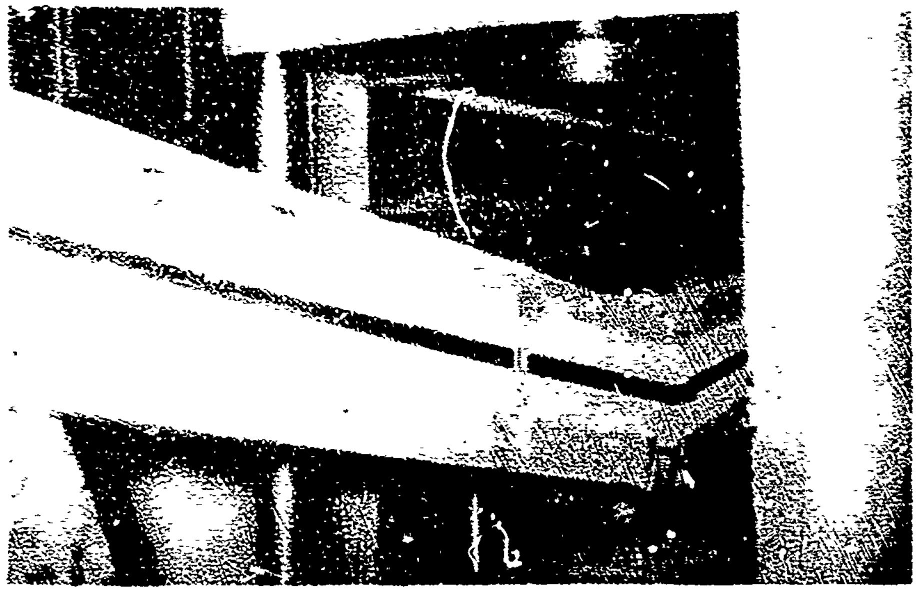

FIBER REINFORCED BEAM 25F DURING STATIC TEST

FIGURE 48

FIBER REINFORCED BEAM 25F AFTER STATIC TEST

FIGURE 49

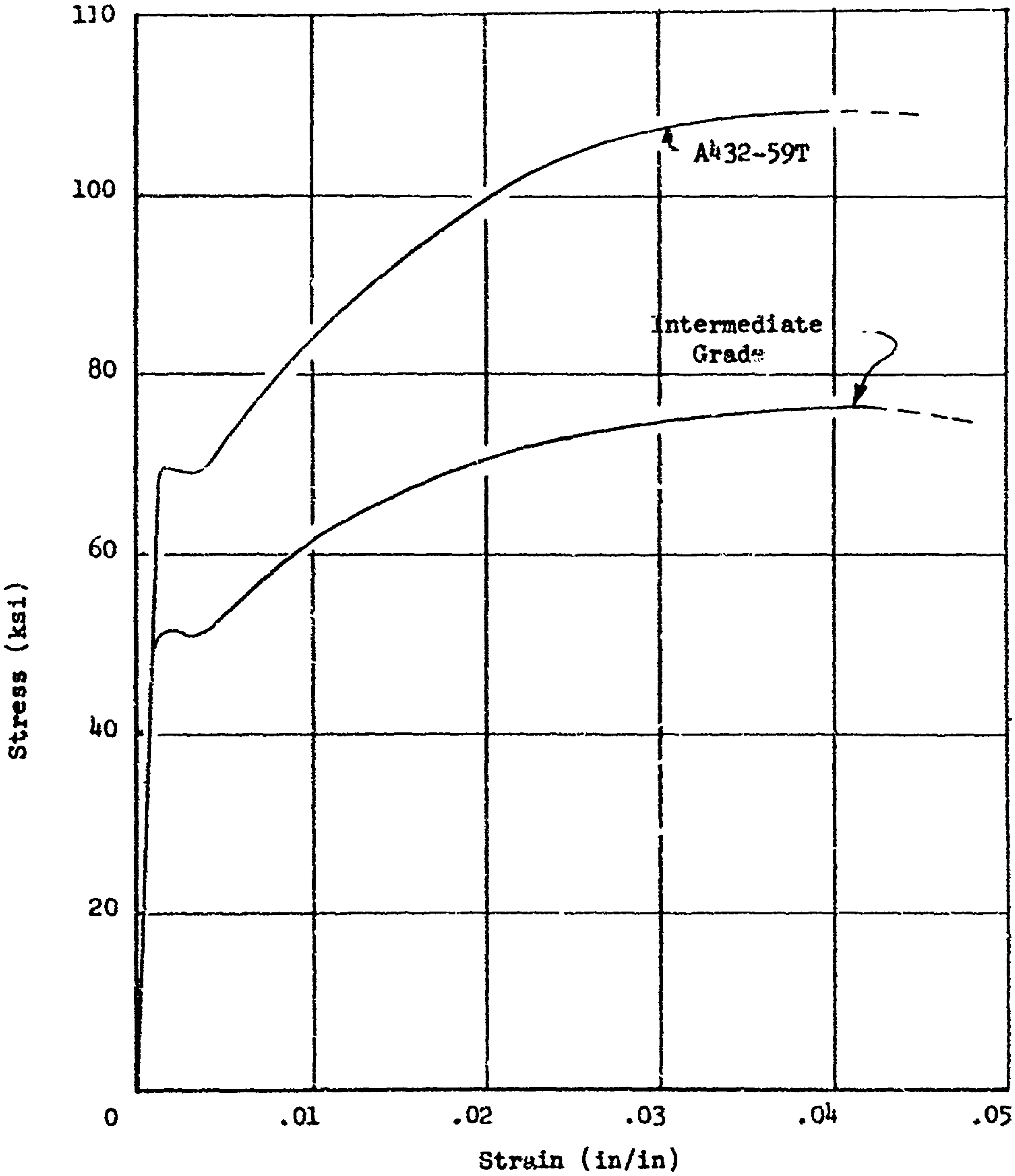

Fig. 50 TENSILE STRESS VS. STRAIN FOR REINFORCING BARS

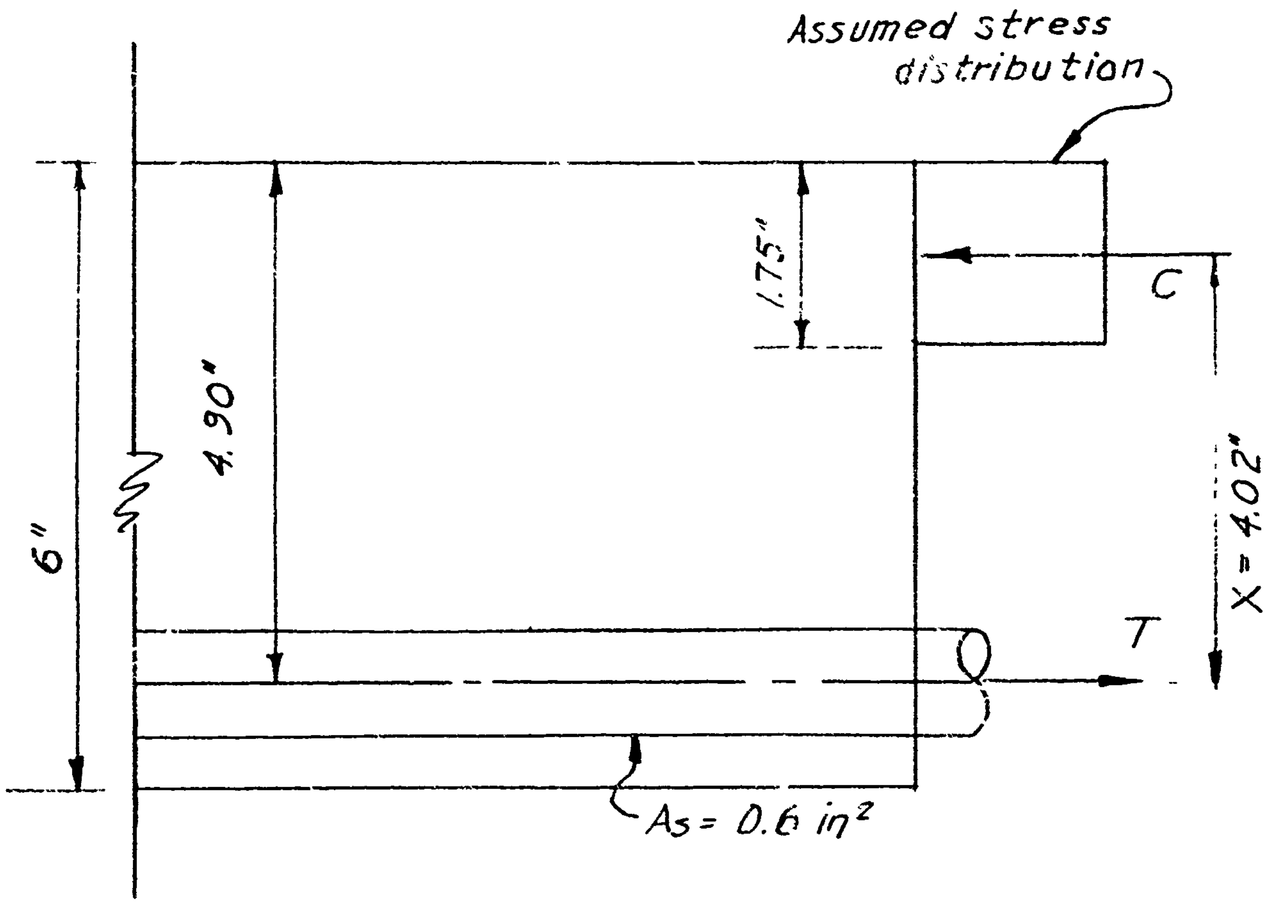

INTERNAL RESISTING COUPLE

FIGURE 51

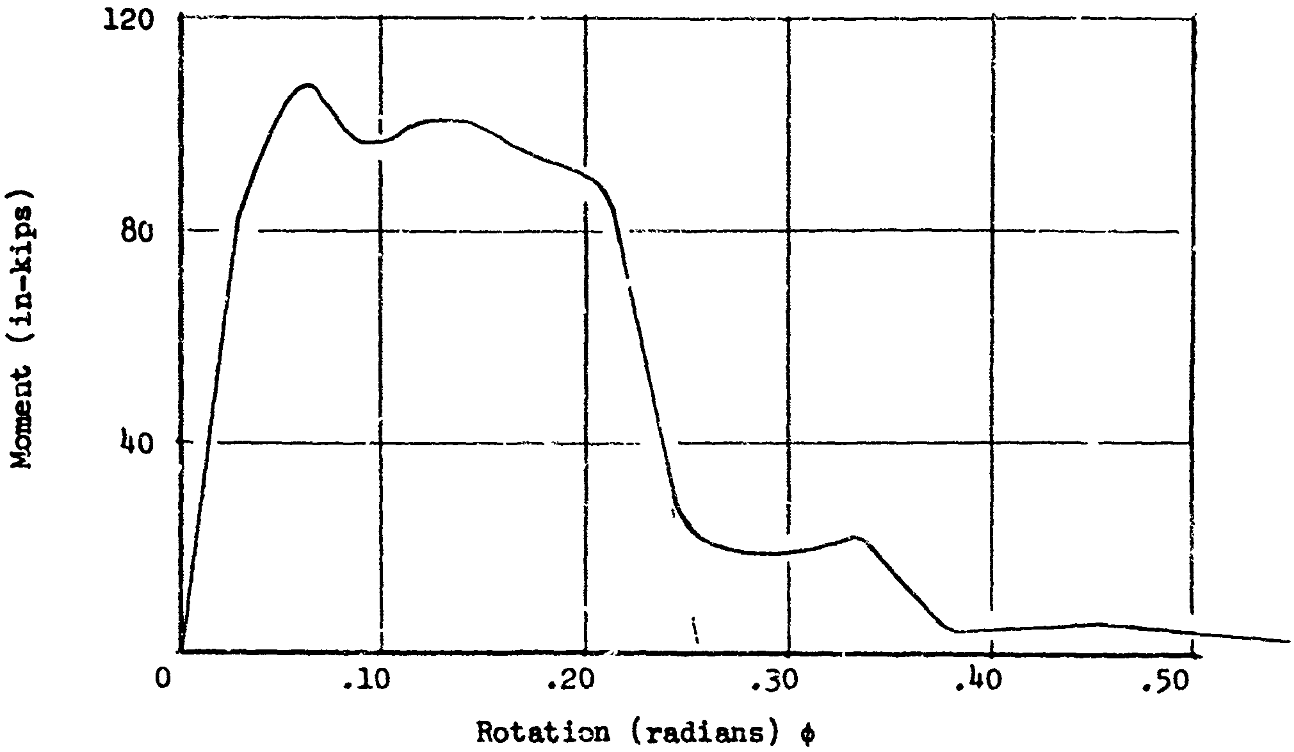

(a) 25PS

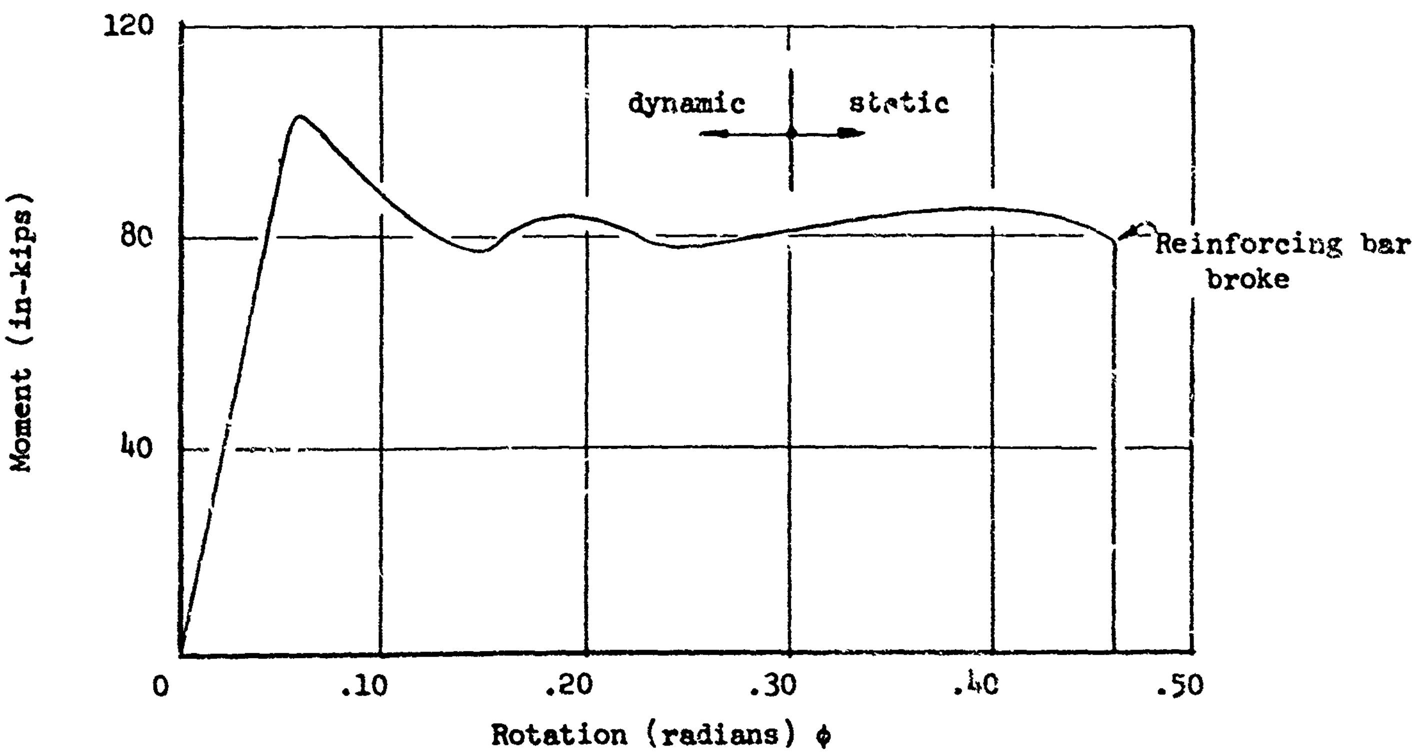

(b) 25F

Fig. 52 MOMENT VS. ROTATION

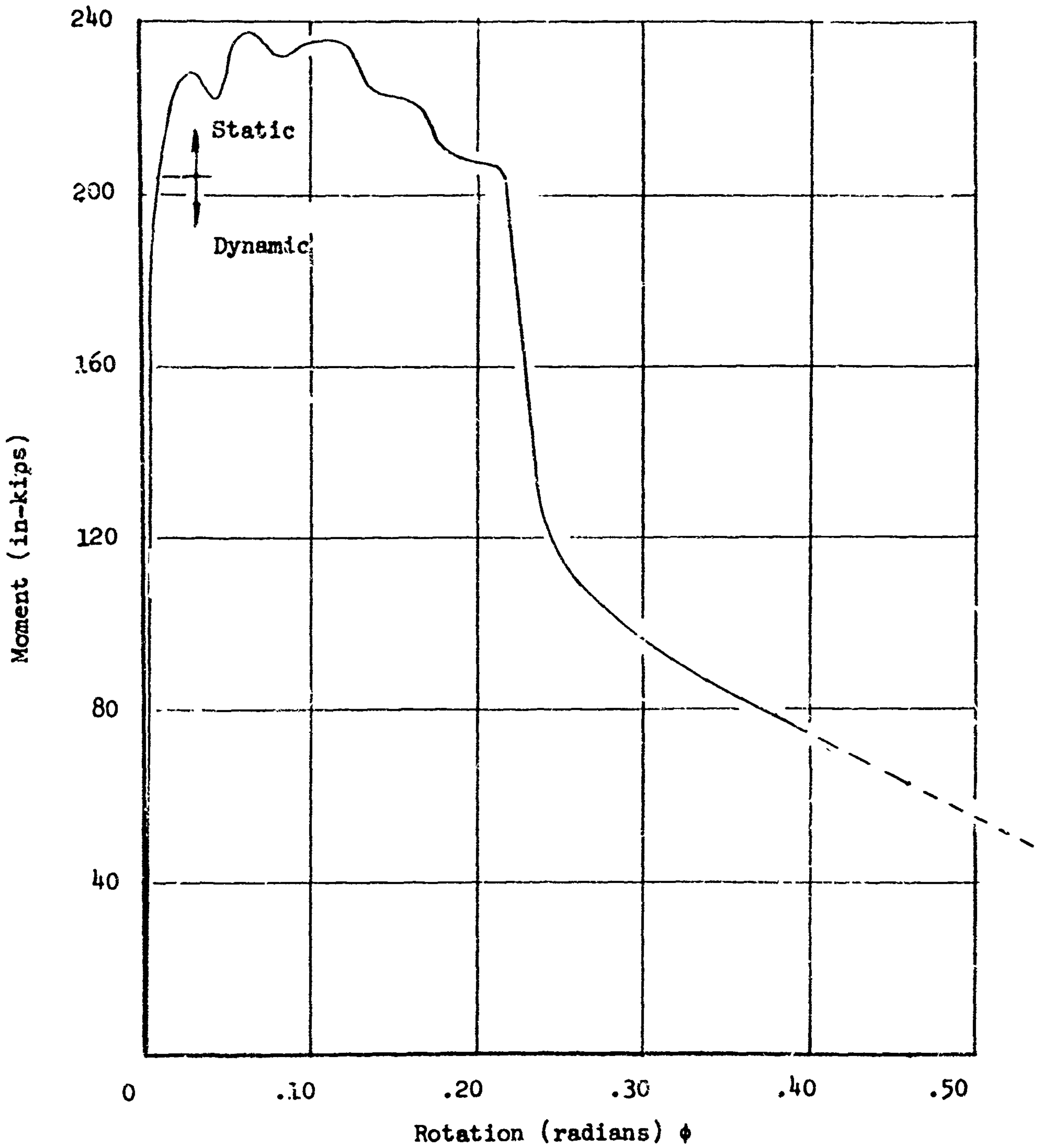

Fig. 53 MOMENT VS. ROTATION BEAM 17F

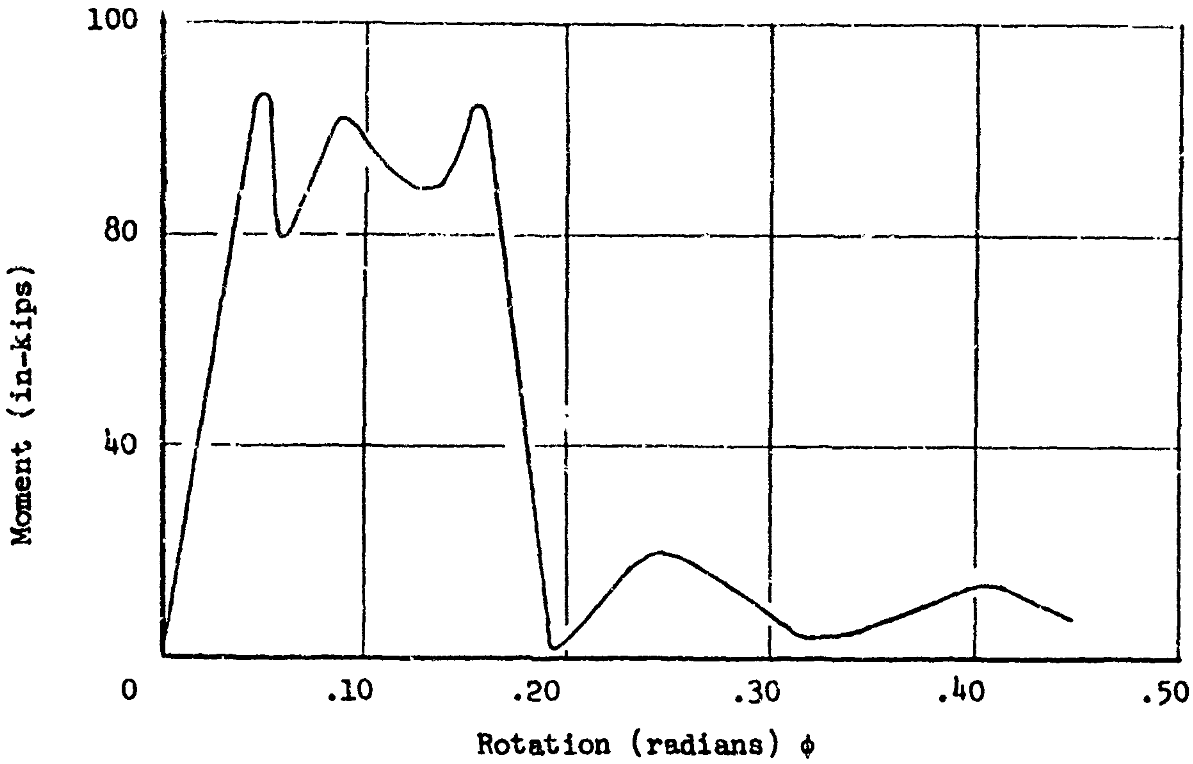

(a) Beam 36PS

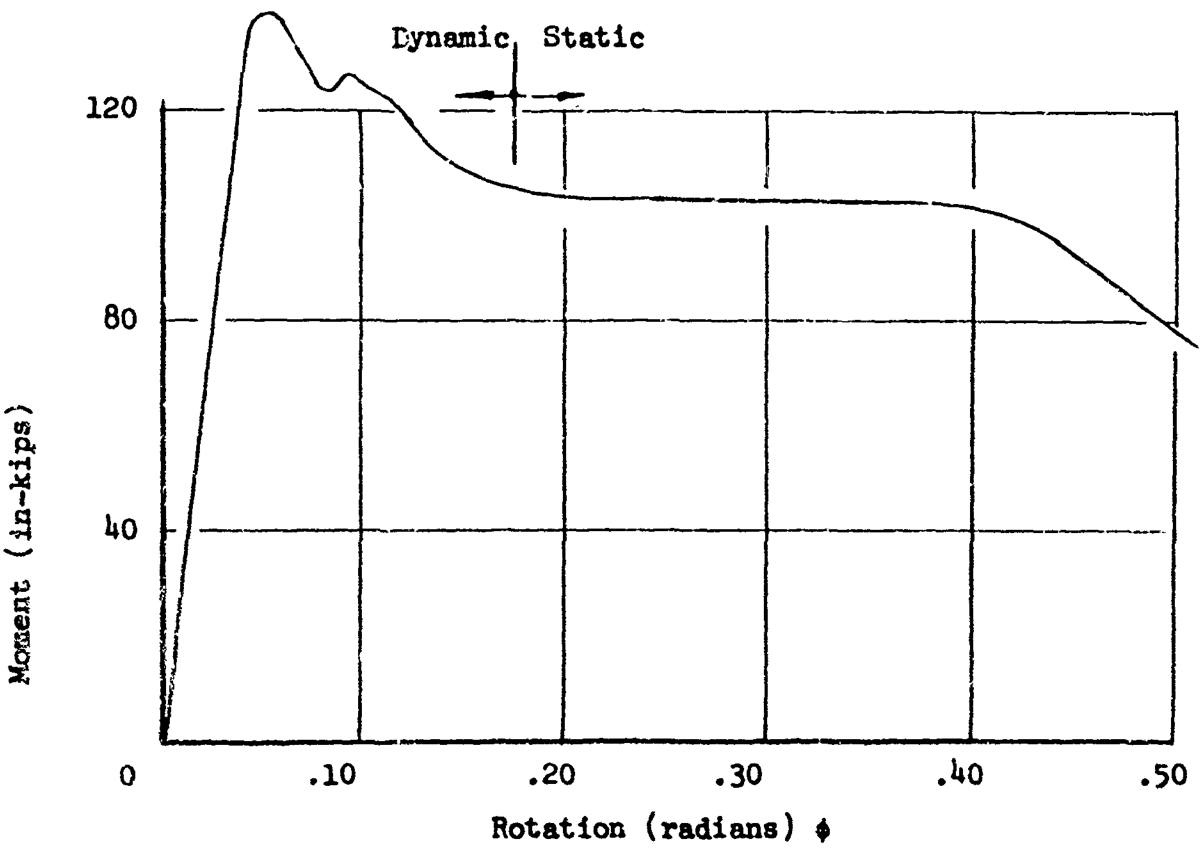

(b) Beam 36F

Fig. 54 MOMENT VS. ROTATION

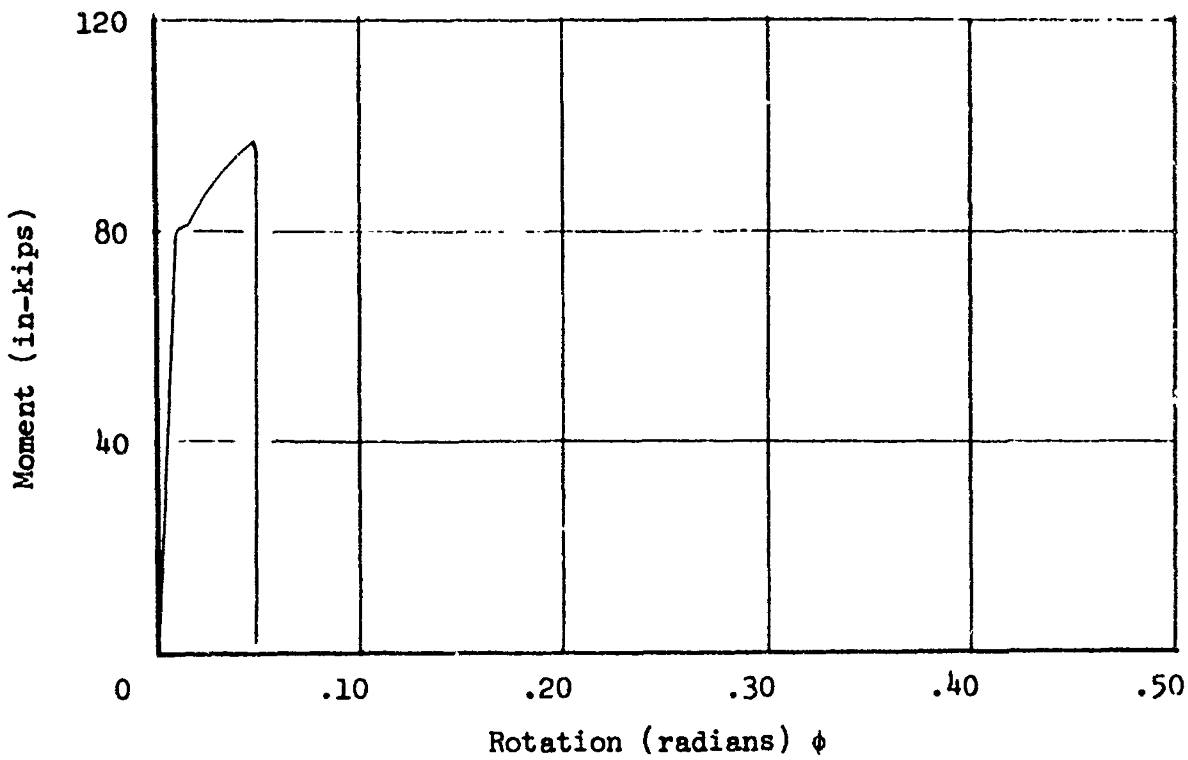

(a) Beam S5P

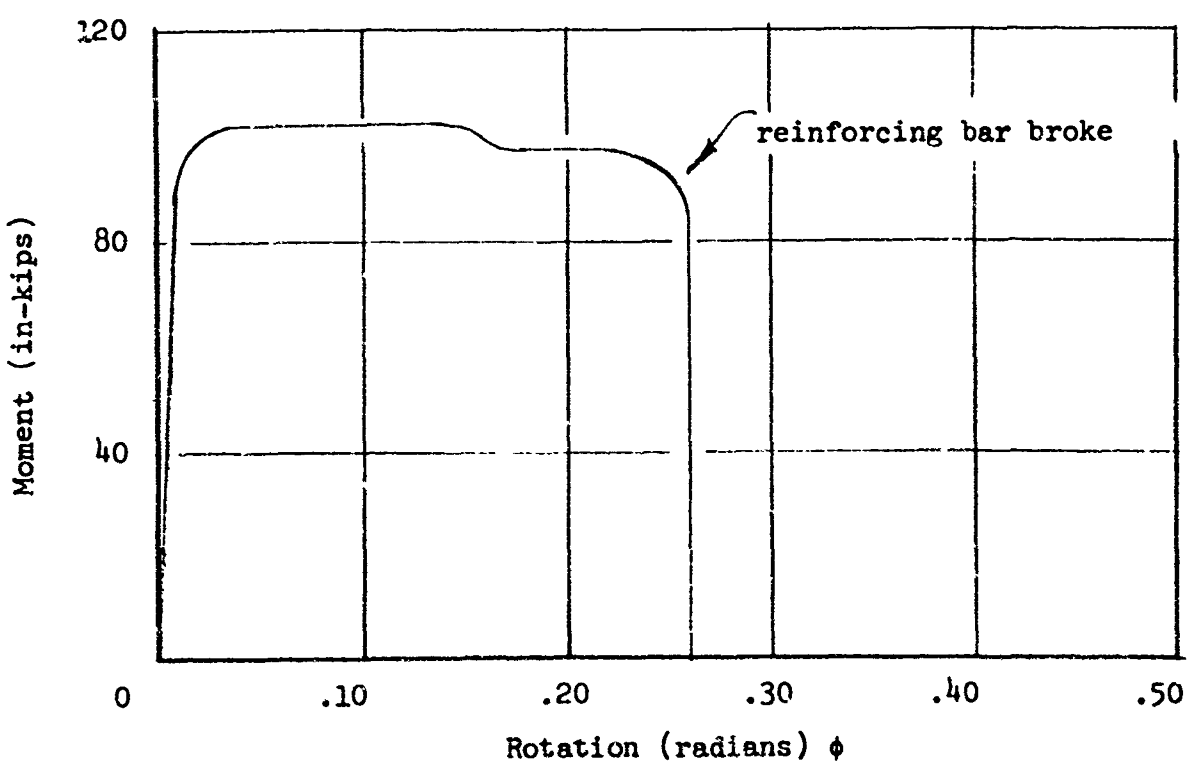

(b) Beam S5F

Fig. 55 MOMENT VS. ROTATION

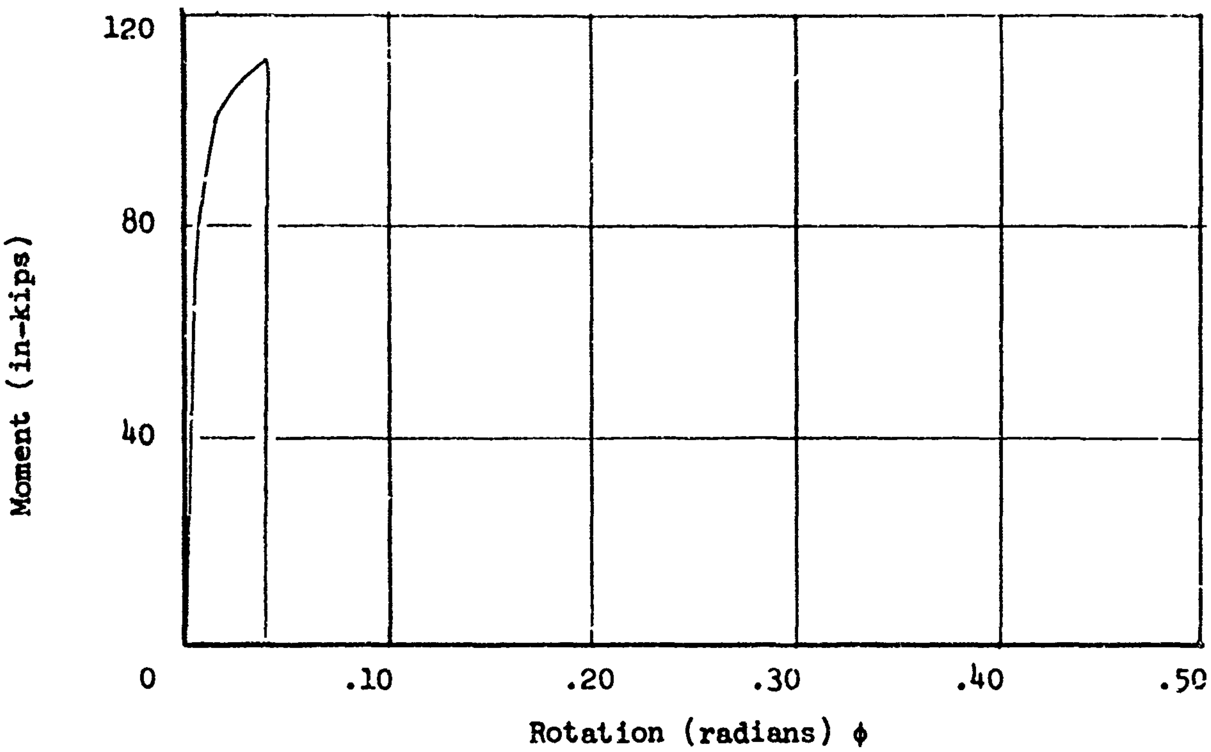

(a) Beam S6P

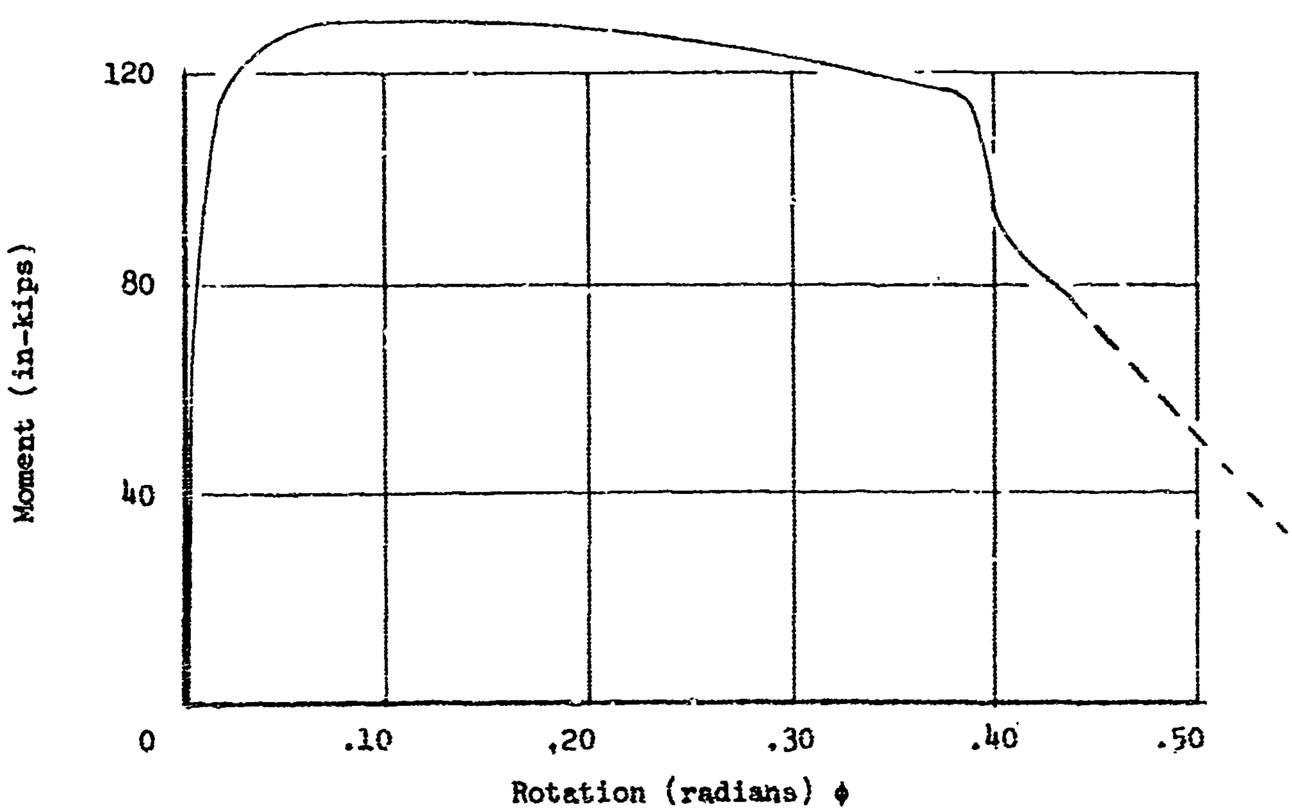

(b) Beam S6F

Fig. 56 MOMENT VS. ROTATION

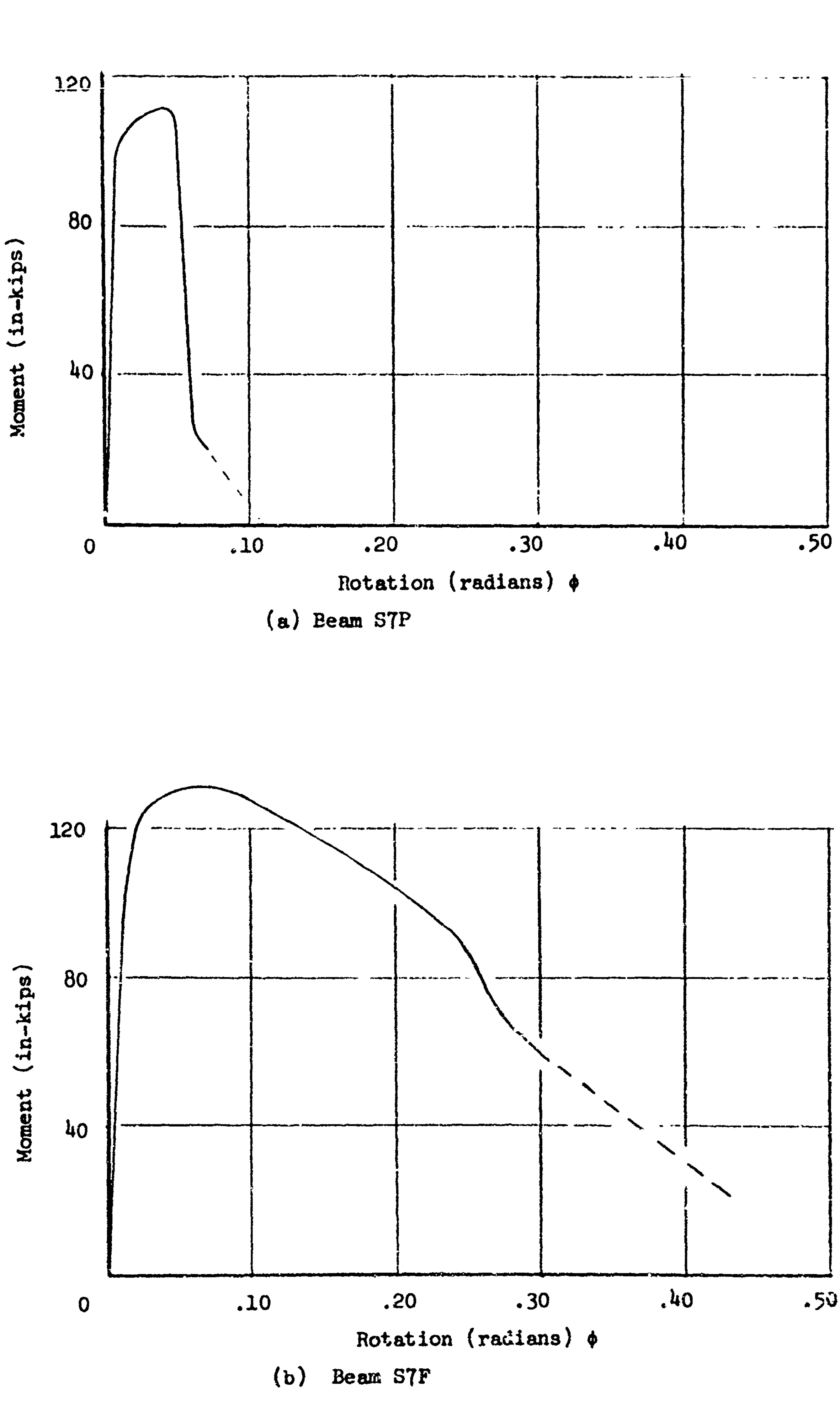

Fig. 57 MOMENT VS. ROTATION

TABLE I

Summary of Beam Data

Beam	Tensile Reinforcement	Shear Reinforcement	
15PS	#5	#3 @ 2"	
15FS	#5	#3 @ 6"	
25PS	#5	#3 @ 2"	
25F	#5	None	
16PS	#6	#3 @ 2"	
16FS	#6	#3 @ 6"	
26PS	#6	#3 @ 2"	
26FS	#6	#3 @ 6"	Dynamic
36PS	#6	#3 @ 2"	
36F	#6	None	
17PS	#7	#3 @ 2"	
17F	#7	None	
27PS	#7	#3 @ 2"	
27FS	#7	#3 @ 6"	
S5P	#5	#3 @ 2"	
S5F	#5	#3 @ 6"	
S6P	#6	#3 @ 2"	Static only
S6F	#6	#3 @ 6"	
S7P	#7	#3 @ 2"	
S7F	#7	#3 @ 6"	

Beam Designations

All beams tested dynamically are designated with four symbols: ABCD

A - Test number (1st, 2nd or 3rd)

B - Size of tensile reinforcement

C - Type of concrete, Plain (P) or fiber (F)

D - Indicates if stirrups are present

i.e., 25FS = second test of beam reinforced with a #5 bar having fiber concrete and stirrups

All beams tested statically have a 3 symbol designation: ABC

i.e., S5P = static, size of tensile reinforcement, plain concrete

TABLE II

Residual Loads After Dynamic Test

Beam	Total Residual Load (kips)
25F	4.90^k
15F	6.41
26FS	10.10
36F	10.90
17F	11.90
15PS	0
25PS	0
36PS	0
27PS	0

TABLE III

Work Done on Plain and Fiber Reinforced Specimens

Beam	Work Done on Beam in-kips	
25F	39.6	
15FS	27.0	
26FS	43.8	
36F	48.0	
17F	60.8	Dynamic-static
15PS	14.6	
25PS	22.6	
36PS	18.0	
27PS	24.0	
S5F	35.0	
S6F	62.0	
S7F	46.0	
S5P	13.4	Static only
S6P	11.2	
S7P	9.8	

TABLE IV

Energy Absorbed by Plain and

Fiber Reinforced Specimens

Beam	Energy Absorbed	
25F	36.6 in-k	Tested Dynamic-Static
36F	47.8	
17F	71.2	
26PS	23.4	
36PS	14.9	
S5F	25.8	Static only
S6F	54.2	
S7F	37.8	
S5P	3.83	
S6P	3.47	
S7P	9.43	

TABLE V

Final Deflections for Dynamic Tests

Main Reinforcement	Beam	Deflection (inches) With Diagonal Tension Reinforcement	Without Diagonal Tension Reinforcement
#5	15FS	2.05	
	25F		2.53
#6	26FS	1.0	
	36F		1.35

Note: Data for #7 bars was not obtained.

78

OCD-PS-64-21

SUMMARY
OF
RESEARCH REPORT

EFFECTS OF IMPULSIVE LOADS ON FIBER-REINFORCED CONCRETE BEAMS

by

JAMES P. ROMUALDI AND MELVIN R. RAMEY
DEPARTMENT OF CIVIL ENGINEERING
CARNEGIE INSTITUTE OF TECHNOLOGY
PITTSBURGH, PENNSYLVANIA 15213

for

OFFICE OF CIVIL DEFENSE
OFFICE, SECRETARY OF THE ARMY
DEPARTMENT OF DEFENSE

CONTRACT NO. OCD-PS-64-21
OCD Work Unit 1122 C

OCD REVIEW NOTICE

This report has been reviewed in the Office of Civil Defense a and approved for publication. Approval does not signify that the contents necessarily reflect the views and policies of the Office of Civil Defense.

OCTOBER 1965

SUMMARY

This study investigates the effects of destructive impulsive loads on concrete made with steel fiber reinforcement. A machine was developed to apply a known impulsive load to concrete beam specimens. Several pairs of specimens were compared. Each pair was identical in geometry and longitudinal steel reinforcement with one exception---one beam of each pair was concrete reinforced with steel fibers and the other of plain concrete. The data were presented in the form of graphs showing the variation of load, time deflection, moment and rotation.

Analysis of the data, including high-speed motion pictures of the beams, has led to the following conclusions:

1. The impulsive loading does not cause the sudden failure in the beams with fiber reinforced concrete that is observed in the case of conventional concrete beams. Figure 38 shows a typical load-deflection diagram for a beam with steel fiber reinforced concrete.

2. The internal resisting moment is significantly greater in the case of beams made with fiber reinforced concrete. This effect permits the beam to absorb more energy and retain its structural integrity while carrying considerable residual loads through relatively large angular distortions. Refer to Figs. 9 and 10 for an illustration of the typical behavior of such beams during a test.

3. Failure of the compressive zone in beams with fiber reinforced concrete is not sudden but is preceded by extensive deformation.

4. The increased tensile strength of fiber reinforced concrete permits its use without special shear reinforcement. The beams with fiber reinforced concrete that were not destroyed during the dynamic tests were tested to destruction in subsequent static bend tests. These tests indicated that significant tensile strains in the steel reinforcing bars could be realized in the beams with fiber reinforced concrete because the compressive concrete zone remained intact throughout a greater range of deformation. In some cases, tensile steel stresses reached the ultimate value. Refer to Figs. 38, 48, and 49.

UNCLASSIFIED

Security Classification

DOCUMENT CONTROL DATA - R&D

(Security classification of title, body of abstract and indexing annotation must be entered when the overall report is classified)

1. ORIGINATING ACTIVITY (Corporate author) Carnegie Institute of Technology Pittsburgh, Pennsylvania	2a. REPORT SECURITY CLASSIFICATION Unclassified 2b. GROUP — — —

3. REPORT TITLE

Effect of Impulsive Loads on Fiber-Reinforced Concrete Beams

4. DESCRIPTIVE NOTES (Type of report and inclusive dates)

Final Report

5. AUTHOR(S) (Last name, first name, initial)

Romualdi, James P., Ramey, Melvin R.

6. REPORT DATE	7a. TOTAL NO. OF PAGES	7b. NO. OF REFS
October 1965	77	7

8a. CONTRACT OR GRANT NO. OCD-PS-64-21 b. PROJECT NO 1100 c. d. Work Unit 1122C	9a. ORIGINATOR'S REPORT NUMBER(S) — — — 9b. OTHER REPORT NO(S) (Any other numbers that may be assigned this report) — — —

10. AVAILABILITY/LIMITATION NOTICES

Distribution of this document is unlimited.

11. SUPPLEMENTARY NOTES — — —	12. SPONSORING MILITARY ACTIVITY Office of Civil Defense Office of the Secretary of the Army Washington, D. C.

13. ABSTRACT (U) This report describes an investigation of the effect of a destructive impulse load upon fibre reinforced concrete beams. Concrete develops tension cracks as a result of minute flaws that are inherent in its nature. A method of arresting these cracks by placing short lengths of randomly spaced fine wire within the concrete mix is described. The result of the studies indicate that (1) the fibres increase the tensile strength of the concrete by as much as 100 percent for static loading, and (2) the material exhibits considerable post-cracking strength. These two effects increase the ability of the material to absorb energy.

14 KEY WORDS	LINK A		LINK B		LINK C	
	ROLE	WT	ROLE	WT	ROLE	WT
fibre-reinforced concrete						
blast shelters						
construction						

INSTRUCTIONS

1. ORIGINATING ACTIVITY: Enter the name and address of the contractor, subcontractor, grantee, Department of Defense activity or other organization *(corporate author)* issuing the report.

2a. REPORT SECURITY CLASSIFICATION: Enter the overall security classification of the report. Indicate whether "Restricted Data" is included. Marking is to be in accordance with appropriate security regulations.

2b. GROUP: Automatic downgrading is specified in DoD Directive 5200.10 and Armed Forces Industrial Manual. Enter the group number. Also, when applicable, show that optional markings have been used for Group 3 and Group 4 as authorized.

3. REPORT TITLE: Enter the complete report title in all capital letters. Titles in all cases should be unclassified. If a meaningful title cannot be selected without classification, show title classification in all capitals in parenthesis immediately following the title.

4. DESCRIPTIVE NOTES: If appropriate, enter the type of report, e.g., interim, progress, summary, annual, or final. Give the inclusive dates when a specific reporting period is covered.

5. AUTHOR(S): Enter the name(s) of author(s) as shown on or in the report. Enter last name, first name, middle initial. If military, show rank and branch of service. The name of the principal author is an absolute minimum requirement.

6. REPORT DATE: Enter the date of the report as day, month, year; or month, year. If more than one date appears on the report, use date of publication.

7a. TOTAL NUMBER OF PAGES: The total page count should follow normal pagination procedures, i.e., enter the number of pages containing information.

7b. NUMBER OF REFERENCES: Enter the total number of references cited in the report.

8a. CONTRACT OR GRANT NUMBER: If appropriate, enter the applicable number of the contract or grant under which the report was written.

8b, 8c, & 8d. PROJECT NUMBER: Enter the appropriate military department identification, such as project number, subproject number, system numbers, task number, etc.

9a. ORIGINATOR'S REPORT NUMBER(S): Enter the official report number by which the document will be identified and controlled by the originating activity. This number must be unique to this report.

9b. OTHER REPORT NUMBER(S): If the report has been assigned any other report numbers *(either by the originator or by the sponsor)*, also enter this number(s).

10. AVAILABILITY/LIMITATION NOTICES: Enter any limitations on further dissemination of the report, other than those imposed by security classification, using standard statements such as:

(1) "Qualified requesters may obtain copies of this report from DDC."

(2) "Foreign announcement and dissemination of this report by DDC is not authorized."

(3) "U. S. Government agencies may obtain copies of this report directly from DDC. Other qualified DDC users shall request through ______."

(4) "U. S. military agencies may obtain copies of this report directly from DDC. Other qualified users shall request through ______."

(5) "All distribution of this report is controlled. Qualified DDC users shall request through ______."

If the report has been furnished to the Office of Technical Services, Department of Commerce, for sale to the public, indicate this fact and enter the price, if known.

11. SUPPLEMENTARY NOTES: Use for additional explanatory notes.

12. SPONSORING MILITARY ACTIVITY: Enter the name of the departmental project office or laboratory sponsoring *(paying for)* the research and development. Include address.

13. ABSTRACT: Enter an abstract giving a brief and factual summary of the document indicative of the report, even though it may also appear elsewhere in the body of the technical report. If additional space is required, a continuation sheet shall be attached.

It is highly desirable that the abstract of classified reports be unclassified. Each paragraph of the abstract shall end with an indication of the military security classification of the information in the paragraph, represented as *(TS), (S), (C), or (U)*.

There is no limitation on the length of the abstract. However, the suggested length is from 150 to 225 words.

14. KEY WORDS: Key words are technically meaningful terms or short phrases that characterize a report and may be used as index entries for cataloging the report. Key words must be selected so that no security classification is required. Identifiers, such as equipment model designation, trade name, military project code name, geographic location, may be used as key words but will be followed by an indication of technical context. The assignment of links, rules, and weights is optional.